Geotechnical Investigation of the Depth of Buried MSW and Rock
Cinder Lake Landfill
City of Flagstaff
Coconino County, Arizona

Submitted to:

City of Flagstaff
Cinder Lake Landfill
6770 East Landfill Road
Flagstaff, Arizona 86004

Submitted by:

Amec Foster Wheeler
Environment & Infrastructure, Inc.
Phoenix, Arizona

March 7, 2016

Project No. 17-2015-4061

Registered Professional Engineer (Civil)
CERTIFICATE NO.
18682
MICHAEL L.
RUCKER
Date Signed 3-7-16
ARIZONA, U.S.A.
Expires 03/31/16

REGISTERED GEOLOGIST
CERTIFICATE NO.
42910
WAYNE A.
HARRISON
Date Signed 3/7/16
ARIZONA U.S.A.
Expires 06/30/2017

March 7, 2016
Project No. 17-2015-4061

City of Flagstaff
Cinder Lake Landfill
6770 East Landfill Road
Flagstaff, Arizona 86004

Attn: Matthew Morales, PE

Re: Geotechnical Investigation of the Depth of Buried MSW and Rock
Cinder Lake Landfill
City of Flagstaff
Coconino County, Arizona

Submitted herewith is the Geotechnical Investigation of the Depth of Buried Municipal Solid Waste (MSW) and Rock for the Cinder Lake Landfill prepared by Amec Foster Wheeler Environment & Infrastructure, Inc. (Amec Foster Wheeler). Included are estimations of the depths and volumes of MSW and basalt rock in relevant portions of Sequences A, C, D, and E, discussions of additional interpretations from the geophysical investigation, and recommendations for boring locations.

Should you have any questions concerning the recommendations presented in this report, please do not hesitate in contacting us.

Respectfully submitted,

Amec Foster Wheeler
Environment & Infrastructure, Inc.

For Kenneth C Fergason, PG
Senior Geologist

Michael L Rucker, PE
Senior Geotechnical Engineer

Reviewed by:

Wayne Harrison, PG
Senior Geologist

REGISTERED GEOLOGIST
CERTIFICATE NO. 42910
WAYNE A. HARRISON
Date Signed 3/7/16
ARIZONA U.S.A.
Expires 06/30/2017

Registered Professional Engineer (Civil)
CERTIFICATE NO. 18682
MICHAEL L. RUCKER
Date Signed 3-7-16
ARIZONA, U.S.A.
Expires 03/31/16

c: Addressee (PDF)

G:\Geotechnical\2015 Projects\17-2015-4061 COF_La

4600 East Washington Street, Suite 600
Phoenix, Arizona 85034-1917
Tel (602) 733-6000
Fax (602) 733-6100
www.amecfw.com

TABLE OF CONTENTS

Page

1.0 EXECUTIVE SUMMARY 1
2.0 INTRODUCTION AND PROJECT DESCRIPTION 2
3.0 INVESTIGATIVE APPROACH 3
3.1 Review of Existing Data 3
3.2 Seismic Refraction and Refraction Microtremor (ReMi) 3
4.0 GEOLOGIC CONDITIONS 4
4.1 Regional Geology 4
4.2 Local Geology 4
5.0 DISCUSSION 6
5.1 Depth of MSW 6
5.2 Depth of Basalt Unit 6
5.2.1 Sequence E 6
5.2.2 Sequence D 7
5.3 Basalt Excavation Assessment 7
5.3.1 Kirsten Excavation Classification System 7
5.3.2 Seismic Velocities 9
5.4 Comparison of Seismic (Horizontal) and Coring (Vertical) Investigations 10
5.5 Basalt Unit Characterization - Low Seismic Velocities and High Strength Samples 11
6.0 RECOMMENDATIONS 12
6.1 Boring Locations 12
7.0 REFERENCES 14

LIST OF FIGURES

Figure 1 Site Map Showing Geologic Profiles, Seismic Line & Proposed Boring Locations
Figure 2 Geologic Profiles in Sequence E (Profiles A & B)
Figure 3 Geologic Profiles in Sequence E (Profile C)
Figure 4 Geologic Profiles in Sequence D (Profile D)
Figure 5 Geologic Profiles in Sequence C (Profile E)
Figure 6 Geologic Profiles in Sequence A (Profiles F & G)

LIST OF APPENDICES

Appendix A Seismic Refraction and Refraction Microtremor

1.0 EXECUTIVE SUMMARY

This report presents an evaluation of the depth of Municipal Solid Waste (MSW) and competent basalt rock intended to aid the City of Flagstaff (City) in evaluating its excavation plans for future expansion of operations at the Cinder Lake Landfill (CLL) and the potential for utilizing basalt rock as an aggregate resource. One goal for the geophysical survey is to provide general information regarding the depths and volume of MSW within specified areas of Sequence A and the southern portion of Sequence C. A second goal of the investigation is to characterize the depth of geologic units to a depth of approximately 200 feet below ground surface in specified areas of Sequence D and E. This is for the purpose of identifying areas where more competent basalt flows that have a potential to be utilized as an aggregate resource are present and to estimate the volume of this potential resource. Additionally, discussions regarding excavation properties of the more competent basalt rock and its potential utilization as aggregate material are included.

In both Cells A and C, the average depth of the MSW was interpreted to be about 18 feet, with some areas of Cell C with depths closer to 12 feet. There were also indications that in portions of Cell A that there is potential that a deeper section of MSW is present to depths of nearly 30 feet that is capped with fill and then more MSW. Approximate volume of MSW was estimated for the portion of Cell C investigated and for Cell A. For both cells, an average depth of MSW of 18 feet was used, it is noted that there is the potential for a deeper MSW section in Cell A that may be partly accounted for in these volume estimates. It is estimated that approximately 360,000 cubic yards of MSW is present in the portions of Cell A investigated and that approximately 180,000 cubic yards of MSW is present in the portion of Cell C investigated.

In Sequence E, the elevation of the top of the Basalt Unit is typically around 6590 to 6600 feet above mean sea level (amsl). The Basalt Unit extends to a depth of about 6400 feet amsl, suggesting that it has a maximum thickness of about 200 feet. As discussed in Section 3.2, the Cinder/Basalt Unit is also present underlying Sequence E and appears to be thickest underlying the eastern and northeastern portions of Sequence E. The bottom of the Basalt Unit and top of the Cinder/Basalt Unit in this area is interpreted to be at about elevation 6520 to 6540 feet amsl. It is estimated that approximately 6.5 million cubic yards of the Basaltic Unit are present within the surface footprint of Sequence E between the surface and elevation 6500 feet amsl. The full potential volume of the Basalt Unit is not planned to be excavated according to the projected excavation plan for Sequence E prepared by the City (Flagstaff 2015). It is estimated that approximately 4.0 million cubic yards of the Basalt Unit are present within the limits of the project excavation plan. Approximately 0.6 million cubic yards of Cinder/Basalt Unit is estimated to be present within the limits of the project excavation plan. Approximately 5.7 million cubic yards of Cinder Unit is estimated to overlie the Basalt Unit within the limits of the project excavation plan.

In Sequence D, the elevation of the top of the Basalt Unit is typically around 6570 to 6600 feet amsl. The Basalt Unit extends to a depth of about 6400 feet amsl, suggesting that it has a maximum thickness of about 200 feet. It is estimated that approximately 4 million cubic yards of the Basaltic Unit are present within Sequence D between the surface and elevation 6500 feet amsl. The full potential volume of the Basalt Unit is not planned to be excavated according to the projected excavation plan for Sequence D prepared by the City (Flagstaff 2015). It is

estimated that approximately 2.1 million cubic yards of the Basalt Unit are present within the limits of the project excavation plan.

It must be understood that the interpreted presence of extensive fissures or large fractures within the Basalt Unit rock mass indicate that blasting for mass excavation may be a difficult and complex operation. Blast energy could be anticipated to seek and be dissipated within such open fissures or fractures, and thus reduce the effectiveness of blasting. It is recommended that consultation with a qualified blasting consultant be included for consideration of these potential issues.

Due to the apparent lateral variations within the Basalt unit rock mass, it is anticipated that sorting suitable aggregate materials from lesser quality rock (otherwise potentially suitable for riprap, rockfill, landscaping, etc.) may be a complex operation. One preliminary indication of rock suitability for crushed aggregate may be the absence of visible vesicles within the rock particles.

Recommendations for boring locations to further investigate the rock quality and depths of the Basalt Unit within Sequences C, D and E are shown on Figure 1. Boring locations were selected to reduce uncertainty of important factors such as the depth of MSW and the thickness and rock quality of the Basalt Unit and the presence or absence of the Cinder/Basalt Unit. In addition to the recommended boring locations discussed in the report, it may be worth considering performing a small-scale excavation (drilling and/or blasting) to further evaluate excavability conditions and the suitability of the Basalt Unit as an aggregate source.

2.0 INTRODUCTION AND PROJECT DESCRIPTION

Amec Foster Wheeler Environment & Infrastructure, Inc. (Amec Foster Wheeler) presents the Geotechnical Investigation of the Depth of Buried MSW and Rock, CLL herein. The report is submitted to the City, CLL as part of an evaluation of the depth of MSW and competent basalt rock intended to aid the City in evaluating its excavation plans for future expansion of operations at the CLL and the potential for utilizing basalt rock as an aggregate resource.

Amec Foster Wheeler understands that the CLL goals for the geophysical survey is to provide general information regarding the depths and volume of MSW within specified areas of Sequence A and the southern portion of Sequence C.

A second aspect of the investigation is to characterize the depth of geologic units to a depth of approximately 200 feet below ground surface in specified areas of Sequence D and E. Amec Foster Wheeler understands that the goal of this portion of the investigation is to identify areas where more competent basalt flows that have a potential to be utilized as an aggregate resource are present and to estimate the volume of this potential resource.

Additionally, Amec Foster Wheeler provides discussion regarding excavation properties of the more competent basalt rock and its potential utilization as aggregate material.

3.0 INVESTIGATIVE APPROACH

To address issues of depths of MSW, deep characterization of the geologic units, material excavatability and strengths, Amec Foster Wheeler performed surface geophysical seismic lines of appropriate length and orientation within the specified sequences at the landfill to obtain the desired information. Additionally, information available from previous investigations, including borehole logs, seismic refraction interpretations, and other geophysical interpretations are correlated with our investigation. Additional information can be obtained from the seismic interpretations beyond what is included in the solicitation including some rock strength parameters (unit weight and unconfined compressive strength [UCS]), excavability/rippability of the materials, and earthwork factors.

3.1 Review of Existing Data

Amec Foster Wheeler reviewed the information and reports specified in the solicitation to gain understanding of the results of previous investigations and to utilize past data to compliment and correlate to this investigation as well as other publications. These included investigations performed by Woodward-Clyde Consultants (WCC 1997), Speedie & Associates (SAI 2012), HydroSystems, Inc. (HydroSystems 2011), City of Flagstaff (Flagstaff-SDB 2014), and other published reports from sources such as the United States Geological Survey (USGS). As part of this task, Amec Foster Wheeler developed a site-specific health and safety plan, prior to performing any field investigations.

3.2 Seismic Refraction and Refraction Microtremor (ReMi)

Two surface seismic methods were utilized. Seismic refraction was performed to interpret subsurface geomaterial profiles and obtain compression wave (p-wave) velocities to assess material strength and excavatability by various mechanical methods or blasting. A 10-pound sledgehammer served as the seismic refraction energy source. ReMi was performed to obtain one dimensional vertical shear wave (s-wave) profiles for dynamic modulus parameters, seismicity assessment and to complement the p-wave results. Table A-1 presents a summary of ReMi s-wave interpretations.

Amec Foster Wheeler has developed correlations to estimate various geomaterial parameters as a function of seismic p-wave and s-wave velocities. These parameters include geomaterial mass density or unit weight, low and high modulus, and UCS. Locations of the seismic lines are shown on Sheet 1 and seismic interpretations are included in Appendix A at the end of this report.

ReMi utilizes ambient ground noise such as traffic vibration as an energy source. If a location lacks sufficient ambient noise, then jumping, jogging or driving the field vehicle in the line vicinity is typically sufficient. The strengths and weaknesses of the seismic refraction and ReMi methods are complementary. Lateral changes in subsurface conditions or materials are interpretable using seismic refraction, while detecting and characterizing weaker, deeper horizons underlying stronger shallower horizons are possible using ReMi. Frozen ground at the surface may form a significant velocity reversal that blinds shallow seismic refraction results; ReMi can provide effective results in such conditions. Seismic refraction signals are strongly

influenced by the water table that can sometimes mask geomaterial conditions, while ReMi signals are minimally influenced by saturation and can characterize geomaterials in a saturated condition. Using a 240-foot long geophone array, seismic refraction provides good detail and resolution in typically the upper 60 feet for the subsurface soils and shallower rock, while ReMi results has a considerably greater depth of investigation, often in excess of 100 feet. Using a 600-foot long geophone array, seismic refraction provides reasonable detail and resolution in the upper 100 feet of the subsurface (depending upon background noise and attenuation of the sledgehammer p-wave signal), while ReMi achieved a depth of investigation of 300 feet or more.

The same 24-channel seismograph, cables and geophone setups are used for both p-wave seismic refraction and s-wave ReMi. We utilized a combination of a 240-foot long setup with geophone spacings of 10 feet (10 lines) and a 600-foot long setup with geophone spacings of 25 feet (10 lines) to achieve reasonable resolution and proper depths of investigation.

Appendix B at the end of this report presents some generalized charts of useful correlations for seismic velocity. Site-specific applications of these principles are discussed Section 5 of this report.

4.0 GEOLOGIC CONDITIONS

4.1 Regional Geology

The CLL is located in the southern portion of the Colorado Plateau physiographic province within the San Francisco Volcanic Field. In northern Arizona, the Colorado Plateau is composed of Cambrian through Mesozoic sedimentary rocks overlain by Tertiary and Quaternary volcanic and sedimentary rocks. Unlike areas to the south and west in the Basin and Range Province, the Colorado Plateau has remained relatively undeformed. The Paleozoic and Mesozoic formations on the Plateau are only slightly faulted and overall dip gently to the northeast. The regional groundwater table roughly follows the same trend, decreasing in elevation to the northeast (Bills, et al. 2000).

4.2 Local Geology

The CLL is located in the San Francisco Volcanic Field, east of the San Francisco Peaks, south of Sunset Crater Cinder Cone. Lava flows and pyroclastic materials are present throughout the site and have been described in detail in several publications (Moore and Wolfe 1976, 1987, Macy et al 2012). Moore and Wolfe (1976, 1987) also identify a small cinder cone as V511 just south of the site. Macy and others (2012) refer to several of the basalt outcrops as possible push-up features.

Previous geologic investigations have been performed at the CLL by others, including studies performed by Woodward-Clyde (WCC 1997), HydroSystems (2011), and Speedie & Associates (SAI 2012). Woodward-Clyde identified two generic geologic units and referred to them as the Cinder Unit and Basalt Unit and subsequent studies have generally utilized this terminology. For consistency with these previous investigations, this report utilizes the terms Cinder Unit and Basalt Unit as well, however we include alluvial components to the surficial Cinder Unit and have identified a third unit that is likely a combination of interlayered cinders and basalt that we

call the Cinder/Basalt Unit. These units are described below. The Basalt Layer is the potential aggregate resource and is discussed below.

Underlying the volcanic deposits are the regional Paleozoic geologic formations. Boring CL-5 located off the northwest corner of the CLL encountered Kaibab Limestone at an elevation of about 6,330 feet amls (Hydrosystems 2011). The Paleozoic Units are not described in detail below since they are found well below the relevant depths for this investigation.

Cinder Unit. As discussed in previous investigations (WCC 1997, SAI 2012), the Cinder Unit appears to be a result of multiple volcanic events identified by black and reddish brown cinders. The Cinder Unit appears to be present from the surface to the elevation of about 6600 feet amsl. The cinder unit consists of materials scoria (cinders), volcanic bombs and possibly thin basalt flows that do not appear to be laterally extensive or more than a few feet in thickness. The surficial portions of the Cinder Unit often contain aeolian/alluvial deposits as well. The cinders, scoria and volcanic bombs are often fused together (agglomerate) creating an undulating surface of variable hardness, thickness and extent. Consistent with patterns of ephemeral surface water flow into the area, portions of the shallow Cinder Unit were previously logged as alluvium (WCC 1997)

Basalt Unit. The Basalt Unit is generally present from about elevation 6600 to around 6400 feet amsl. The Basalt Unit is likely underlain by Paleozoic sedimentary rocks of either the Moenkopi or Kaibab Formations (Macy et al 2012). The upper portion of the Basalt Unit near the surface was generally weathered to a predominately decomposed state and was very soft to medium hard (SAI 2012). Below the surficial weathering the basalt was classified as slightly weathered to fresh and hard to very hard. Vesicles are present in the basalt but typically represent less than 3 percent of the mass (SAI 2012). Larger voids are possible in basalt formations of this type. Rock core obtained as part of the Speedie & Associates investigation (SAI 2012) described fractures within the basalt that are spaced close to moderately close. The fractures are generally closed and contain some minor surficial iron oxide staining. However it appears likely that a series of large, widely-spaced, sub-vertical fractures are present within the Basalt Unit, which is common in these environments and consistent with interpretations of push up features in the area (Macy et al 2012).

The Basalt Unit is the potential aggregate resource and therefore what otherwise may be subtle changes in the rock characteristics may have a significant impact on the unit's suitability for use as aggregate. For example, the presence, amount and size of vesicles (void space within the basalt rock) can impact the quality of the rock as an aggregate resource because interconnected vesicles could provide surface area to absorb asphalts / oils, but would not be in contact with adjacent aggregate particles. Those oils / asphalts on internal vesicle surfaces would not contribute to the overall bonding of different aggregate particles as asphaltic concrete mix, and would essentially waste a relatively larger fraction of the asphalt in the mix.

Cinder/Basalt Unit. Underlying portions of Cell E, there appears to be a deeper unit referred to as the Cinder/Basalt Unit that has notably lower seismic velocities. No previous investigations have drilled deep enough in this area to directly observe this unit. Based on its seismic velocity, it could be a combination of relatively thin basalt flows and pyroclastic deposits similar to the Cinder Unit, potentially associated with V511 as mapped by Moore and Wolfe (1976, 1987). The thickness and extent of this unit are not well understood. It appears to be present at about elevation 6550 feet amsl and in places may extend to elevations as low as 6500 feet amsl or

even 6400 feet amsl. Indications are that this unit is thicker underlying the southeast portion of Cell E. The Cinder/Basalt Unit may be similar to the anomalous conditions that have been observed in the southwest corner of Cell D.

5.0 DISCUSSION

The following volume estimate calculations are based on review of the Flagstaff excavation plan (Flagstaff 2015). Volume estimate calculations were developed based on average end-area method from shallow borings by others combined with Amec Foster Wheeler seismic interpretations to estimate the extent and thickness of the geologic units within the excavation limits shown on the excavation plan provided for review (Flagstaff 2015).

5.1 Depth of MSW

Seismic lines located in Sequences A and C were performed to estimate the depth of MSW and estimate an approximate volume of MSW in those areas. Profile E (Figure 4) shows depths of the MSW in Cell C and Profiles F and G (Figure 5) show the depths of MSW in Cell A. In both Cells A and C, the average depth of the MSW was about 18 feet, with some areas of Cell C with depths closer to 12 feet. There were also indications that in portions of Cell A that there is potential that a deeper section of MSW is present to depths of nearly 30 feet that is capped with fill and then more MSW.

Approximate volume of MSW was estimated for the portion of Cell C investigated and for Cell A. For both cells, an average depth of MSW of 18 feet was used, it is noted that there is the potential for a deeper MSW section in Cell A that may be partly accounted for in these volume estimates. It is estimated that approximately 360,000 cubic yards of MSW is present in the portions of Cell A investigated and that approximately 180,000 cubic yards of MSW is present in the portion of Cell C investigated.

5.2 Depth of Basalt Unit

Interpreted thickness of the Basalt Unit are shown next to seismic lines on Figure 1 for Sequences D and E. The elevations of the top of the Basalt Unit interpreted from this geophysical investigation compared well with earlier investigations by Woodward-Clyde (WCC 1997) and Speedie & Associates (SAI 2012). The depth contours to the top of the Basalt Unit published in the Woodward-Clyde (WCC 1997) report is extremely useful.

5.2.1 Sequence E

In Sequence E, the elevation of the top of the Basalt Unit is typically around 6590 to 6600 feet amsl. Geologic profiles A, B, and C (see Figures 2 and 3) illustrate this. The Basalt Unit extends to a depth of about 6400 feet amsl, suggesting that it has a maximum thickness of about 200 feet. As discussed in Section 3.2, the Cinder/Basalt Unit is also present underlying Sequence E and appears to be thickest underlying the eastern and northeastern portions of Sequence E. The bottom of the Basalt Unit and top of the Cinder/Basalt Unit in this area is interpreted to be at about elevation 6520 to 6540 feet amsl. Profile 3 indicates that Paleozoic units (likely the Kaibab Limestone) are reasonably interpreted to be encountered at an elevation of approximately 6390 feet amsl.

The approximate volume of the Basalt Unit present within Sequence E between the surface and elevation 6500 feet amsl was estimated based on the thickness of the unit indicated from the geophysical interpretations and top of the Basalt Unit from previous borings. It is estimated that approximately 6.5 million cubic yards of the Basaltic Unit are present within the surface footprint of Sequence E between the surface and elevation 6500 feet amsl. The full potential volume of the Basalt Unit is not planned to be excavated according to the projected excavation plan for Sequence E prepared by the City (Flagstaff 2015). It is estimated that approximately 4.0 million cubic yards of the Basalt Unit are present within the limits of the project excavation plan. It must be understood that the Basalt Unit volume consists of in-place material that includes probable fissures or large fracture volumes, and weak basalts as will be discussed in Section 4.5. It is anticipated that the basalt rock material usable as potential aggregate material will bulk (swell) as part of the excavation process; that anticipated swell may roughly compensate for the portion of the Basalt Unit that would be unusable as aggregate material. Approximately 0.6 million cubic yards of Cinder/Basalt Unit is estimated to be present within the limits of the project excavation plan. Approximately 5.7 million cubic yards of Cinder Unit is estimated to overlie the Basalt Unit within the limits of the project excavation plan.

5.2.2 Sequence D

In Sequence D, the elevation of the top of the Basalt Unit is typically around 6570 to 6600 feet amsl. Geologic profile D (see Figures 2 and 3) illustrate this. The Basalt Unit extends to a depth of about 6400 feet amsl, suggesting that it has a maximum thickness of about 200 feet.

The approximate volume of the Basalt Unit present within Sequence D between the surface and elevation 6500 feet amsl was estimated based on the thickness of the unit indicated from the geophysical interpretations. It is estimated that approximately 4 million cubic yards of the Basaltic Unit are present within Sequence D between the surface and elevation 6500 feet amsl. The full potential volume of the Basalt Unit is not planned to be excavated according to the projected excavation plan for Sequence D prepared by the City (Flagstaff 2015). It is estimated that approximately 2.1 million cubic yards of the Basalt Unit are present within the limits of the project excavation plan.

5.3 Basalt Excavation Assessment

5.3.1 Kirsten Excavation Classification System

The Kirsten (1982; 1988) excavation system uses a Class Rating to categorize ground into eight classes of excavatability based on excavation power as shown in Table 1. It has been adapted for analysis of erodability as documented in the ‘Field Procedures Guide for the Headcut Erodability Index’ (NRCS, 2001); that document, with instructions for developing class rating N is available on the internet. Excavation class ratings are numeric and based on powers of 10 of the product or quotient of various ground mass parameters. The wide range of ground strength addressed and variety of usable parameters makes the Kirsten method especially useful for geomaterials with a wide range of strengths.

The overall calculation for Class Rating is as follows:

Class Rating = M_s * (RQD / J_n) * J_s * (J_r / J_a)

Where:

M_s	= mass strength	J_s	= relative ground structure number
RQD / J_n	= block size	J_r / J_a	= joint strength number

Each of these parameters will be discussed relative to basalt geo-material masses. The mass strength or consistency parameter M_s is based on uniaxial UCS, either estimated or measured, and is characterized in Table 2. Most of the UCS tests performed in 2012 (SAI 2012) range from about 10,000 to 25,000 psi, and result in an M_s range of about 70 to 175.

Table 1 – Kirsten Excavatability Classes as Reported by Kirsten (1982; 1988); Check Current Trackhoe and Bulldozer Models for Power.

Class	Excavation Class Rating N	Excavatability Description	Trackhoe/ Dozer Type	Trackhoe/ Dozer Power	Approx Seismic Velocity ft/sec *Basalt Becomes Unrippable*	
1	< 0.01	Hand spade				
2	0.01 – 0.099	Hand pick and spade	Cat 215	63 kW 85 hp	**P-wave**	**S-wave**
3	0.1 – 0.99	Power tools	Cat 225, D6D	101 kW 136 hp	~3,000	~1,500
4	1.0 – 9.99	Easy ripping	Cat 235, D7G	145 kW 195 hp	~5,200*	~2,600
5	10 – 99	Hard ripping	Cat 245, D8K	242 kW 325 hp	~8,600*	~4,300
6	100 – 999	Very hard ripping	Cat D9H	306 kW 411 hp	~8,900*	~4,500
7	1000 – 9999	Extreme rip/blasting	Cat D10	522 kW 701 hp	~9,200*	~4,600
8	10000 +	Blasting				

Note:
*indicates data from Caterpillar (CAT 1984, 1993).

Table 2 – Mass strength or consistency parameter M_s.

UCS testing indicated that most of the cored basalt samples qualified as 'extremely hard rock'.

Material Type	Consistency	Average UCS psi	Average UCS MPa	Average Mass Strength M_s
Granular / cohesive soil	Very loose / very soft	5	0.035	0.02
	Loose / soft	10	0.069	0.04
	Med dense / firm	20	0.14	0.09

Material Type	Consistency	Average UCS psi	Average UCS MPa	Average Mass Strength M_s
	Dense / stiff	41	0.28	0.19
	Very dense / very stiff	80	0.55	0.41
Rock	Very soft rock	160	1.1	0.87
		319	2.2	1.9
	Soft rock	638	4.4	4.0
		1276	8.8	8.4
	Hard rock	2552	17.7	17.7
	Very hard rock	5104	35.4	35
	Extremely hard rock	20400	141.3	140

Block size is determined as the RQD divided by the joint set number J_n. Assuming primarily three orthogonal joint sets characteristic of shrinkage cracking, J_n is 2.73. The maximum for J_n is 5 for multiple joint sets. For basalt cores obtained in 2012 (SAI 2012) with RQD typically greater than 50 and commonly 100, block size ranges from about 10 to 37 (RQD/J_n = 50/5 to 100/2.73) in the sampled basalt rock mass.

The relative ground structure number J_s is taken to be 1.0 since joint sets are assumed to be roughly oriented vertical and horizontal, or randomly oriented in an undefined geometry.

Joint strength number is the joint roughness number divided by the joint alteration number. Joint roughness number J_r is 1.5 for rough or irregular planar joints that are tight or closing during excavation, and 1.0 for joints being sufficiently thick to prevent joint wall contact during excavation. Joint alteration number J_a ranges from 1.0 for unaltered joint walls in effective contact to 6.0 with joint wall separation greater than 5 millimeters. For the basalt cores obtained in 2012, joint strength number ranges from 1.5 (J_r/J_a or 1.5/1) to 0.17 (J_r/J_a or 1/6).

J_n was assumed to reflect shrinkage cracking of the basalt, essentially 3 orthogonal joint sets as it cooled into relatively cubic shaped particles. With a maximum J_n of 5 (random cracking with joint sets), the difference in the overall excavatability number is minimal. The range of the J_n assumption being 2.73 or 5 is captured in the calculation range of the Excavation Class Rating of 119 to 9,720.

Given this range of parameters, the overall Excavation Class Rating for the basalts sampled in Sequence D (SAI 2012) is estimated to range from a low of about 119 to a high of about 9,720. This range covers the low end of very hard ripping to the high end of extreme ripping or blasting (Kirsten Class 6 to 7).

5.3.2 Seismic Velocities

The approximate maximum p-wave seismic velocities (high end of the marginal rippability range) for which ripping can be effectively accomplished by various heavy bulldozers as summarized from the Caterpillar Performance Handbook (CAT 1984, 1993) are also summarized in Table 1. Estimated equivalent s-wave velocities (assumed to be half the p-wave velocities consistent with a Poissons Ratio of 0.33) are included in Table 1; the ReMi results provided generalized characterization of the basalt rock mass to much greater depth than the

seismic refraction results. Based on the seismic velocities interpreted in this and in previous investigations (WCC 1997), it would be anticipated that the basalt rock mass can be classified as easy ripping to hard ripping (Kirsten Class 4 to 5).

5.4 Comparison of Seismic (Horizontal) and Coring (Vertical) Investigations

The various outcrops in the landfill area are mapped on USGS Maps I-953 and MF-1960 (Moore and Wolfe 1976, 1987) as basalt flows and cinder cones (Vent V511 is located immediately south of Sequence E) or basaltic pyroclastic deposits. Basalt outcrops are further described in USGS Open File Report 2012-1018 (Macy et al 2012) as possible push-up features. Seismic Lines S-19 and S-20 were completed in Sequence D at and near one of these basalt outcrops, and in the same area as the Speedie & Associates (SAI 2012) drilling and coring investigation. In the Basalt Unit sampled by coring, s-wave velocities of 1,900 to 2,100 f/s (feet per second) were interpreted from the ReMi results. This range of velocities would indicate easy ripping (Kirsten Class 4) of the Basalt Unit rock mass. However, the logging and laboratory testing of the basalt cores indicate that the Basalt Unit is very hard ripping to extreme ripping to blasting (Kirsten Class 6 to 7).

The difference in rippability assessment is attributed to the orientation of the coring and seismic investigation methods. Drilling and coring operations advance vertically into the rock mass and produce a vertical sample. Relatively large vertical fractures or fissures can be present in the rock mass, and unless directly drilled into, would not be detected or sampled by drilling. Of 14 borings drilled in Sequence D (SAI 2012) and summarized in Table 3, only one boring (B-901) appears to have been drilled into a large vertical fracture or fissure. Two other borings (B-908 and B-910) were auger drilled anomalously deep, indicating possible fissures or fractures, before encountering hollow stem auger refusal and coring began. These three borings indicated that large fissures or fractures could occur along perhaps 10 to 20 percent of the lateral (horizontal) extent of the rock mass. Due to the relatively small area that such fractures or fissures would occupy within the top surface of the basalt rock mass, a relatively small proportion of vertical oriented borings would encounter such fractures or fissures.

Seismic energy from seismic refraction and surface wave methods propagates primarily in sub-horizontal (refractive angles) to horizontal directions. Thus, surface seismic energy encounters and propagates through the large low velocity soil-like materials bridging fissures and fractures in the rock mass, or, if the fissures or fractures are open voids, around them. Thus, seismic energy will tend to be strongly influenced (seismic velocities reduced and seismic signals attenuated) by vertically oriented fissures and fractures in the rock mass even if they are not effectively sampled by drilling methods.

Table 3 - Summary of Drilling Results in Basalt in Sequence D (SAI 2012)

Boring No.	Depth to Top of Basalt (feet)	Depth to Auger Refusal (feet)	Thickness of Augered Basalt (feet)	Total Boring Depth (feet)	Thickness of Cored Basalt (feet)	Percentage of Cored Basalt (%)	Percent of Visibly Non-Vesicular Basalt (%)
900	7.5	10.0	2.5	40.5	30.5	92.4	44

Boring No.	Depth to Top of Basalt (feet)	Depth to Auger Refusal (feet)	Thickness of Augered Basalt (feet)	Total Boring Depth (feet)	Thickness of Cored Basalt (feet)	Percentage of Cored Basalt (%)	Percent of Visibly Non-Vesicular Basalt (%)
901*	41.0	43.2	2.2	51.8	8.6	79.6	0
902	20.0	24.5	4.5	53.6	29.1	86.6	0
903	9.0	14.7	5.7	51.4	36.7	86.6	5
904	27.5	31.2	3.7	53.3	22.1	85.7	0
905	24.5	27.6	3.1	61.3	33.7	91.6	68
906	19.0	26.5	7.5	50.1	23.6	75.9	0
907	6.0	16.3	10.3	54.9	38.6	78.9	4.5
908*	40.0	41.5	1.5	53.9	12.4	89.2	33
909	28.0	31.3	3.3	58.3	27.0	89.1	69
910*	36.6	39.3	2.7	54.2	14.9	84.7	0
911	28.0	29.8	1.8	52.3	22.5	92.6	0
912	31.8	31.8	0.0	53.4	21.6	100.0	9
913	31.5	34.7	3.2	55.4	20.7	86.6	34
914	18.5	19.5	1.0	46.4	26.9	96.4	0
*boring may have encountered large vertical fracture/fissure					average % =	87.7	17.8

5.5 Basalt Unit Characterization - Low Seismic Velocities and High Strength Samples

To combine the aspects of vertical and horizontal characterization, a simple seismic model consisting of high and low velocity inter-layers was assembled using the ReMi seismic interpretation software. The low velocity layers represented cinder-type s-wave velocities of 500 to 700 f/s. For a 100-foot length of seismic model, ten layers, each layer representing a cinder-filled vertical fissure of 1 to 2 feet in width, comprised 10 to 20 percent of the model. The high velocity layers represented high strength basalt. Each high velocity layer was 8 to 9 feet in width and had low velocity layers representing vertical fissures on each side. Normal fracturing (represented by high RQD) reduced the seismic velocities in these basalts from the very high velocities (perhaps 8,000 to 10,000 f/s s-wave velocities) of intact, unfractured material. S-wave velocities of 4,000 f/s representing basalt flows at depths less than about 100 feet, and 6,000 f/s representing basalt flows at depths greater than about 100 feet, consisted of 70 to 80 percent of the model. Finally, the first high velocity layer was replaced with a layer of weak, augerable basalts having s-wave velocities of 2,000 f/s to represent the hollow-stem augered portion of the basalt flows. This weak basalt layer represented 10 percent of the basalt rock mass in the model. Results of this modeling are shown in Table 4.

Table 4 – Estimated Seismic S-wave Velocities for Basalt Unit with 10% to 20% of Rock Mass Volume as Cinder-filled Fissures / Fractures and 10% of Rock Mass Volume as Weak Basalt

% Cinders > % Weak Basalt >	10% @ 500 f/s 10% @ 2,000 f/s	20% @ 500 f/s 10% @ 2,000 f/s	10% @ 700 f/s 10% @ 2,000 f/s	20% @ 700 f/s 10% @ 2,000 f/s
Basalt @ 4,000 f/s	2,200 f/s	1,600 f/s	2,500 f/s	1,900 f/s
Basalt @ 6,000 f/s	2,600 f/s	1,700 f/s	3,100 f/s	2,200 f/s

Estimated s-wave velocities shown in Table 4 are consistent with interpreted s-wave velocities in the Basalt Unit across the site.

6.0 RECOMMENDATIONS

It must be understood that the interpreted presence of extensive fissures or large fractures within the Basalt Unit rock mass indicate that blasting for mass excavation may be a difficult and complex operation. Blast energy could be anticipated to seek and be dissipated within such open fissures or fractures, and thus reduce the effectiveness of blasting. It is recommended that consultation with a qualified blasting consultant be included for consideration of these potential issues.

Due to the apparent lateral variations within the Basalt unit rock mass, it is anticipated that sorting suitable aggregate materials from lesser quality rock (otherwise potentially suitable for riprap, rockfill, landscaping, etc) may be a complex operation. One preliminary indication of rock suitability for crushed aggregate may be the absence of visible vesicles within the rock particles. As shown in Table 3, a relatively small percentage of the rock, perhaps on the order of 20 percent or less based on photographs of recovered core in Sequence D, might be free from visible vesicles.

6.1 Boring Locations

Recommendations for boring locations to further investigate the rock quality and depths of the Basalt Unit within Sequences C, D and E are shown on Figure 1. These locations are modified from the City's projected excavation plan (Flagstaff 2015). No modifications are suggested for planned borings in Sequence A, which will likely not encounter the Basalt Unit. Boring locations were selected to reduce uncertainty of important factors such as the depth of MSW and the thickness and rock quality of the Basalt Unit and the presence or absence of the Cinder/Basalt Unit.

For Sequence E the number of recommended borings (eleven) is lower than the 24 proposed in the City's plan (Flagstaff 2015). We recommend a lesser number of borings because the elevation of the top of the Basalt Unit is typically around 6600 feet amsl, and therefore it appears more beneficial to only drill borings in areas where the projected excavation is to elevations notably lower than 6600 feet amsl where the intended purpose of the boring is for characterization of the Basalt Unit in regard to volume and rock quality assessment. Two borings in the western portion of Sequence E were retained to verify anticipated conditions.

For Sequence D the number of recommended borings (seven) is similar in number and placement to those proposed in the City's plan (Flagstaff 2015). We recommend minor adjustments to the location of one of the borings, an additional boring at the west end of the proposed excavation underlying Sequence C, and an additional boring at the east end of Sequence C.

In addition to the recommended boring locations discussed above, it may be worth considering performing a small-scale excavation (drilling and/or blasting) to further evaluate excavability conditions and the suitability of the Basalt Unit as an aggregate source.

7.0 REFERENCES

Bills, D.J., Truini, M., Flynn, M.E., Pierce, H.A., Catchings, R.D., and Rymer, M.J., 2000, *Hydrogeology of the regional aquifer near Flagstaff, Arizona, 1994–97*: United States Geological Survey Water-Resources Investigations Report 00-4122.

Caterpillar Tractor Company, (Cat), 1984, Caterpillar Performance Handbook, Edition 15, Peoria, Illinois, October.

Cat, 1993, Caterpillar Performance Handbook, Edition 24, Peoria, Illinois, October.

City of Flagstaff, SDB, Inc. (Flagstaff-SDB), 2014. *Cinder Lake Landfill Feasibility Study – Landfill Mining and Excavation Plan – Cells A, C, & D*. City of Flagstaff File Number 20-431-00, Project Number SW-0631, September 14.

HydroSystems, Inc. (HydroSystems), 2011. *Geophysical Survey and Drilling Program*, City of Flagstaff, Cinder Lake Landfill. Prepared for the City of Flagstaff, Prepared in association with SDB Contracting Services, June.

Kirsten, H.A.D., 1982, A Classification System for Excavation in Natural Materials, Civil Engineer in South Africa, Vol. 24, No. 7, July, pp. 293-308.

Kirsten, H.A.D., 1988, Case Histories of Groundmass Characterization for Excavatability, Rock Classification Systems for Engineering Purposes, ASTM STP 984, Louis Kirkaldie, Ed., American Society for Testing and Materials, Philadelphia, Pennsylvania, pp. 102-120.

Macy, J.P., Amoroso, L., Kennedy, J., and J. Unema, 2012. *Depth of Cinder Deposits and Water-Storage Capacity at Cinder Lake*, Coconino County, Arizona. United States Geological Survey Open-File Report 2012-1018.

Moore, R. B. and Wolfe, E. F., 1976. *Geologic Map of the Eastern San Francisco Volcanic Field*, Arizona, United States Geologic Survey Map I-953.

Moore, R. B. and Wolfe, E. F., 1987. *Geologic Map of the East Part of the San Francisco Volcanic Field*, North-Central Arizona, United States Geological Survey Miscellaneous Field Studies Map MF-1960.

National Resources Conservation Service (NRCS), 2001, Field procedures guide for the headcut erodability index, Chapter 52, Part 628, National Engineering Handbook: U.S. Department of Agriculture Natural Resources Conservation Service, 210-VI-NEH, rev. 1, March.

Speedie & Associates, Inc. (SAI), 2012. *Report of Subgrade Investigation*, Cinder Lake Landfill South Borrow Pit. Prepared for the City of Flagstaff, Speedie Project Number 121372SF, December 31.

Woodward-Clyde Consultants (WCC), 1997. *Geotechnical Investigation Cinder Lake Landfill Expansion*. Prepared for the City of Flagstaff Department of Public Works. Woodward-Clyde Project Number 96A199-0400. February 4.

FIGURES

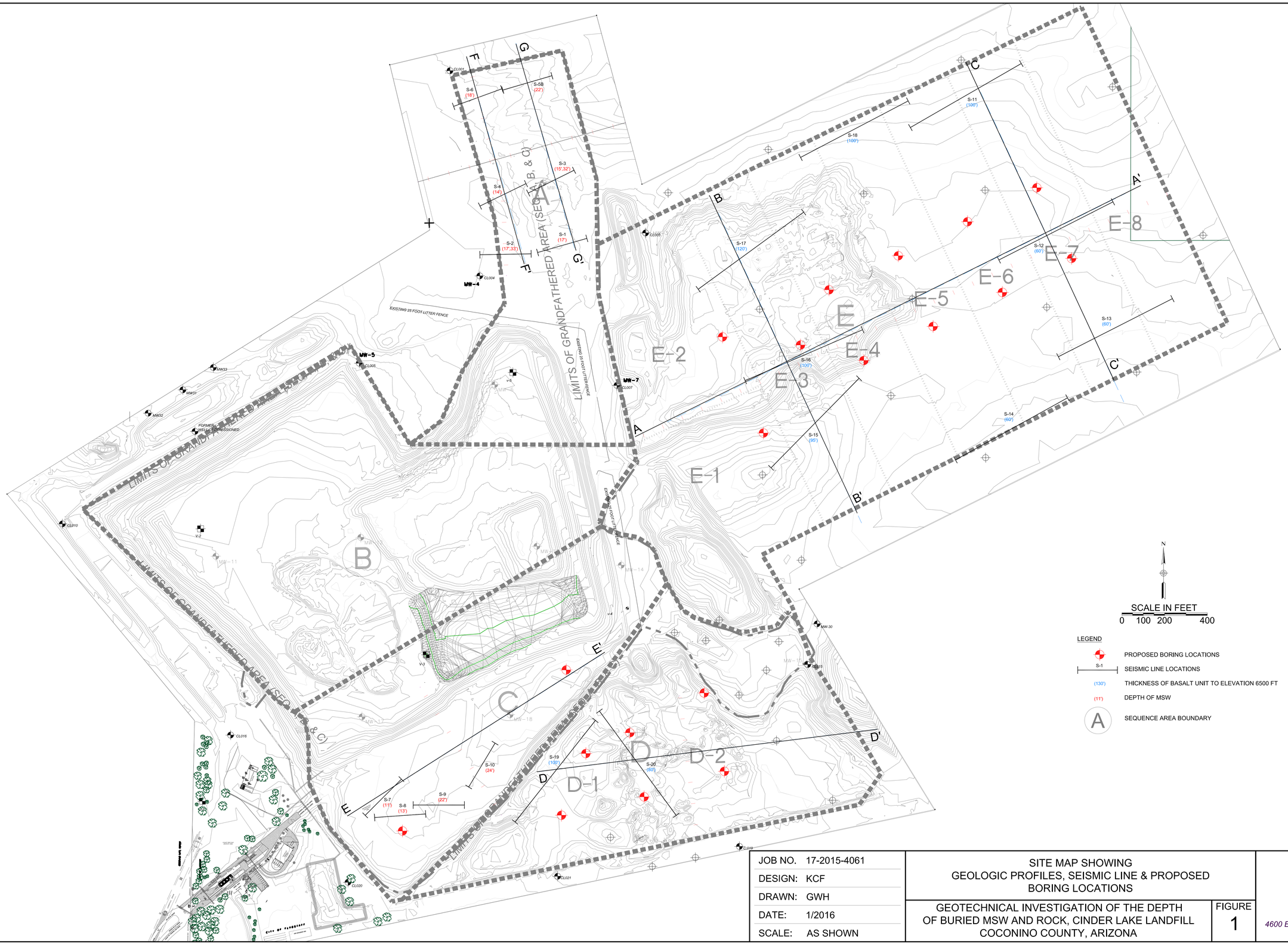

JOB NO.	17-2015-4061
DESIGN:	KCF
DRAWN:	GWH
DATE:	1/2016
SCALE:	AS SHOWN

SITE MAP SHOWING
GEOLOGIC PROFILES, SEISMIC LINE & PROPOSED
BORING LOCATIONS

GEOTECHNICAL INVESTIGATION OF THE DEPTH
OF BURIED MSW AND ROCK, CINDER LAKE LANDFILL
COCONINO COUNTY, ARIZONA

FIGURE
1

amec foster wheeler
4600 East Washington Street, Suite 600
Phoenix, Arizona

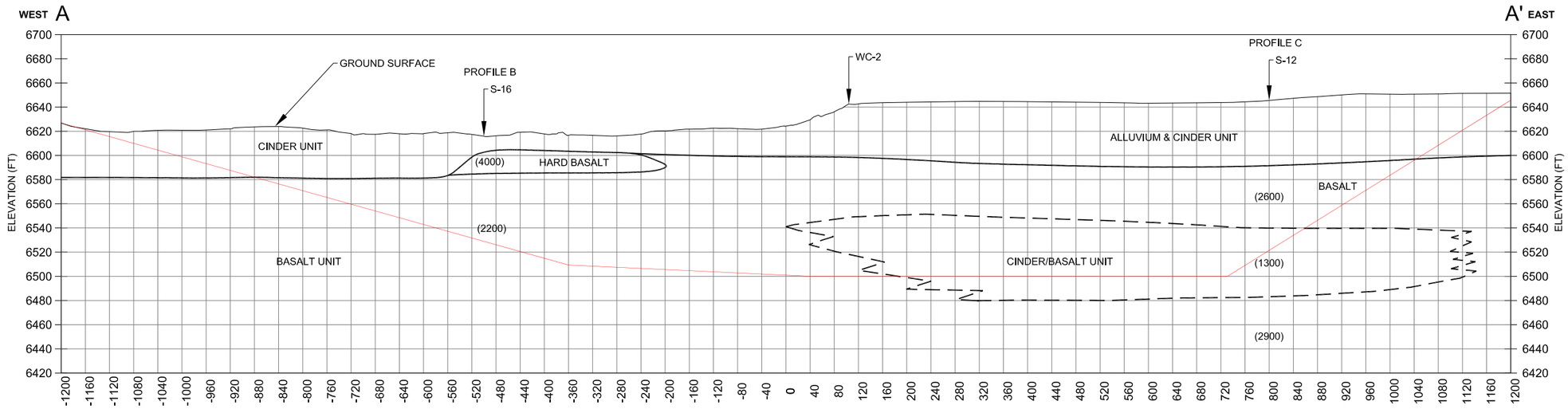

SCALE: HORIZONTAL: 1" = 200', VERTICAL: 1" = 100'

(4000) - S-WAVE VELOCITIES

APPROXIMATE CONCEPTUAL EXCAVATION LIMITS (FLAGSTAFF - SDC 2014)

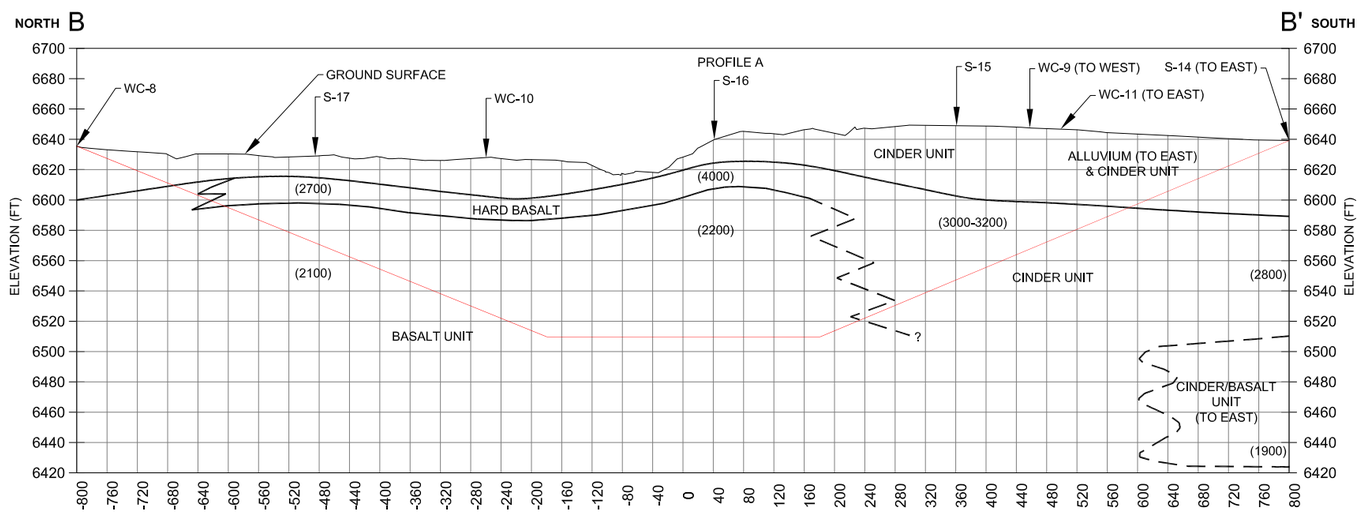

SCALE: HORIZONTAL: 1" = 200', VERTICAL: 1" = 100'

(4000) - S-WAVE VELOCITIES

APPROXIMATE CONCEPTUAL EXCAVATION LIMITS (FLAGSTAFF - SDC 2014)

KEY MAP (NTS)

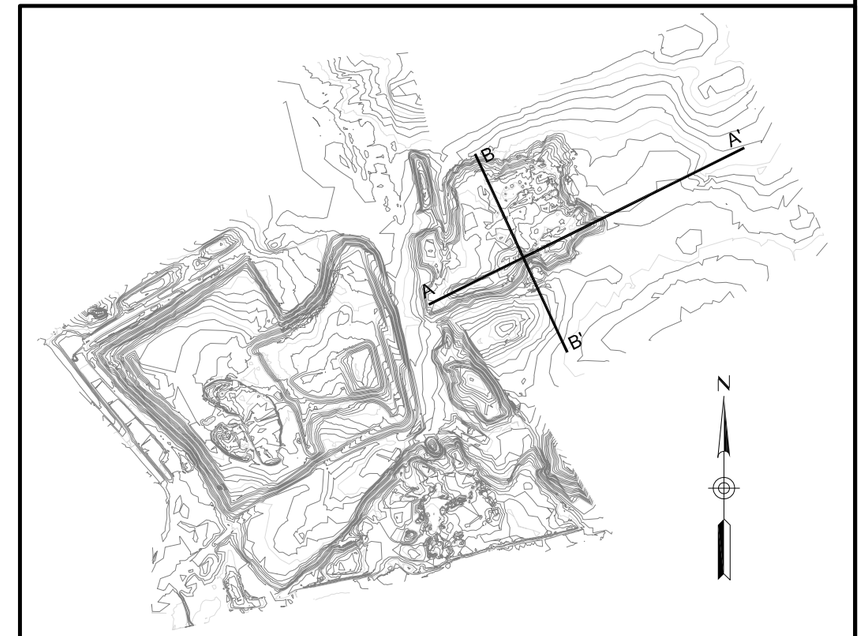

NO.	REVISION	MADE	CKD.	DATE
1				

JOB NO.	17-2015-4061
DESIGN:	KCF
DRAWN:	GWH
DATE:	1/2016
SCALE:	AS SHOWN

GEOLOGIC PROFILES IN SEQUENCE E (PROFILES A & B)

GEOTECHNICAL INVESTIGATION OF THE DEPTH OF BURIED MSW AND ROCK, CINDER LAKE LANDFILL COCONINO COUNTY, ARIZONA

FIGURE 2

amec foster wheeler

4600 East Washington Street, Suite 600
Phoenix, Arizona

G:\Geotechnical\2015 Projects\17-2015-4061 COF_Landfill Geophysical Survey\CAD\Base.dwg

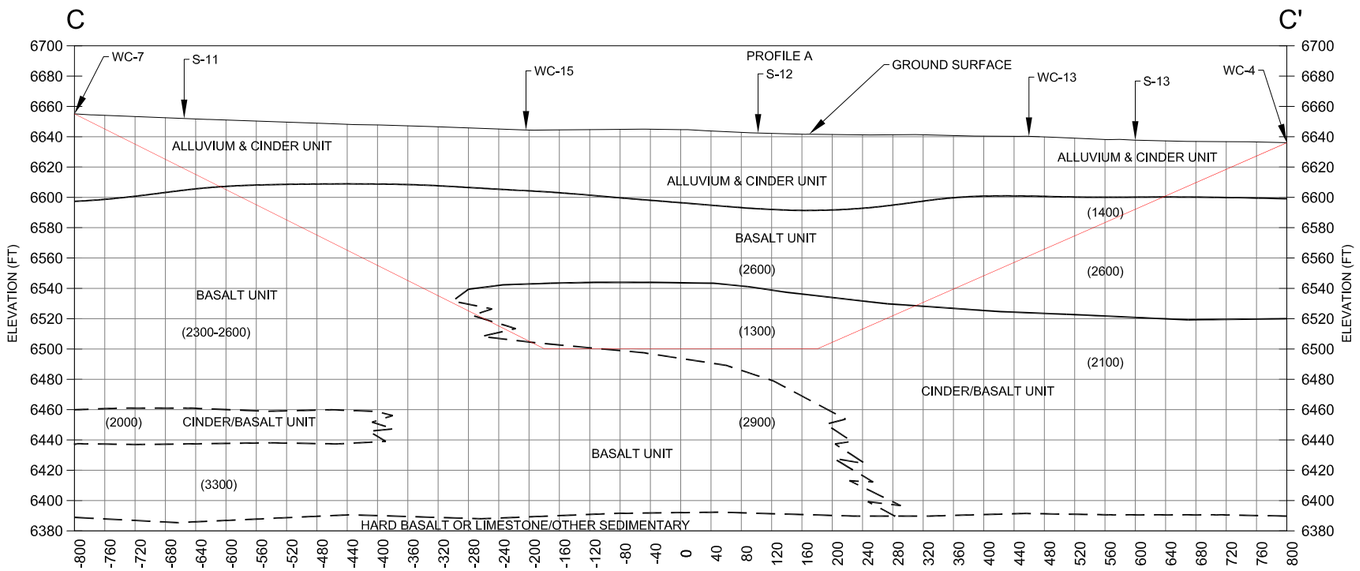

SCALE: HORIZONTAL: 1" = 200', VERTICAL: 1" = 100'

(2900) - S-WAVE VELOCITIES

APPROXIMATE CONCEPTUAL EXCAVATION LIMITS (FLAGSTAFF - SDC 2014)

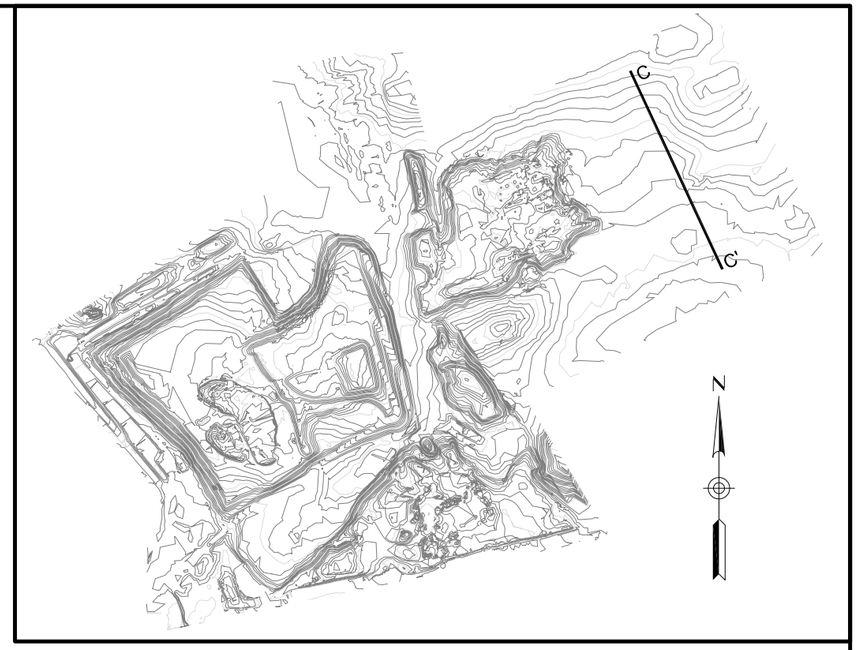

KEY MAP (NTS)

NO.	REVISION	MADE	CKD.	DATE
1				

JOB NO.	17-2015-4061
DESIGN:	KCF
DRAWN:	GWH
DATE:	1/2016
SCALE:	AS SHOWN

GEOLOGIC PROFILES IN SEQUENCE E (PROFILE C)

GEOTECHNICAL INVESTIGATION OF THE DEPTH OF BURIED MSW AND ROCK, CINDER LAKE LANDFILL COCONINO COUNTY, ARIZONA

FIGURE 3

amec foster wheeler
4600 East Washington Street, Suite 600
Phoenix, Arizona

G:\Geotechnical\2015 Projects\17-2015-4061 COF_Landfill Geophysical Survey\CAD\Base.dwg

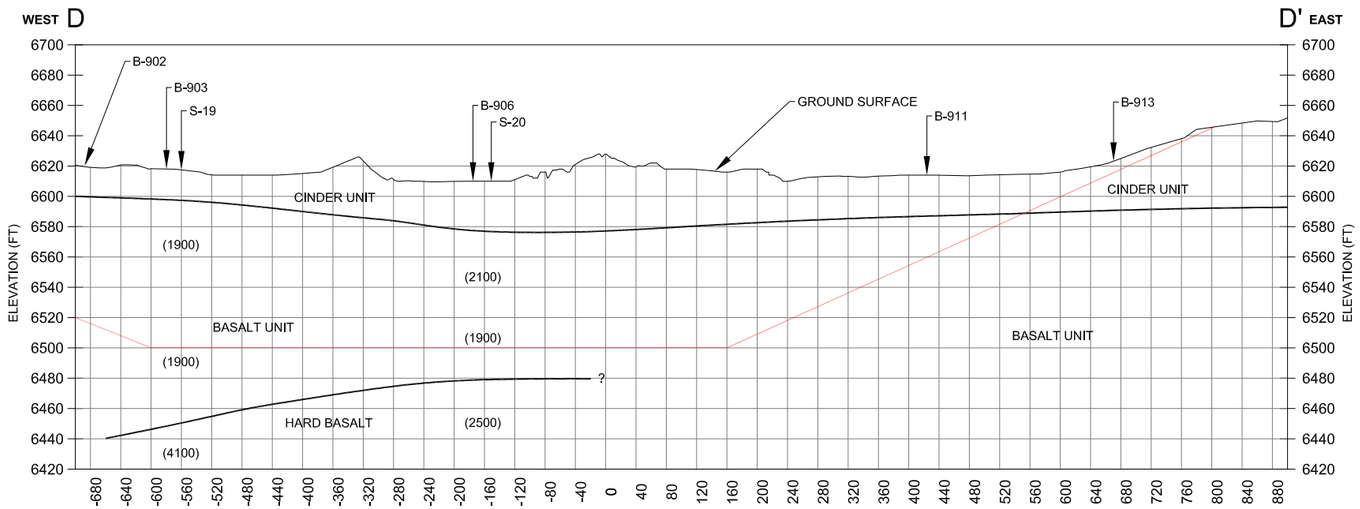

SCALE: HORIZONTAL: 1" = 200', VERTICAL: 1" = 100'

(2300) - S-WAVE VELOCITIES

APPROXIMATE CONCEPTUAL EXCAVATION LIMITS (FLAGSTAFF - SDC 2014)

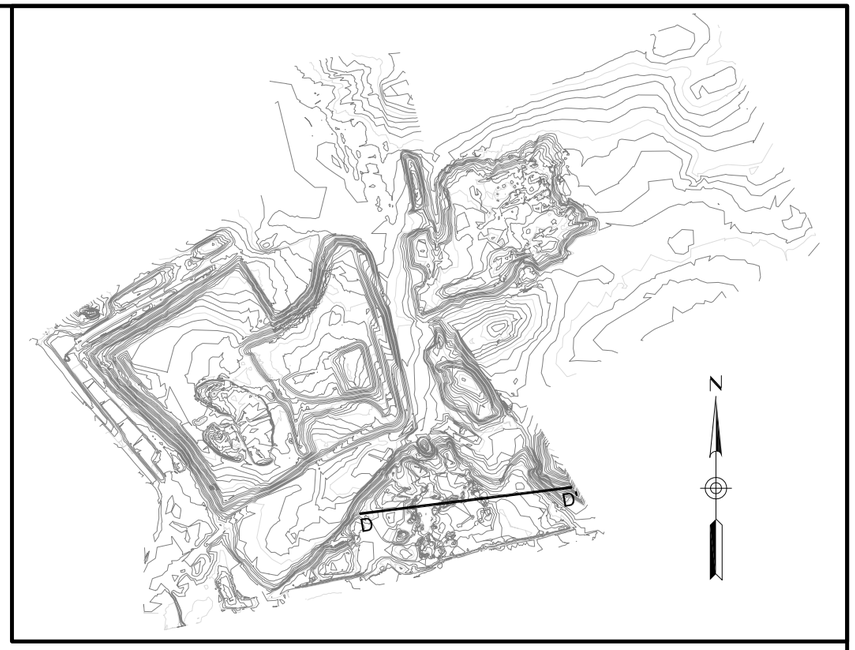

KEY MAP (NTS)

NO.	REVISION	MADE	CKD.	DATE
1				

JOB NO.	17-2015-4061
DESIGN:	KCF
DRAWN:	GWH
DATE:	1/2016
SCALE:	AS SHOWN

GEOLOGIC PROFILES IN SEQUENCE D (PROFILE D)

GEOTECHNICAL INVESTIGATION OF THE DEPTH OF BURIED MSW AND ROCK, CINDER LAKE LANDFILL COCONINO COUNTY, ARIZONA

FIGURE 4

amec foster wheeler
4600 East Washington Street, Suite 600
Phoenix, Arizona

G:\Geotechnical\2015 Projects\17-2015-4061 COF_Landfill Geophysical Survey\CAD\Base.dwg

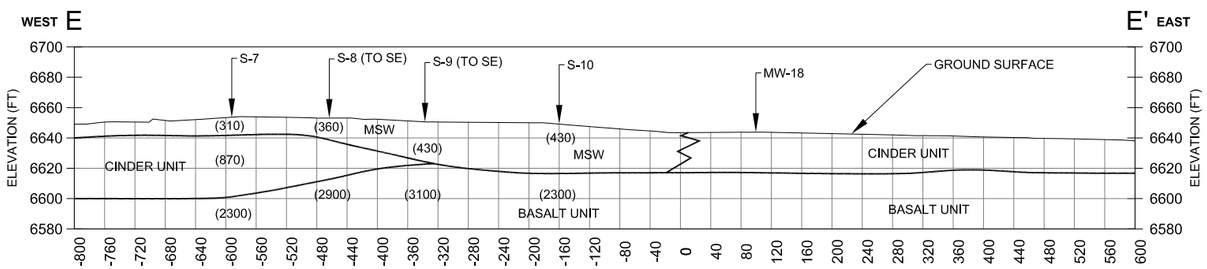

SCALE: HORIZONTAL: 1" = 200', VERTICAL: 1" = 100'

(2300) - S-WAVE VELOCITIES

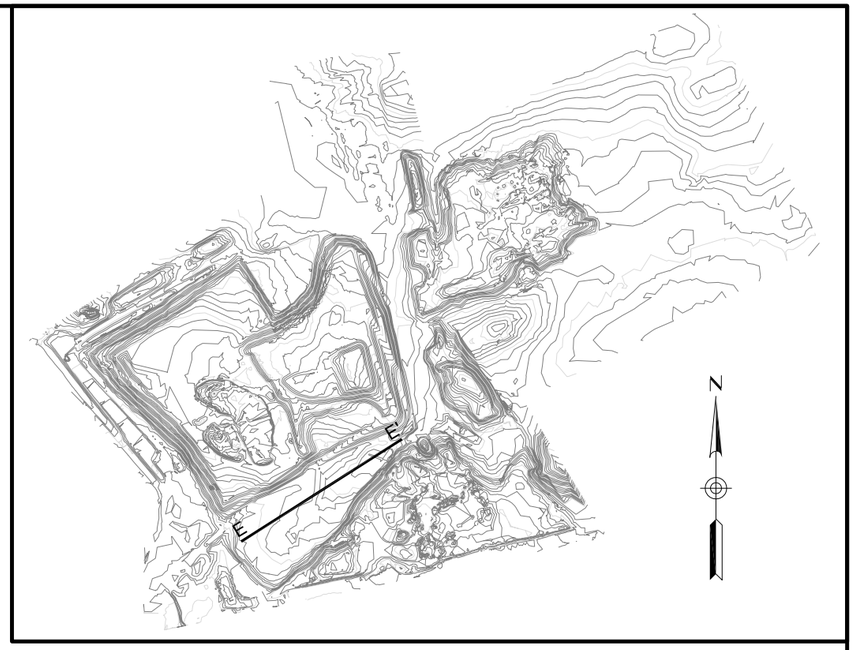

KEY MAP (NTS)

NO.	REVISION	MADE	CKD.	DATE
1				

JOB NO.	17-2015-4061
DESIGN:	KCF
DRAWN:	GWH
DATE:	1/2016
SCALE:	AS SHOWN

GEOLOGIC PROFILES IN SEQUENCE C (PROFILE E)

GEOTECHNICAL INVESTIGATION OF THE DEPTH
OF BURIED MSW AND ROCK, CINDER LAKE LANDFILL
COCONINO COUNTY, ARIZONA

FIGURE
5

amec foster wheeler
4600 East Washington Street, Suite 600
Phoenix, Arizona

G:\Geotechnical\2015 Projects\17-2015-4061 COF_Landfill Geophysical Survey\CAD\Base.dwg

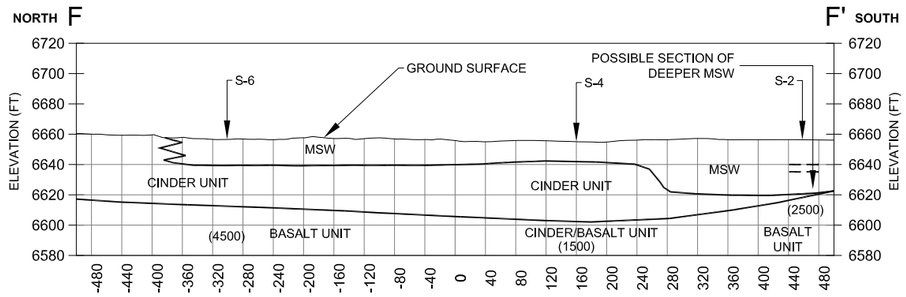

SCALE: HORIZONTAL: 1" = 200', VERTICAL: 1" = 100'

(4500) - S-WAVE VELOCITIES

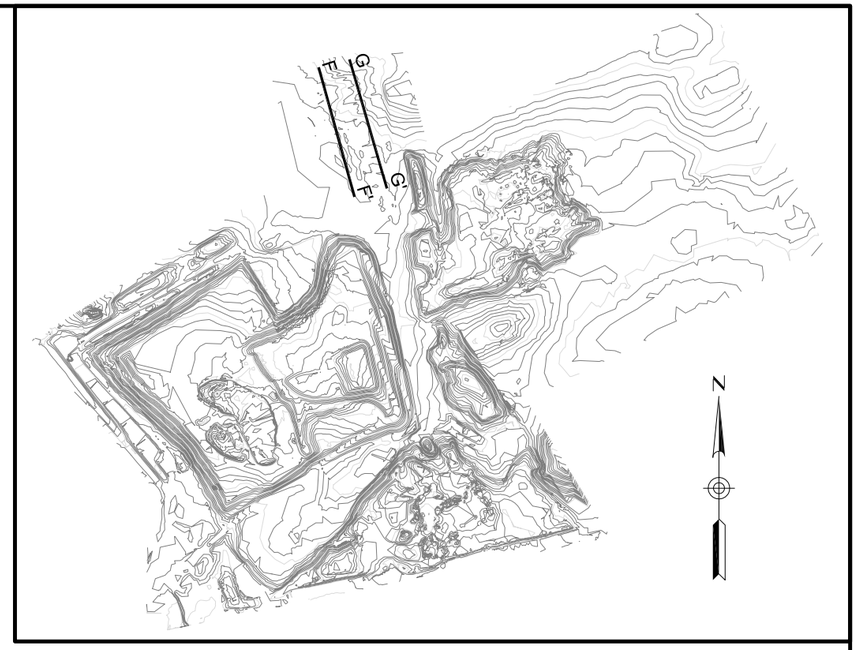

KEY MAP (NTS)

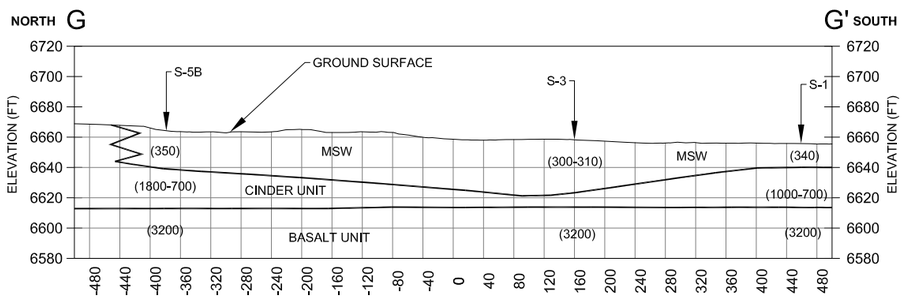

SCALE: HORIZONTAL: 1" = 200', VERTICAL: 1" = 100'

(350) - S-WAVE VELOCITIES

NO.	REVISION	MADE	CKD.	DATE
1				

JOB NO.	17-2015-4061
DESIGN:	KCF
DRAWN:	GWH
DATE:	1/2016
SCALE:	AS SHOWN

GEOLOGIC PROFILES IN SEQUENCE A (PROFILES F & G)

GEOTECHNICAL INVESTIGATION OF THE DEPTH OF BURIED MSW AND ROCK, CINDER LAKE LANDFILL COCONINO COUNTY, ARIZONA

FIGURE 6

amec foster wheeler
4600 East Washington Street, Suite 600
Phoenix, Arizona

G:\Geotechnical\2015 Projects\17-2015-4061 COF_Landfill Geophysical Survey\CAD\Base.dwg

APPENDIX A

SEISMIC REFRACTION AND REFRACTION MICROTREMOR

REFRACTION SEISMIC EQUIPMENT AND PROCEDURES

Refraction seismic surveys are performed in general conformance with the guidelines presented in ASTM D5777-95 Standard Guide for Using the Seismic Refraction Method for Subsurface Investigation for refraction surveys using compression waves (p-waves). ASTM D5777 does not address shear wave (s-wave) surveys; standard practice is followed for refraction surveys using s-waves. In some investigations, such as seeking and tracing earth fissures or other significant discontinuities (Rucker and Keaton, 1998), non-standard procedures and analyses, such as signal amplitude analysis, are used as part of the investigation process.

Seismic Equipment - Refraction seismic surveys are performed using a Geometrics Smartseis SE-12 or SE-24 signal enhancement seismograph. These instruments have the capability to simultaneously record 12 or 24 channels of geophone data and produce hard copies of that data. The Smartseis also has the capability of digitally storing geophone data. Signal enhancement capability permits the use of a sledgehammer as the seismic energy source. A timing sensor is attached to the hammer, and for p-waves, a metal plate is set securely on the ground surface and struck. Generating horizontally polarized s-waves typically involves setting the plate against the end of a wooden plank or railroad tie oriented perpendicular to the axis of the geophone array and striking with a horizontal motion of the sledgehammer. A truck is usually driven onto the plank or tie to effectively couple the plank or tie to the ground.

Because of the signal enhancement capability, signals from several or many strikes can be added together to increase the total signal available relative to noise to obtain the seismic record. Although explosives can also be used as a p-wave seismic energy source, a sledgehammer does not require licenses or permits, or involve special limitations, regulations and liabilities. Explosive energy sources may be needed for long geophone arrays. Geophone cables with 12 geophone takeouts at 10-foot, 25-foot or 20-meter spacings are presently used. Vertical geophones are used to obtain p-wave data and horizontal geophones are used to obtain s-wave data. The seismograph system is extremely portable. In areas where vehicular access is not possible, the equipment can be mobilized by various means, including backpacking, packhorse, helicopter and canoe.

Field Procedures - The field operations are directed by our experienced engineer or geologist, who operates the equipment, prepares the records and examines the data in the field. Refraction seismic lines are generally laid out using the standard spacings on the geophone cables. A maximum depth of investigation of about 75 to 100 feet may be possible using a 300-foot array. For shorter lines with improved near-surface resolution, 10-foot spacings between geophones with a 120-foot array have a maximum depth of investigation of about 30 to 40 feet, and with a 240-foot array have a maximum depth of investigation of about 60 to 80 feet. Other geophone spacings can also be used. To improve the resolution of near-surface interfaces, energy source positions generally are set at 12.5 feet from the ends of a 25-foot spacing geophone array or at 5 feet from the ends of a 10-foot geophone spacing array. Several shots locations are utilized along the length of an array. When three shots are obtained, there is a foreshot and a backshot at the array ends and a midshot at the array center. The midshot is usually placed midway between the two centermost geophones. When five shots are obtained, the additional shotpoints are located midway between the foreshot-midshot and the midshot-backshot. For 240-foot 24-channel arrays, shotpoints are arrayed at 30-foot intervals along the array. These multiple shot points permit interpretation of near-surface interfaces at various locations along the array as well as near the endpoints for variable subsurface profiles, and permits more refined overall interpretations of shallow and mid-depth subsurface velocities and interfaces. In cases when both enhanced depth of investigation and improved shallow resolution are needed, multiple geophone arrays are completed end to end and combined into longer composite geophone arrays with greater depths of investigation. Additional energy shotpoints are then, at a minimum, performed at the midpoint and far endpoint of each adjacent geophone array to provide seismic energy travel path coverage over the extended array.

Surface wave data is also typically collected for each seismic line setup and interpreted for vertical shear wave profiles using the Refraction Microtremor method. This procedure is described separately. To facilitate the collection of low frequency surface wave data, 4.5 Hz geophones are typically used for surface seismic work.

REFRACTION SEISMIC EQUIPMENT AND PROCEDURES (Cont.)

P-wave data are recorded for general exploration work. S-wave data are also recorded when dynamic subsurface material properties are desired. An s-wave arrival is verified by obtained two sets of horizontal data that are 180 degrees out of phase. The phase reversal is obtained by either reversing the horizontal geophone orientation or reversing the hammer impact direction. Hard copy printouts of all field data are made and inspected as the information is collected. Field notes, including line number and orientation, topographic variations and other notes as appropriate are made on the hard copy printout. Locations and other notes are made on site maps and in notebooks as appropriate. Initial first arrival picks are made in the field and array endpoint arrival times are checked for immediate data adequacy verification as part of the quality control process.

Interpretation - Although preliminary or quality control initial refraction seismic data interpretations may sometimes be performed in the field, full interpretations are completed in the office. At the present time, two interpretation methods are being used; the intercept time method (ITM) and an optimization software routine based on finite difference optimization software. ITM breaks an interpretation into several distinct layers. It is simple, can be performed with a calculator, and can provide excellent interpretations of near surface layer depths and velocities. Optimization provides a continuously variable velocity interpretation through a discrete grid. Interpretations using optimization also indicate zones where interpretation has occurred, thus providing quality control on the depths to which the interpretation can be relied upon. However, the discrete grid used by optimization results in a low resolution near surface interpretation. The combination of both ITM and, when appropriate, optimization methods provides two separate interpretations with complimentary strengths and cross-checking capability. These interpretation methods are applied as appropriate to a particular project.

Refraction seismic data interpretation using the intercept time method is detailed by Mooney (1973). A personal computer spreadsheet is used to perform the necessary calculations to obtain depths and layer velocities, and print out time-distance plots and depth interpretations. This method is used for interpretations of up to three layers. It is considered that more than three layers cannot be effectively interpreted using twelve geophone data points. Interpretations are then completed manually to produce a final interpreted geologic profile and layer depths.

Refraction seismic data interpretation using optimization is performed using the SeisOpt2D (presently Version 4.0) software package by Optim, L.L.C., 1999-2007, of Reno, Nevada. Energy source and geophone receiver locations and elevations, and first arrival times are entered into the software package, and first arrival travel times are optimized through a process of repeated (typically 10,000 to 100,000) iterations. Multiple seismic lines combined end to end into a longer composite line can be effectively interpreted using this software. Model grid dimensions and element sizes are selected, with larger grids containing smaller elements providing greater potential resolution. However, very large grids containing small elements may become unstable, and several runs may need to be made to obtain stable, robust interpretations. Once a robust interpretation has been obtained, the resulting seismic velocity profile is printed out with varying colors indicating the interpreted velocities.

References:

Mooney, H.M., 1973, Engineering Seismology Using Refraction Methods, Bison Instruments, Inc., Minneapolis, Minnesota.

Rucker, M.L. and Keaton, J.R., 1998, Tracing an Earth Fissure Using Seismic-Refraction Methods with Physical Verification, in Land Subsidence Case Studies and Current Research: Proceedings of the Dr. Joseph F. Poland Symposium on Land Subsidence, Edited by Borchers, J.W., Special Publication No. 8, Association of Engineering Geologists, Star Publishing Company, Belmont, California, p. 207-216.

REFRACTION MICROTREMOR (ReMi) SHEAR WAVE EQUIPMENT AND PROCEDURES

Refraction microtemor or ReMi surveys are performed in general accordance with the method described by Louie (2001) to develop vertical one-dimensional shear wave (s-wave) velocity profiles. The same equipment used for ReMi is also used for refraction seismic. When appropriate, both p-wave and s-wave data can be collected with the same physical seismic line setup.

ReMi Seismic Equipment - ReMi surveys are performed using a Geometrics SE-12 or SE-24 Smartseis signal enhancement seismograph. These instruments have the capability to digitally record and store up to 12 or 24 channels of geophone data in SEG2 format. Up to 16,384 samples can be acquired for each geophone channel at sample intervals as long as 0.25, 0.5, 1 and 2 milliseconds. Sampling events to collect ReMi field data may typically last 6, 12 or 24 seconds. Geophone cables with 12 geophone takeouts at 10-foot or 20-meter spacings are presently used. Vertical geophones with resonant frequencies of 28 Hz and 4.5 Hz are used to obtain surface wave data for s-wave vertical profile analysis. High frequency geophones are used for shorter arrays with shallower depths of investigation, and low frequency geophones are used for longer arrays with greater depths of investigation. Broad band ambient site noise may be used as a surface wave energy source. Controlled surface wave energy sources include jogging alongside shorter geophone arrays and driving a field vehicle alongside longer geophone arrays. The seismograph system is extremely portable. In areas where vehicular access is not possible, the equipment can be mobilized by various means, including backpacking, packhorse, helicopter and canoe.

ReMi Field Procedures - The field operations are directed by our experienced engineer or geologist, who operates the equipment, prepares the records and examines the data in the field. ReMi seismic lines are generally laid out using the standard spacings on the geophone cables. A depth of investigation of about 100 meters or more may be possible using a 240 meter array. For shorter lines with improved near-surface resolution, 10-foot array spacings between geophones have a shallowr depth of investigation. Other geophone spacings can also be used.

Data collection consists of the system sampling the ambient or generated surface waves (a sampling event) at the geophone array for several to many seconds. Typical sampling times and intervals for a sampling event may be 6 seconds at 0.5 milliseconds, 12 seconds at 1 millisecond and 24 seconds at 2 milliseconds for array lengths of 60 feet, 120 to 240 feet, and 240 meters, respectively. Several sampling events are collected at each ReMi setup. For shorter arrays where ReMi with surface wave energy generated by jogging is conducted in concert with seismic refraction data collection, four sampling events may typically be recorded. For longer arrays where urban ambient noise or a field vehicle generates the surface wave energy, six to ten sampling events may be recorded. Field notes, including line number and orientation, topographic variations and other notes as appropriate are made on hard copy of traces. Locations and other notes are made on site maps and in notebooks as appropriate. Sample data files may be transferred by 3.5-inch floppy to the laptop computer and preliminary interpretations made for immediate data adequacy verification as part of the quality control process.

Interpretation - Although preliminary or quality control initial ReMi seismic data interpretations may sometimes be performed in the field, full interpretations are completed in the office. Data files, typically about 580kb each in size, are transferred from the seismograph to the laptop computer using 3.5-inch floppy disks. Interpretation is performed using the SeisOpt ReMi Version 3.0 (2004) software package by Optim, L.L.C., of Reno, Nevada. The software consists of two modules. The ReMiVsSpect module is used to convert the SEG2 files into a spectral energy shear wave frequency versus shear wave velocity presentation for a ReMi seismic setup. The interpreter then selects a dispersion curve consisting of the lower bound of the spectral energy shear wave velocity versus frequency trend, and that dispersion curve is saved to disk. Tracing the lower bound (slowest) of the shear wave velocity at each frequency selects the ambient energy propagating parallel to the geophone array, since energy propagating incident to the array will appear to have a faster propagating velocity. The second module, ReMiDisper, is then invoked. The interpreter models a dispersion curve with multiple layers and s-wave velocities to match the selected dispersion curve from the field data. An interpreted vertical s-wave profile is obtained through this process. It must be understood that this type of interpretation may not result in a unique solution.

Louie, J.L., 2001, Faster, Better: Shear-wave velocity to 100 meters depth from refraction microtremor arrays, Bulletin of the Seismological Society of America, Vol. 91, 347-364.

TABLE A-1
Seismic Line Summary (ReMi Results)

Line	Elev	Layer 1		Layer 2		Layer 3		Layer 4		Layer 5				
	feet amsl	velocity	depth	velocity	depth	velocity	depth	velocity	depth	velocity	depth	velocity	depth	velocity
1	**6656**	440	2.1	340	16.6	1000	30.4	700	40.7	3200				
2	**6656**	2000	2.1	300	16.6	850	21.7	350	33.3	2500				
3 alt A	**6657**	690	2.1	300	15.5	3200	20.8	310	27.9	2700	3200			
3 alt B		2600	2.1	270	15	1100	24.9	360	32	3300				
4	**6654**	1800	2	270	13.7	740		740	52.8	1500				
5b	**6663**	1200	2	350	22	1800	35.8	700	51	2400	3200			
6	**6656**	1400	0.09	300	17.9	700		700	43.5	2400				
7	**6644**	580	1.2	310	11	2300		2300	48.6	1400				
7 alt		580	1.2	290	9.1	870	50.8	870	50.8	2300				
8	**6643**	1800	1.5	360	13.1	730	34.2			2900	3300			
9	**6644**			430	21.7	770	34.1			3300				
9 alt				430	18.2	660	26.6			3100				
10	**6646**	1000	2	430	24.4	2300								
11a	**6656**	430	7.2	1100	18.4	860	41.3	2300		2300	177	2000	214	3300
11b		400	5.4	800	24.9	1500	58.9	2600		2600	194.6	2000	214	3300
12	**6647**	410	7	1300		1300	52.9	2600		2600	107.4	1300	153.6	2900
13a	**6640**	390	5	1100	16.9	770	25.4	1400	80.4	2600	127.4	2100	234	5000
13b		390	5	1100	16.9	770	25.4	1400	60.6	2600	107.6	2100	254	5000
14	**6635**	390	5	1100	16.2	710	24.7	2800		2800	142.2	1900	233	5000
15a	**6649**	390	5	960		960	49.2	3000						
15b		390	5	930		930	42.4	3200						
16a	**6616**	360	4.1	1500	8.8	580	15.9	?	32.7	2200		2200	327	4300
16b		360	4.1	1500	8.8	580	15.9	4000	32.7	2200		2200	327	4300
17	**6629**	400	5.6	1500	8.2	670	15.3	2700	32.1	2100				
18	**6653**	400	5.6	920	8.3	670	19.4	1200	36.2	2200		2200	295	4200
19	**6620**	400	4.8	1200		1200	28.5	1900		1900	167	4100		
20	**6609**	320	5.1	1300		1300	39.1	2100	72.8	1900	126	2500		

Municipal Solid Waste (MSW)
Cinders Unit
Basalt Unit
Cinders/Basalt Unit
Isolated pyroclastics

Note:
Velocities shown are S-Wave, feet per second

Line 1

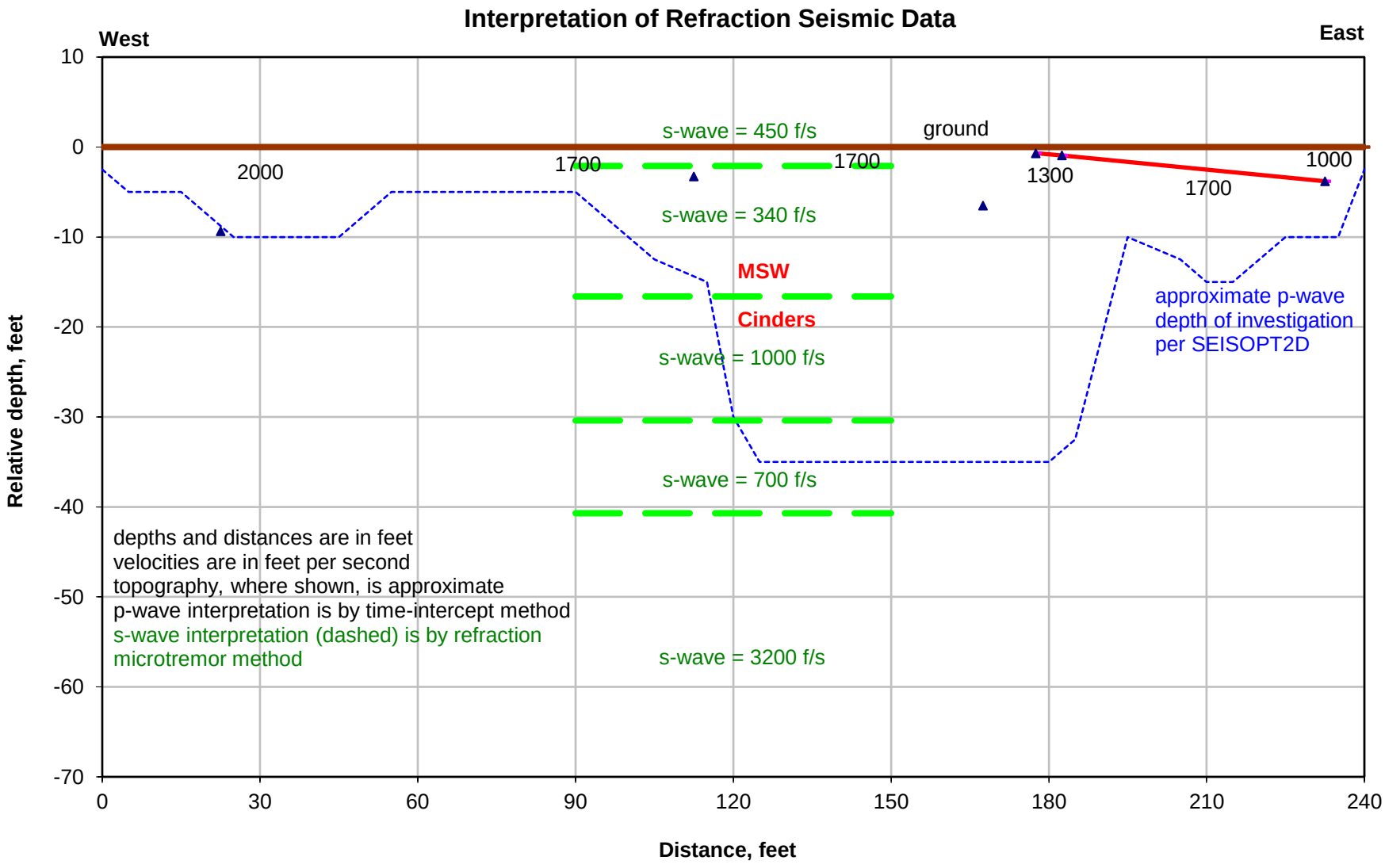
Interpretation of Refraction Seismic Data
West
East
ground
s-wave = 450 f/s
2000
1700
1700
1300
1700
1000
s-wave = 340 f/s
MSW
Cinders
s-wave = 1000 f/s
s-wave = 700 f/s
s-wave = 3200 f/s
approximate p-wave
depth of investigation
per SEISOPT2D
depths and distances are in feet
velocities are in feet per second
topography, where shown, is approximate
p-wave interpretation is by time-intercept method
s-wave interpretation (dashed) is by refraction
microtremor method
Relative depth, feet
10
0
-10
-20
-30
-40
-50
-60
-70
0
30
60
90
120
150
180
210
240
Distance, feet

Line 1

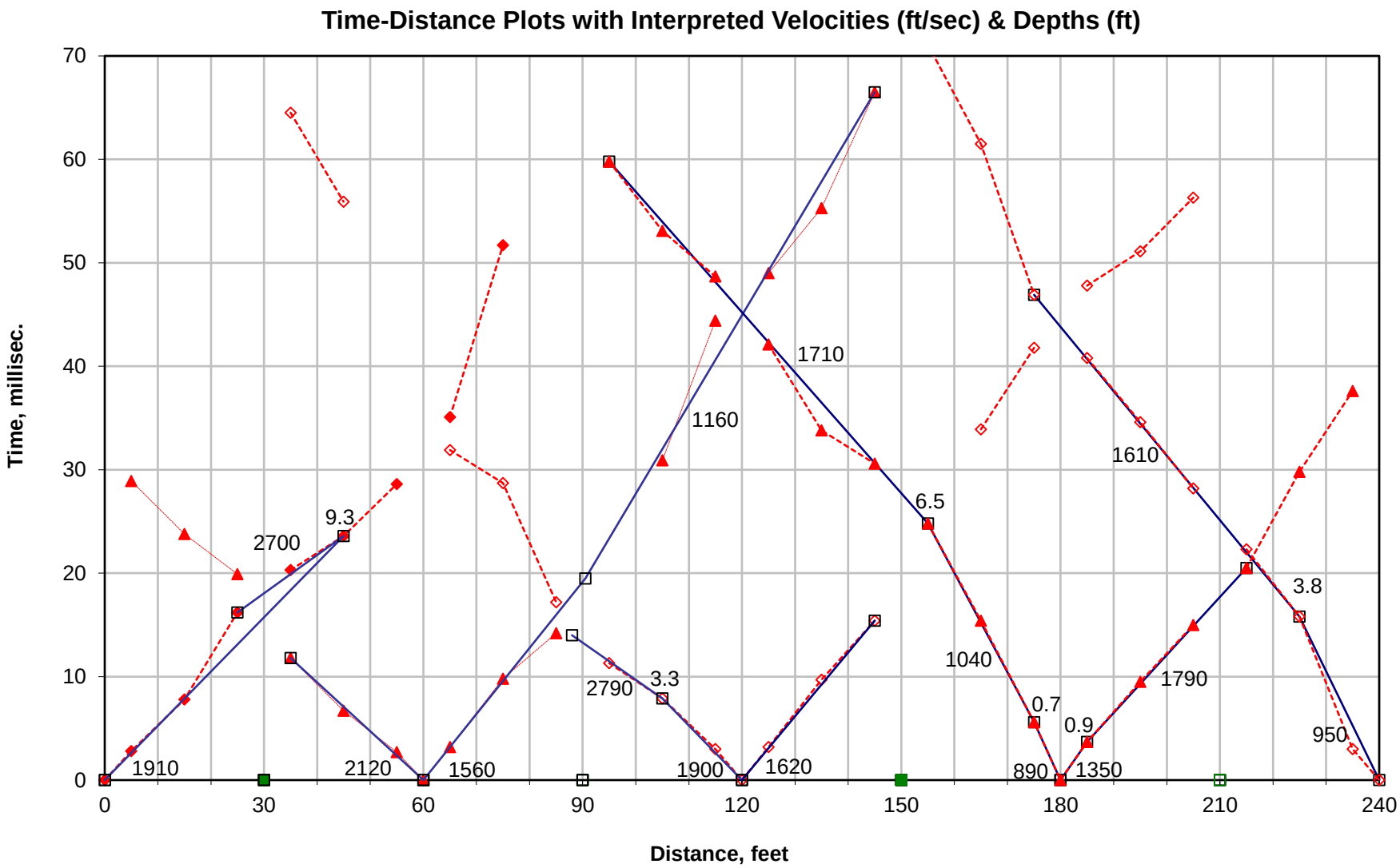
Time-Distance Plots with Interpreted Velocities (ft/sec) & Depths (ft)
Time, millisec.
Distance, feet
0
10
20
30
40
50
60
70
0
30
60
90
120
150
180
210
240
1910
2700
9.3
2120
1560
1160
1710
2790
3.3
1900
1620
6.5
1040
0.7
890
0.9
1350
1610
1790
3.8
950

Line 2

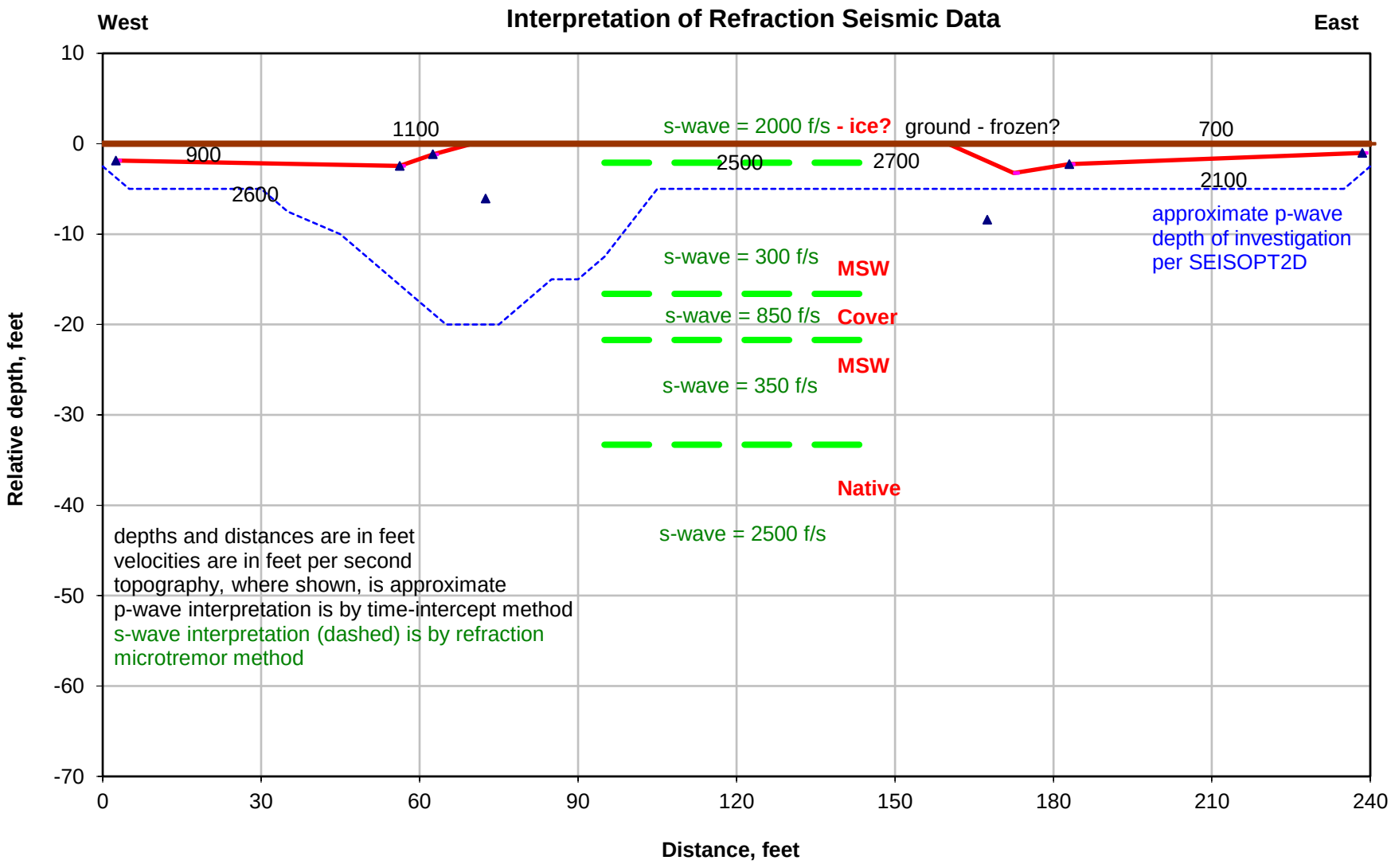
Interpretation of Refraction Seismic Data
West
East
Relative depth, feet
Distance, feet
10
0
-10
-20
-30
-40
-50
-60
-70
0
30
60
90
120
150
180
210
240
900
1100
2600
2500
2700
700
2100
s-wave = 2000 f/s - ice?
ground - frozen?
s-wave = 300 f/s
MSW
s-wave = 850 f/s
Cover
MSW
s-wave = 350 f/s
Native
s-wave = 2500 f/s
approximate p-wave
depth of investigation
per SEISOPT2D
depths and distances are in feet
velocities are in feet per second
topography, where shown, is approximate
p-wave interpretation is by time-intercept method
s-wave interpretation (dashed) is by refraction
microtremor method

Line 2

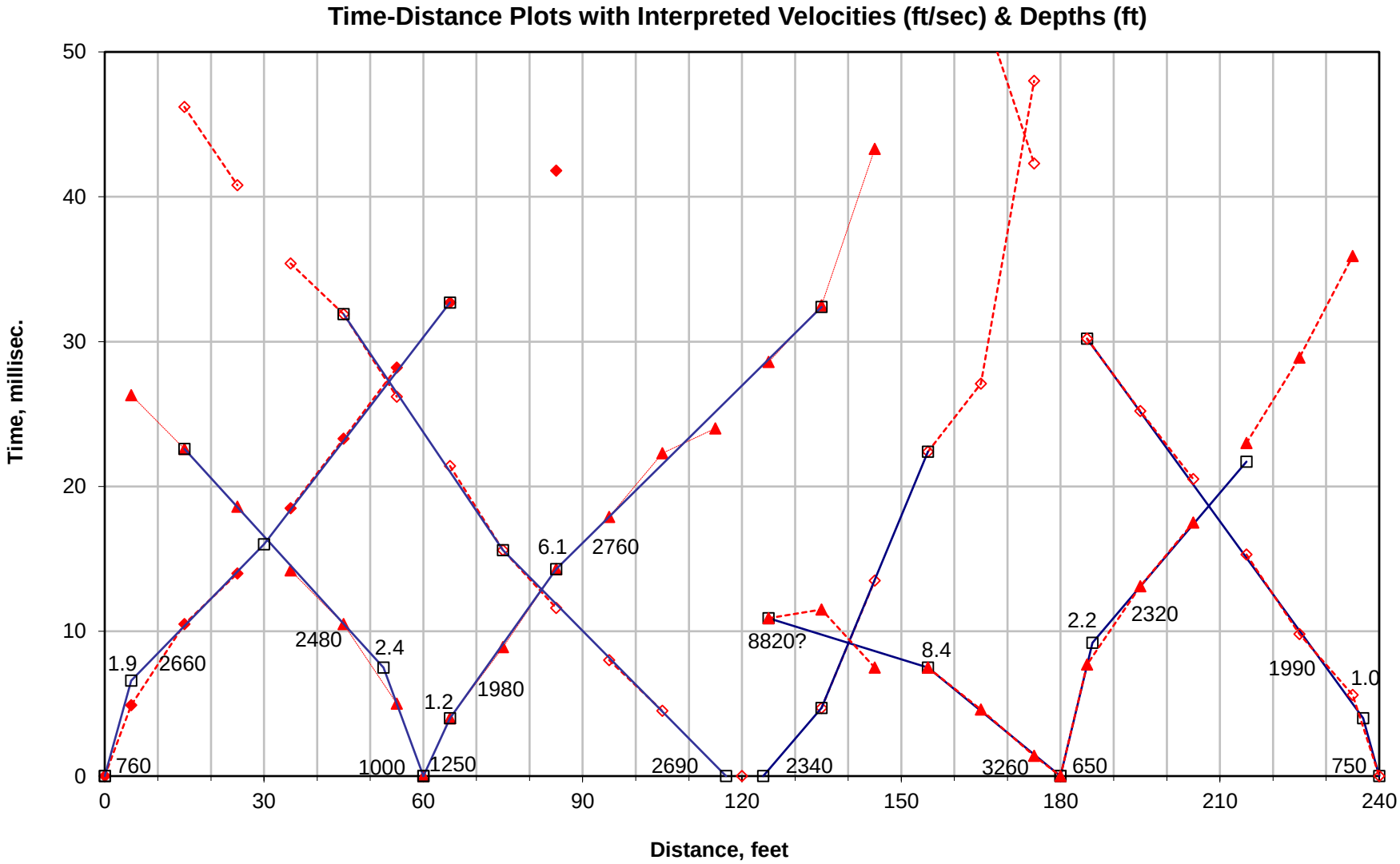
Time-Distance Plots with Interpreted Velocities (ft/sec) & Depths (ft)
Time, millisec.
Distance, feet
0
10
20
30
40
50
0
30
60
90
120
150
180
210
240
760
1.9
2660
2480
2.4
1000
1.2
1250
1980
6.1
2760
2690
2340
8820?
8.4
3260
2.2
650
2320
1990
1.0
750

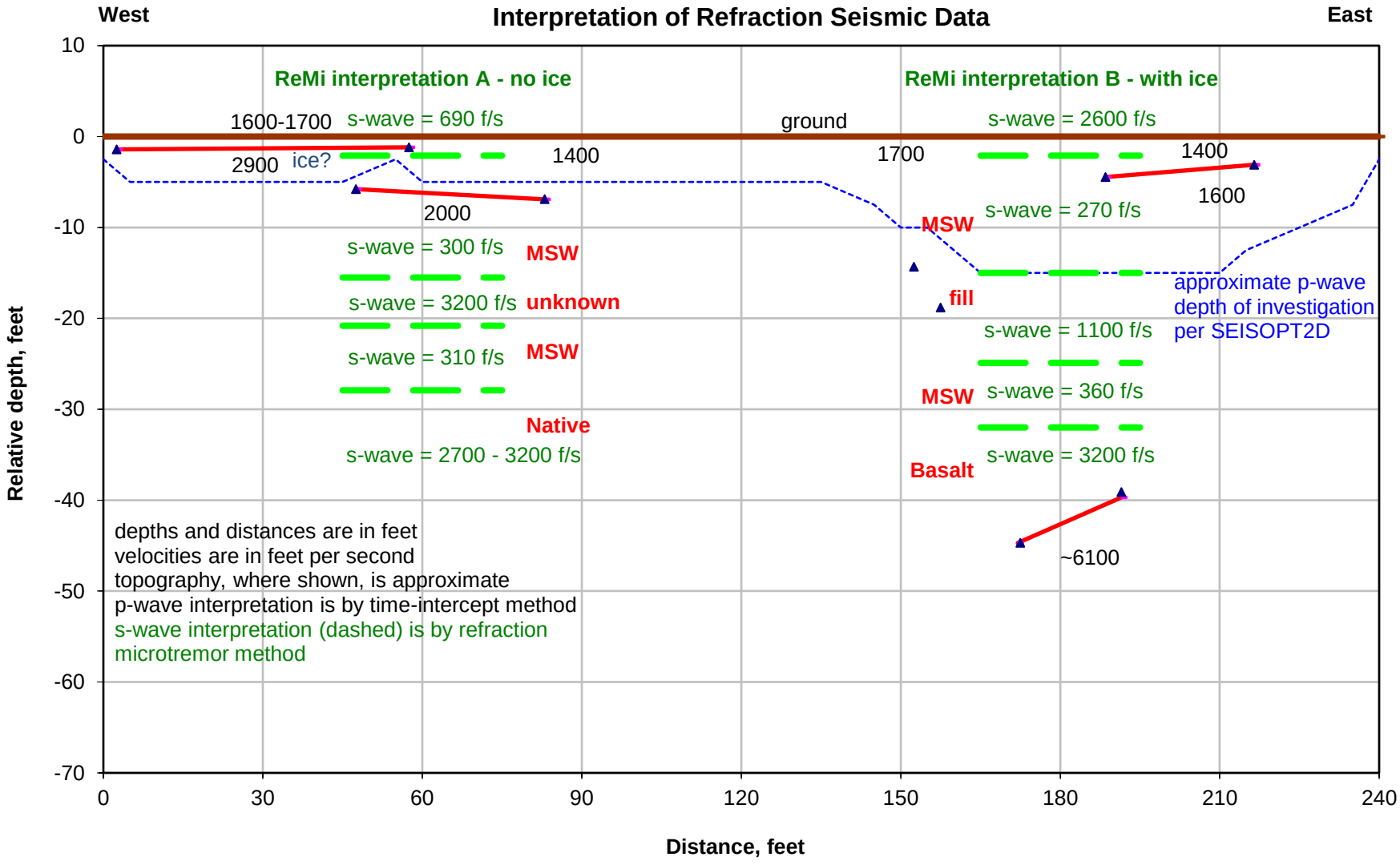
West
Interpretation of Refraction Seismic Data
East
ReMi interpretation A - no ice
ReMi interpretation B - with ice
1600-1700
s-wave = 690 f/s
ground
s-wave = 2600 f/s
2900
ice?
1400
1700
1400
1600
2000
s-wave = 270 f/s
MSW
s-wave = 300 f/s
MSW
fill
approximate p-wave
depth of investigation
per SEISOPT2D
s-wave = 3200 f/s
unknown
s-wave = 1100 f/s
s-wave = 310 f/s
MSW
MSW
s-wave = 360 f/s
Native
s-wave = 2700 - 3200 f/s
Basalt
s-wave = 3200 f/s
~6100
depths and distances are in feet
velocities are in feet per second
topography, where shown, is approximate
p-wave interpretation is by time-intercept method
s-wave interpretation (dashed) is by refraction
microtremor method
Relative depth, feet
Distance, feet
10
0
-10
-20
-30
-40
-50
-60
-70
0
30
60
90
120
150
180
210
240

Line 3

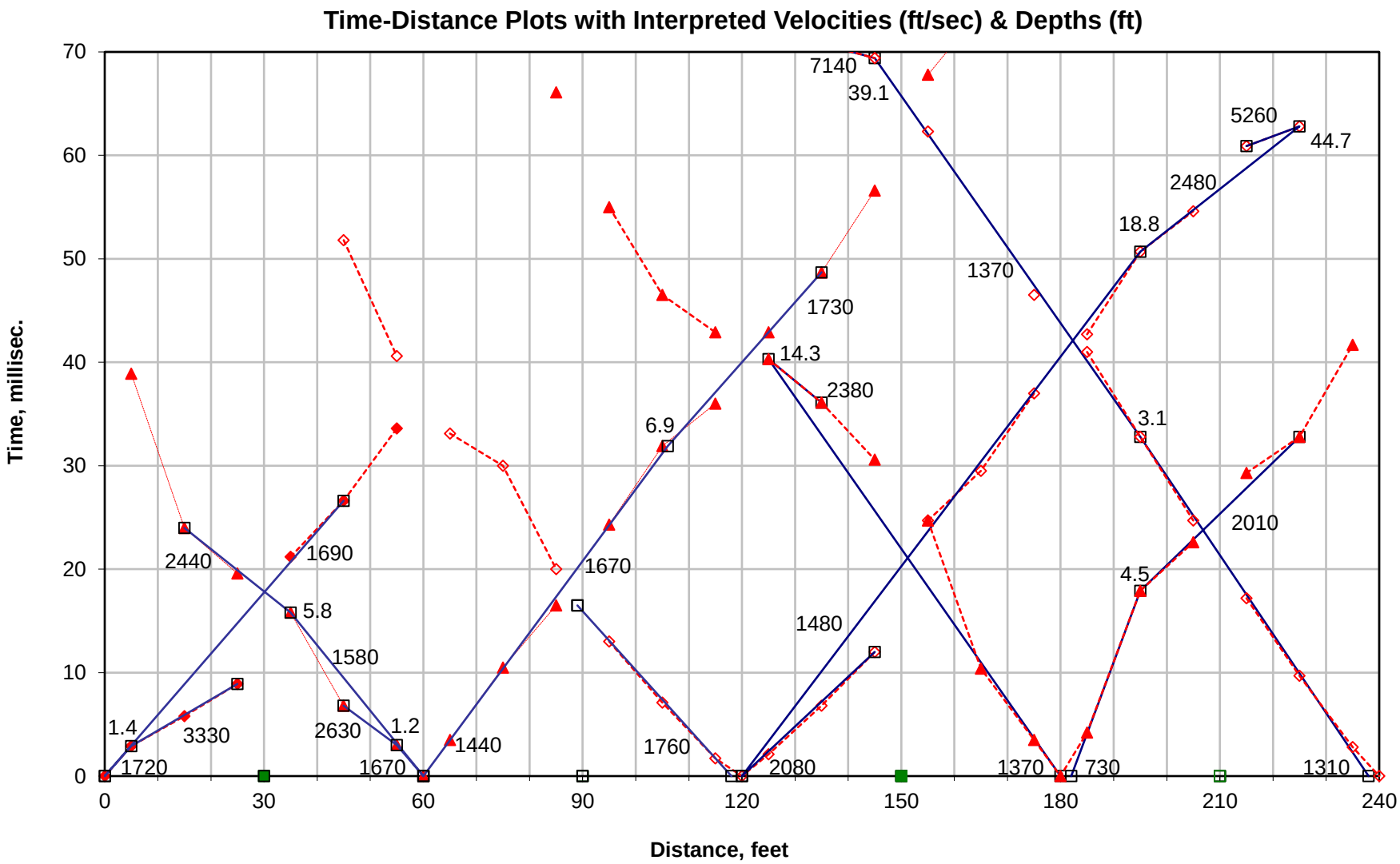
Time-Distance Plots with Interpreted Velocities (ft/sec) & Depths (ft)
Time, millisec.
Distance, feet
0
10
20
30
40
50
60
70
0
30
60
90
120
150
180
210
240
1.4
1720
3330
2440
1690
5.8
1580
2630
1.2
1670
1440
1670
6.9
1760
14.3
1730
2380
2080
1480
7140
39.1
1370
1370
730
3.1
18.8
2480
5260
44.7
4.5
2010
1310

Line 4

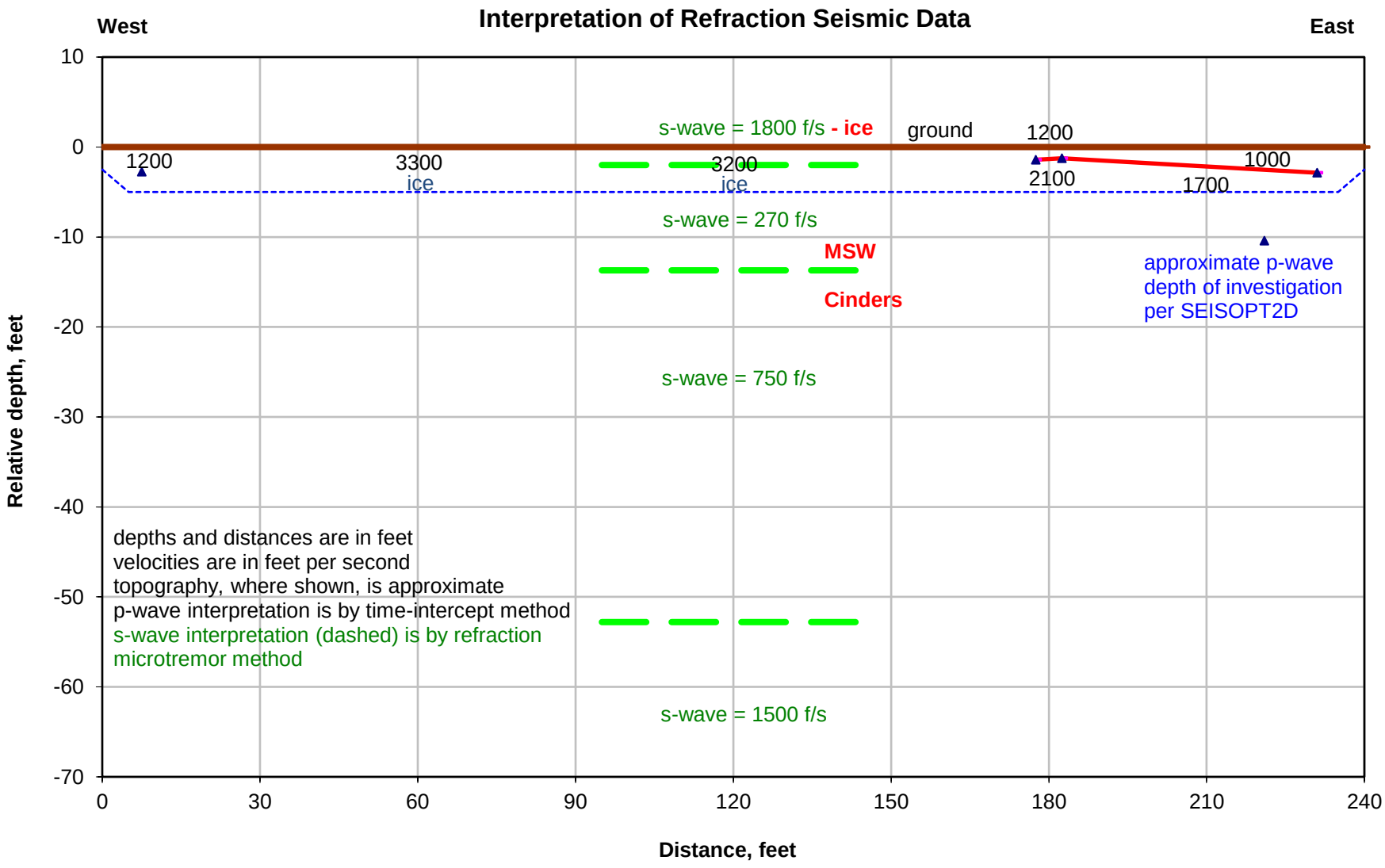
Interpretation of Refraction Seismic Data
West
East
s-wave = 1800 f/s - ice
ground
1200
1200
3300
ice
3200
ice
2100
1700
1000
s-wave = 270 f/s
MSW
Cinders
approximate p-wave
depth of investigation
per SEISOPT2D
s-wave = 750 f/s
depths and distances are in feet
velocities are in feet per second
topography, where shown, is approximate
p-wave interpretation is by time-intercept method
s-wave interpretation (dashed) is by refraction
microtremor method
s-wave = 1500 f/s
Relative depth, feet
10
0
-10
-20
-30
-40
-50
-60
-70
0
30
60
90
120
150
180
210
240
Distance, feet

Line 4

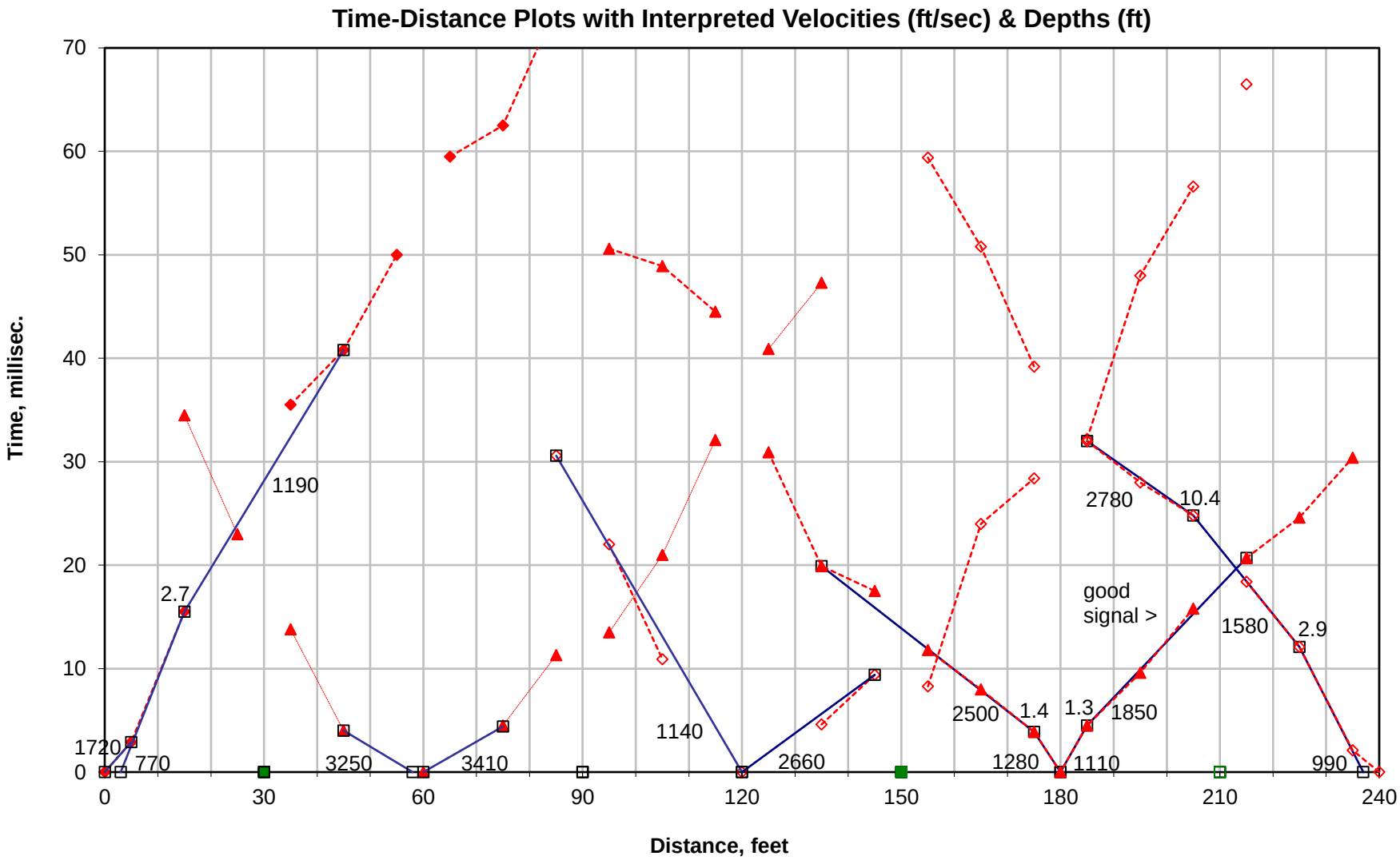
Time-Distance Plots with Interpreted Velocities (ft/sec) & Depths (ft)
Time, millisec.
Distance, feet
0
10
20
30
40
50
60
70
0
30
60
90
120
150
180
210
240
1720
770
2.7
1190
3250
3410
1140
2660
2500
1.4
1.3
1280
1110
2780
10.4
good
signal >
1850
1580
2.9
990

Line 5B

Interpretation of Refraction Seismic Data

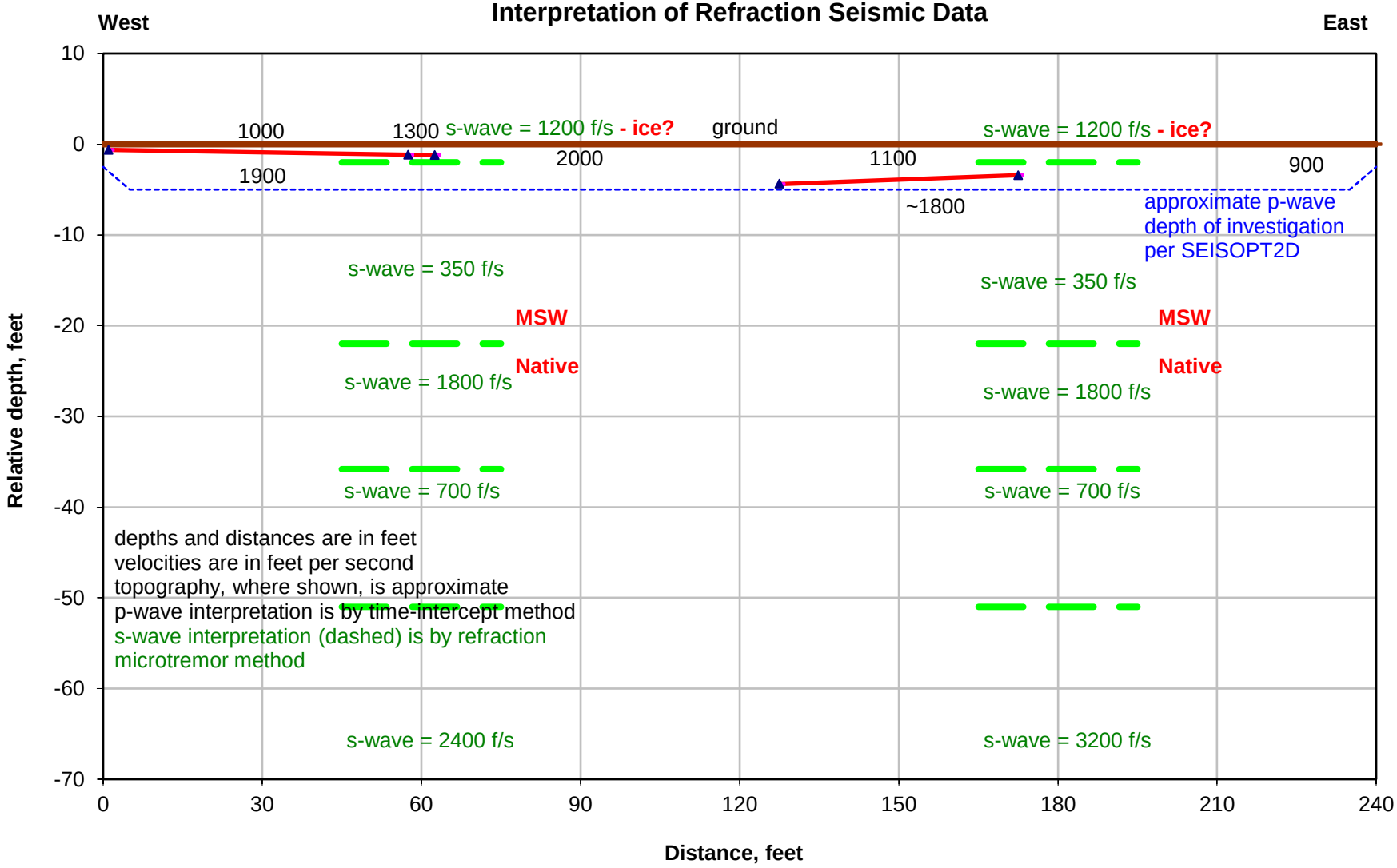

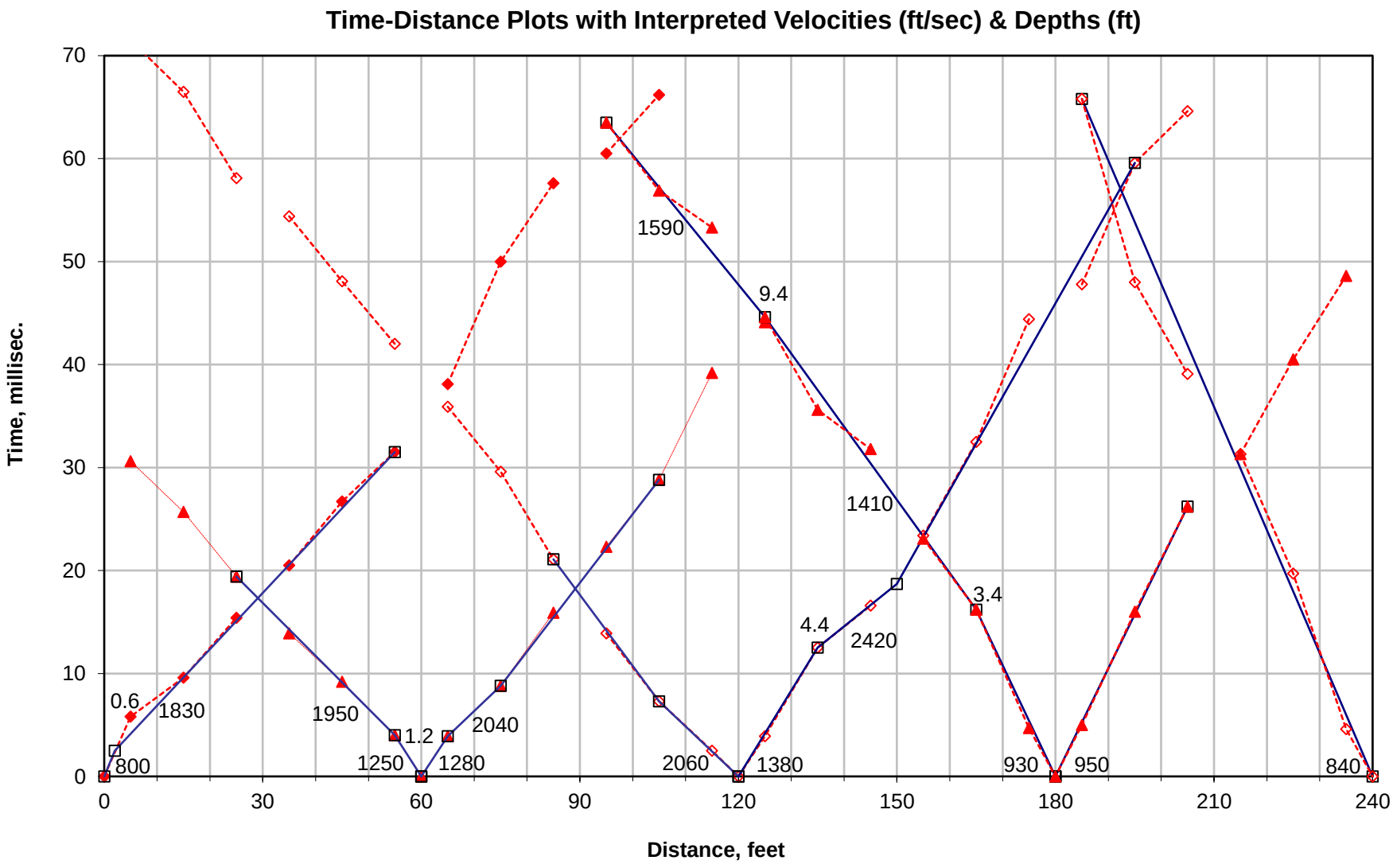
Time-Distance Plots with Interpreted Velocities (ft/sec) & Depths (ft)
Time, millisec.
Distance, feet
0
10
20
30
40
50
60
70
0
30
60
90
120
150
180
210
240
0.6
1830
800
1950
1.2
1250
1280
2040
1590
9.4
2060
1380
1410
3.4
4.4
2420
930
950
840

Line 6

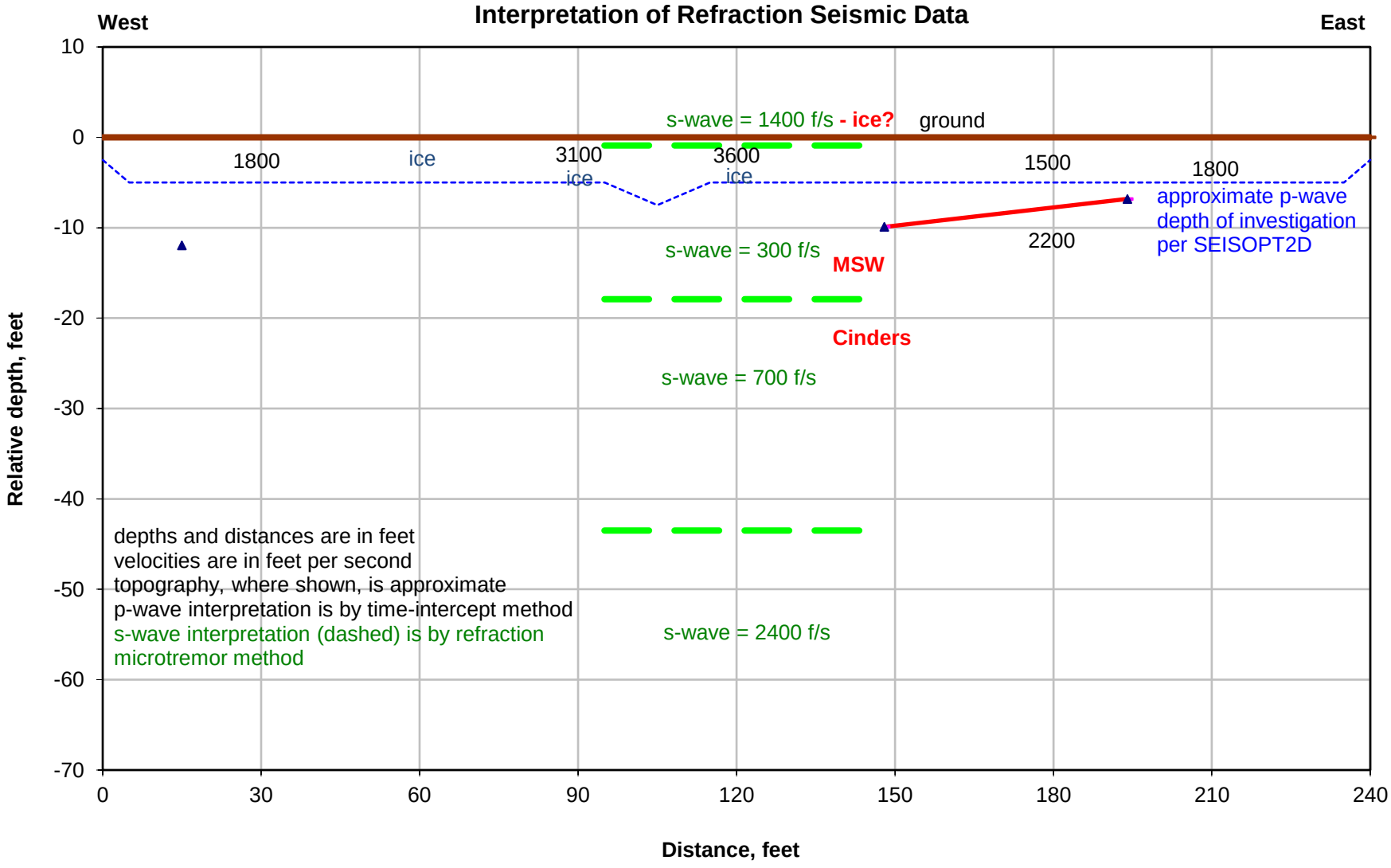
Interpretation of Refraction Seismic Data
West
East
s-wave = 1400 f/s - ice?
ground
1800
ice
3100
ice
3600
ice
1500
1800
approximate p-wave
depth of investigation
per SEISOPT2D
2200
s-wave = 300 f/s
MSW
Cinders
s-wave = 700 f/s
s-wave = 2400 f/s
depths and distances are in feet
velocities are in feet per second
topography, where shown, is approximate
p-wave interpretation is by time-intercept method
s-wave interpretation (dashed) is by refraction
microtremor method
Relative depth, feet
Distance, feet
10
0
-10
-20
-30
-40
-50
-60
-70
0
30
60
90
120
150
180
210
240

Line 6

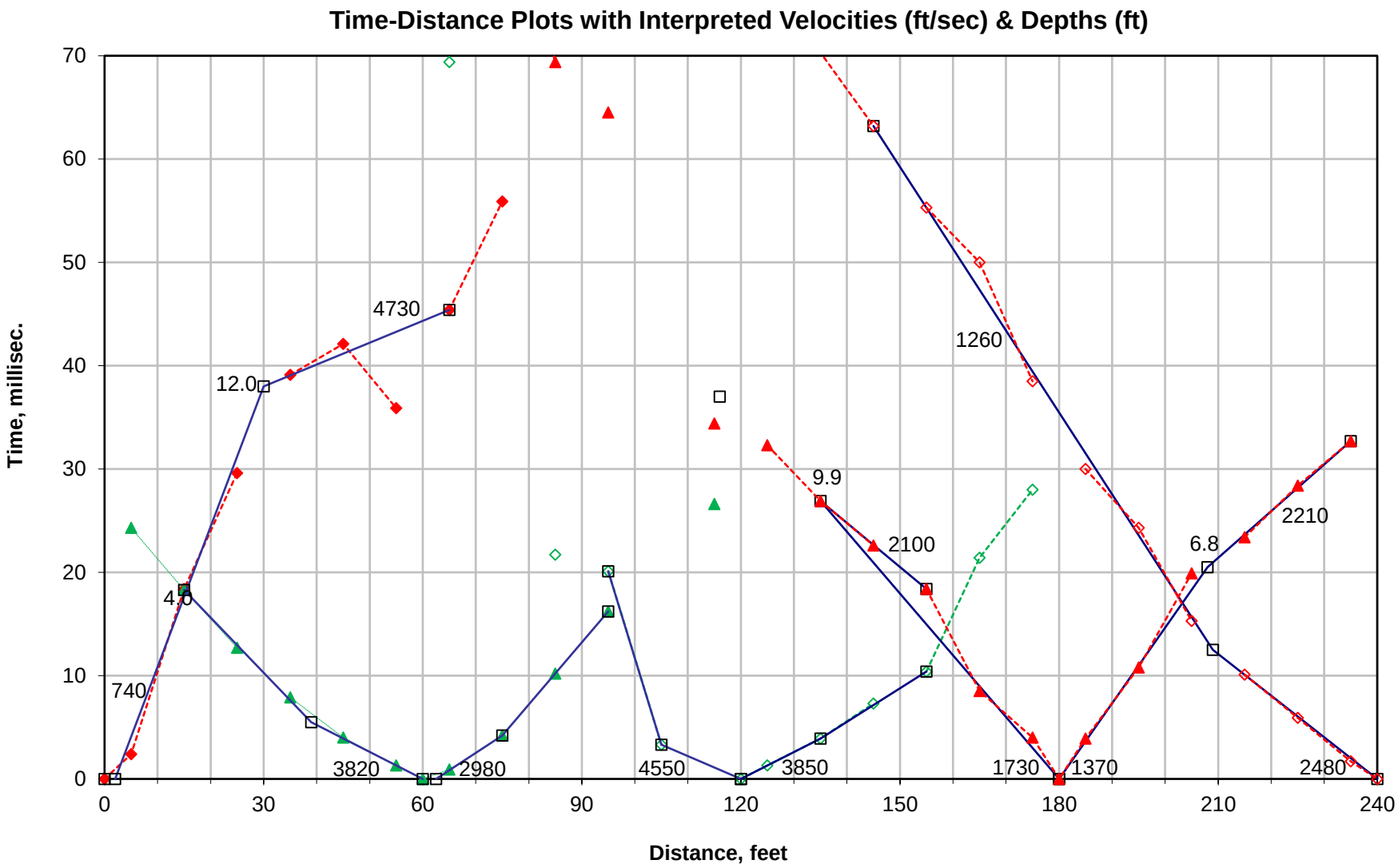
Time-Distance Plots with Interpreted Velocities (ft/sec) & Depths (ft)
Time, millisec.
Distance, feet
0
10
20
30
40
50
60
70
0
30
60
90
120
150
180
210
240
4730
12.0
1260
9.9
2100
6.8
2210
740
3820
2980
4550
3850
1730
1370
2480

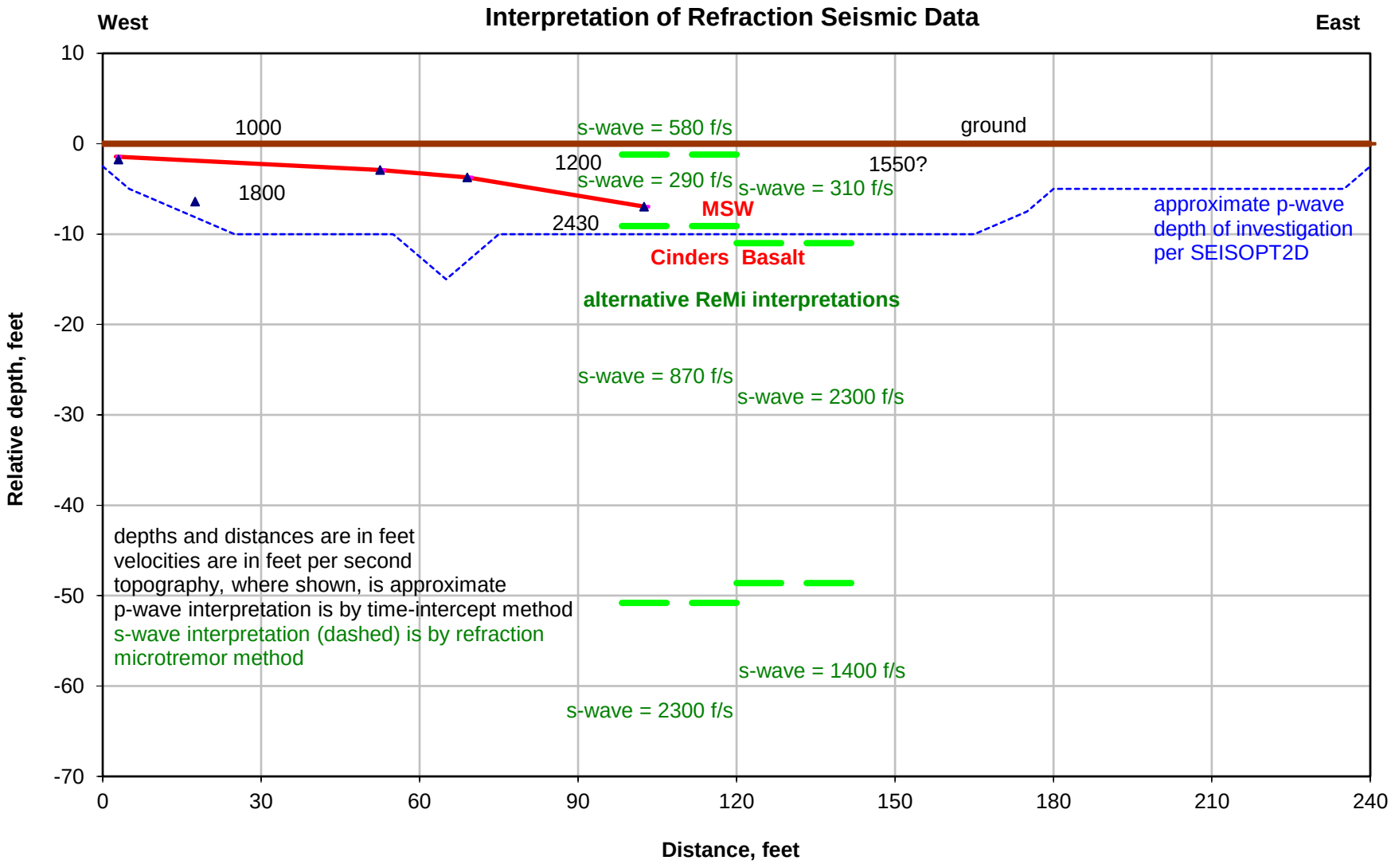
Interpretation of Refraction Seismic Data
West
East
Relative depth, feet
Distance, feet
10
0
-10
-20
-30
-40
-50
-60
-70
0
30
60
90
120
150
180
210
240
1000
1800
1200
2430
1550?
ground
s-wave = 580 f/s
s-wave = 290 f/s
s-wave = 310 f/s
MSW
Cinders
Basalt
approximate p-wave
depth of investigation
per SEISOPT2D
alternative ReMi interpretations
s-wave = 870 f/s
s-wave = 2300 f/s
s-wave = 1400 f/s
s-wave = 2300 f/s
depths and distances are in feet
velocities are in feet per second
topography, where shown, is approximate
p-wave interpretation is by time-intercept method
s-wave interpretation (dashed) is by refraction
microtremor method

Line 7

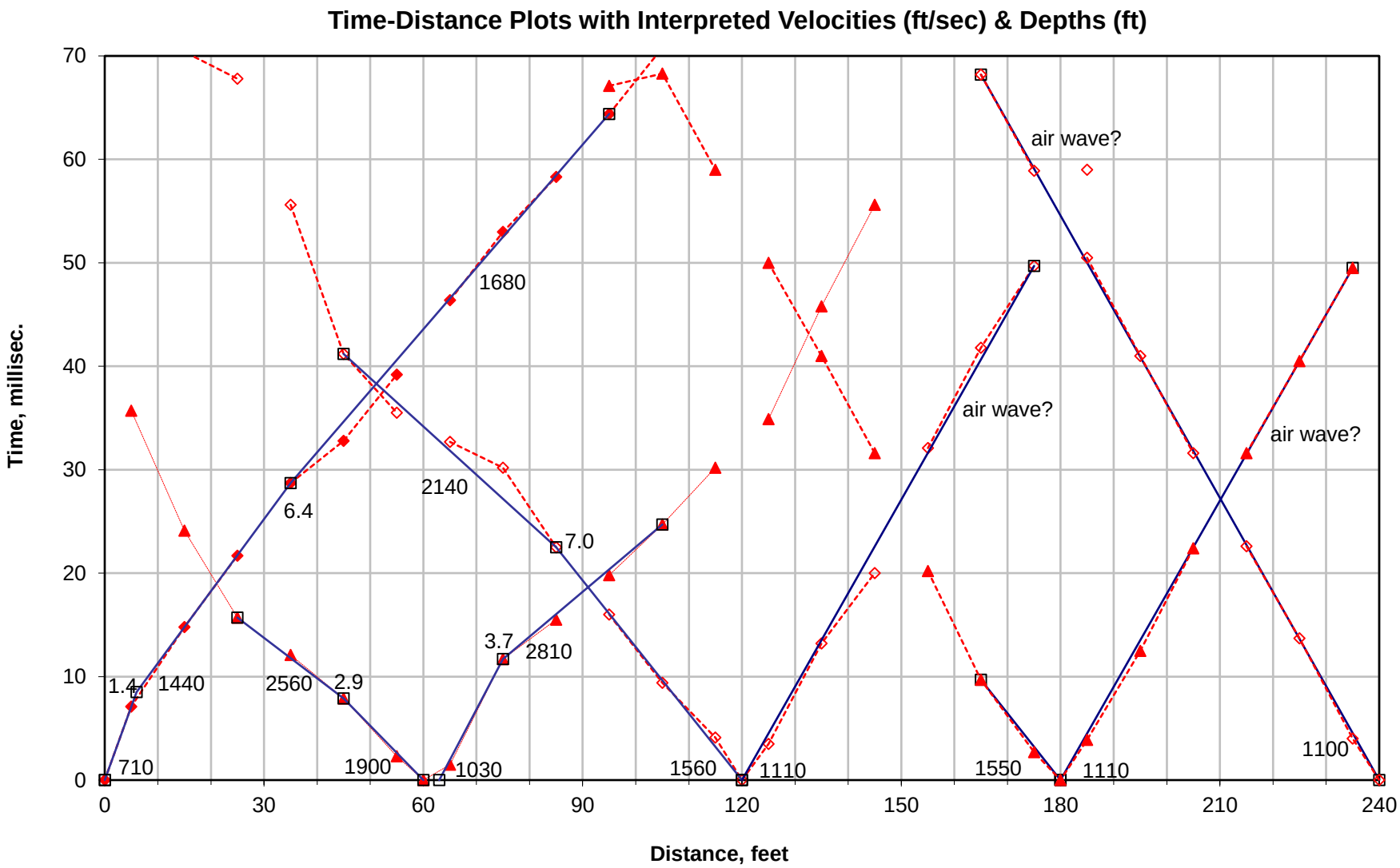
Time-Distance Plots with Interpreted Velocities (ft/sec) & Depths (ft)
Time, millisec.
Distance, feet
0
10
20
30
40
50
60
70
0
30
60
90
120
150
180
210
240
air wave?
air wave?
air wave?
1680
2140
6.4
7.0
3.7
2810
1.4
1440
2560
2.9
710
1900
1030
1560
1110
1550
1110
1100

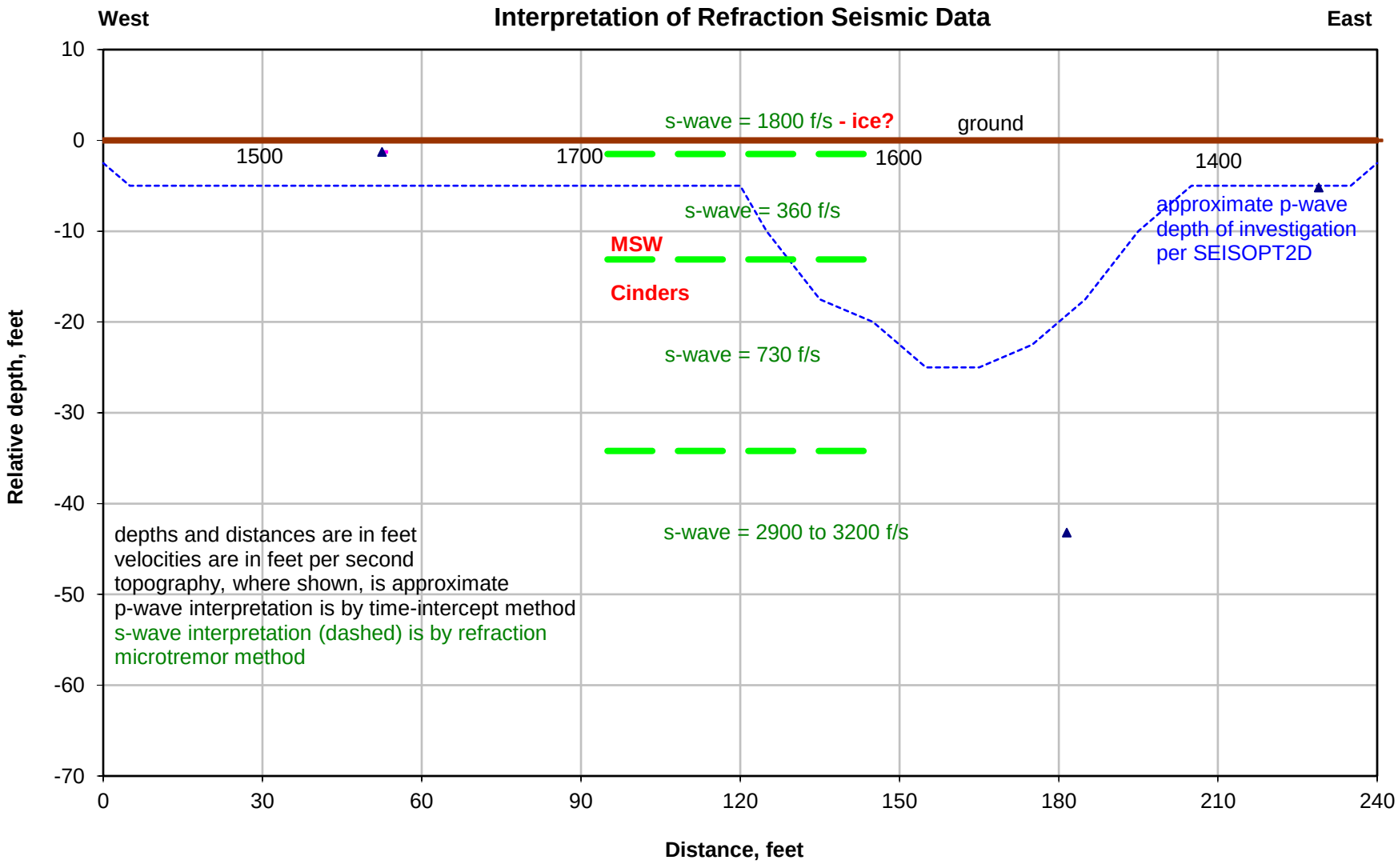
West
Interpretation of Refraction Seismic Data
East
s-wave = 1800 f/s - ice?
ground
1500
1700
1600
1400
s-wave = 360 f/s
MSW
Cinders
s-wave = 730 f/s
s-wave = 2900 to 3200 f/s
approximate p-wave
depth of investigation
per SEISOPT2D
depths and distances are in feet
velocities are in feet per second
topography, where shown, is approximate
p-wave interpretation is by time-intercept method
s-wave interpretation (dashed) is by refraction
microtremor method
Relative depth, feet
10
0
-10
-20
-30
-40
-50
-60
-70
0
30
60
90
120
150
180
210
240
Distance, feet

Line 8

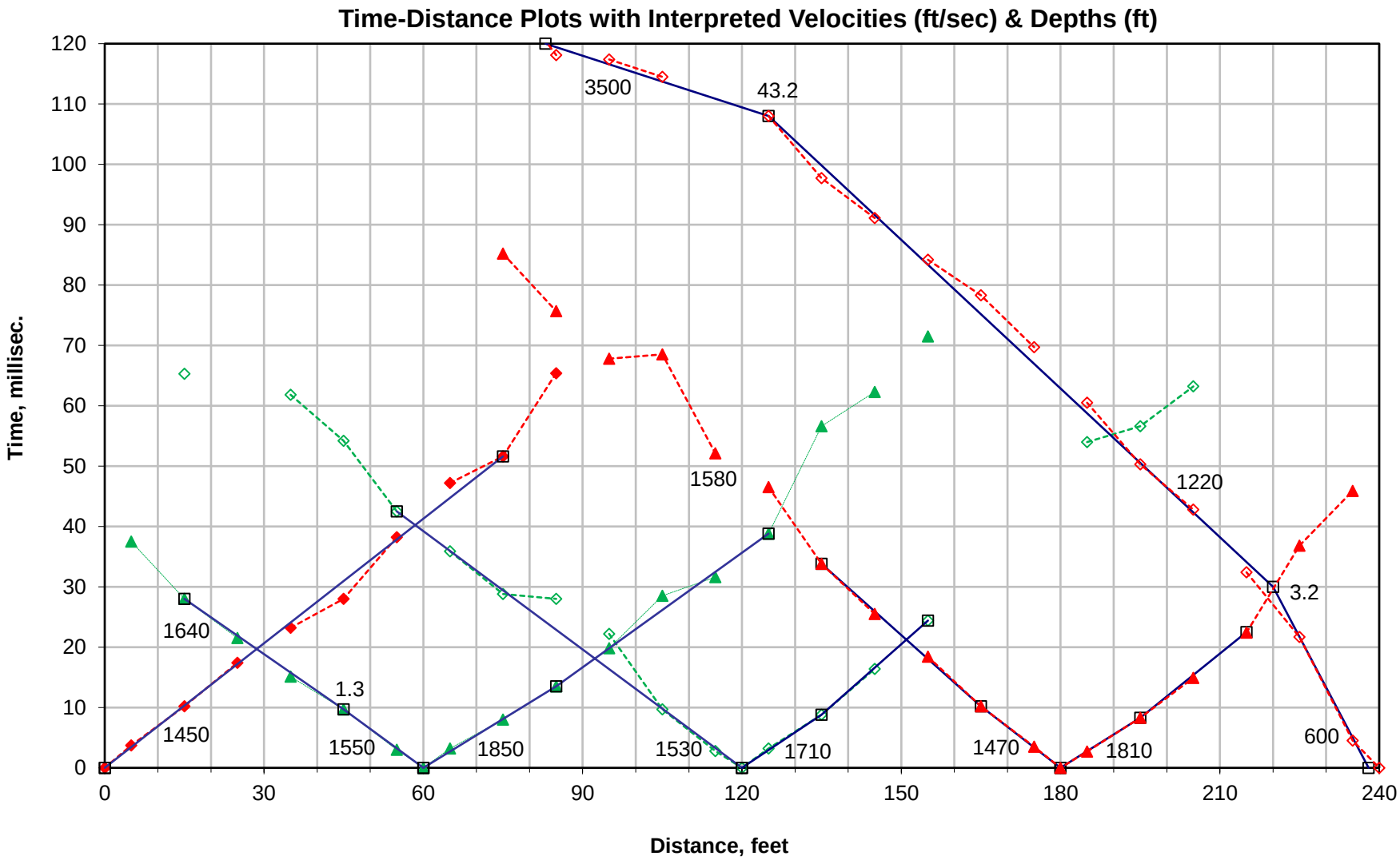
Time-Distance Plots with Interpreted Velocities (ft/sec) & Depths (ft)
Time, millisec.
Distance, feet
0
10
20
30
40
50
60
70
80
90
100
110
120
0
30
60
90
120
150
180
210
240
3500
43.2
1580
1220
3.2
1640
1.3
1450
1550
1850
1530
1710
1470
1810
600

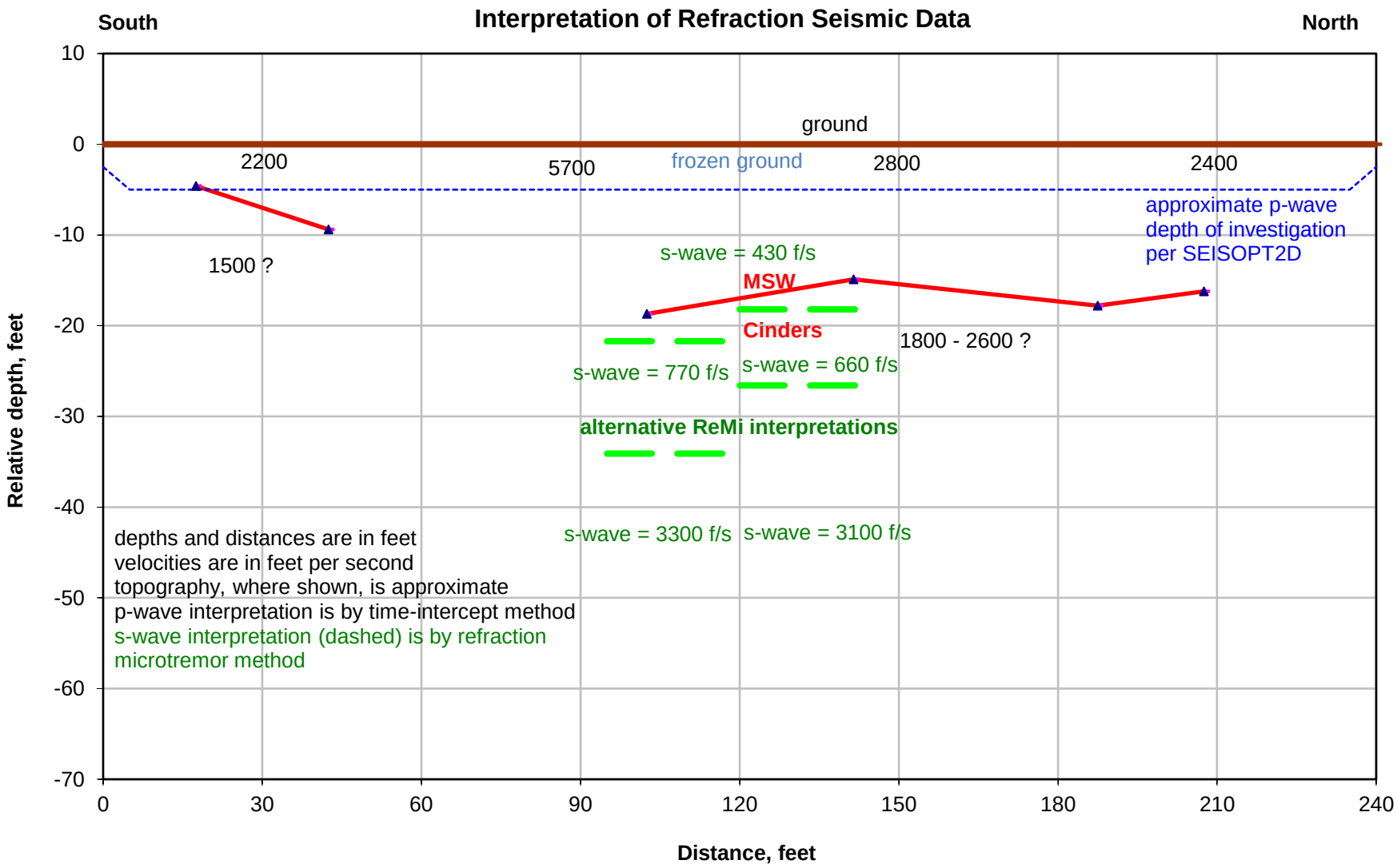
Interpretation of Refraction Seismic Data
South
North
ground
frozen ground
2200
5700
2800
2400
approximate p-wave
depth of investigation
per SEISOPT2D
1500 ?
s-wave = 430 f/s
MSW
Cinders
1800 - 2600 ?
s-wave = 770 f/s
s-wave = 660 f/s
alternative ReMi interpretations
s-wave = 3300 f/s
s-wave = 3100 f/s
depths and distances are in feet
velocities are in feet per second
topography, where shown, is approximate
p-wave interpretation is by time-intercept method
s-wave interpretation (dashed) is by refraction
microtremor method
Relative depth, feet
10
0
-10
-20
-30
-40
-50
-60
-70
0
30
60
90
120
150
180
210
240
Distance, feet

Line 9

Time-Distance Plots with Interpreted Velocities (ft/sec) & Depths (ft)

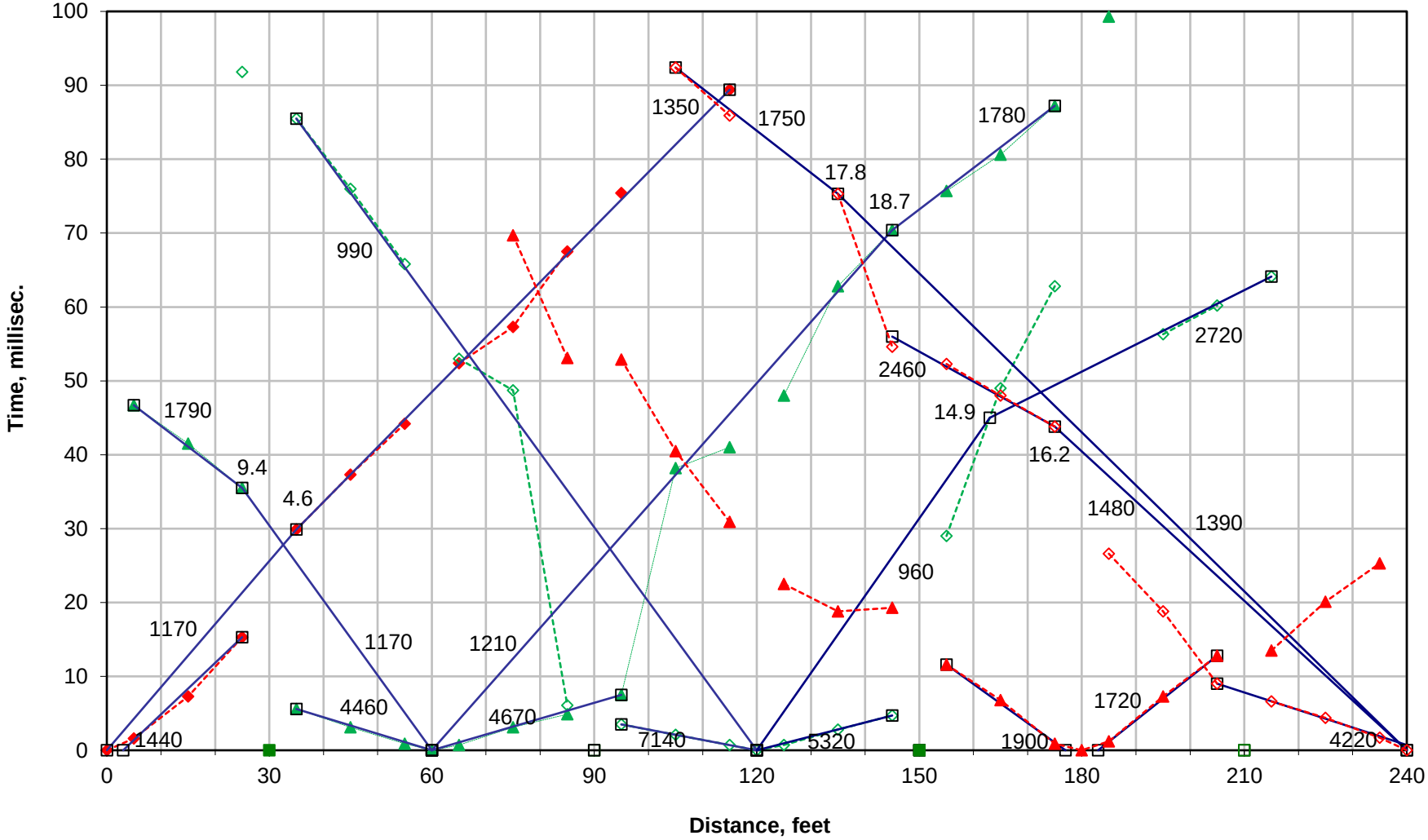

Line 10

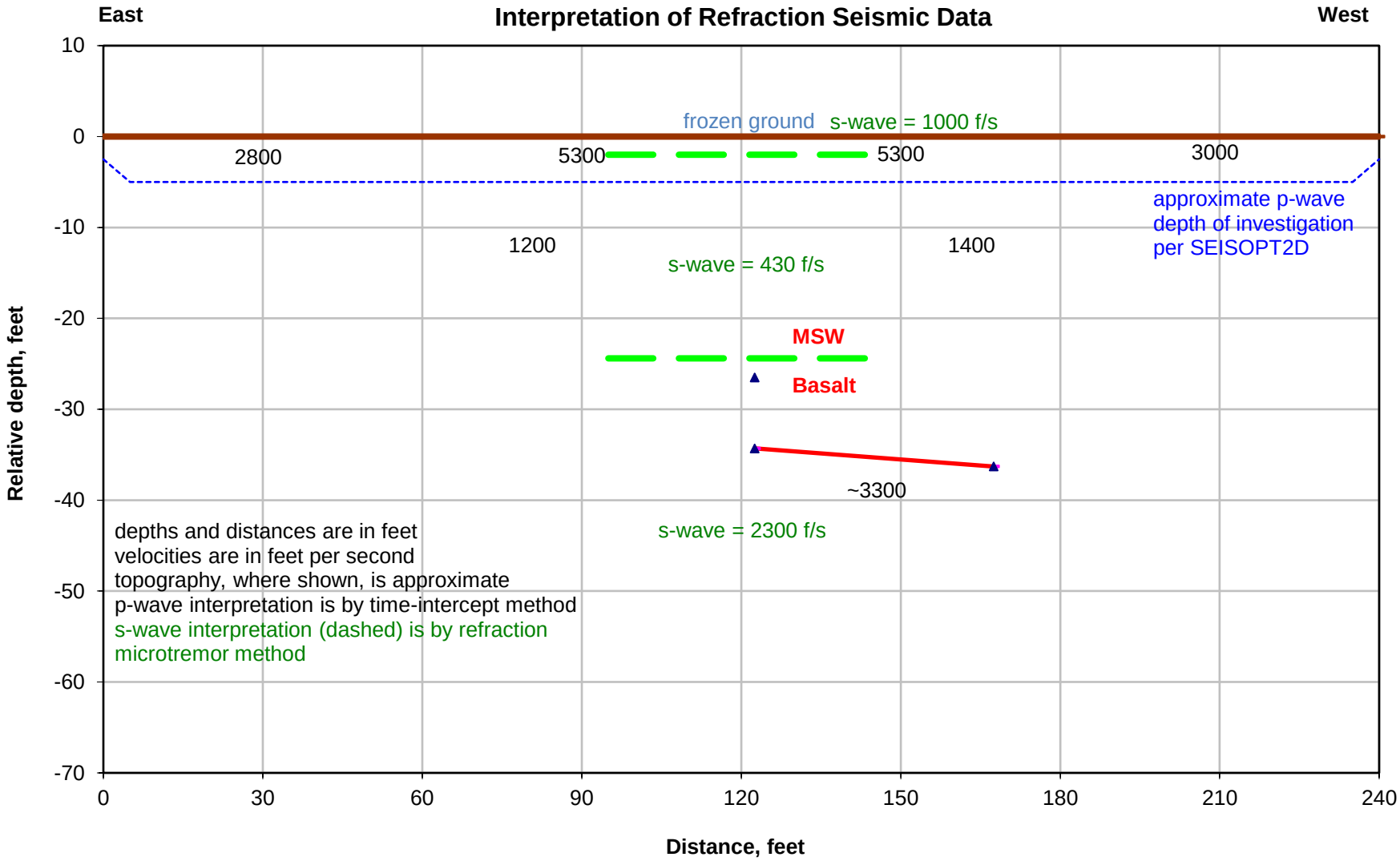
East
Interpretation of Refraction Seismic Data
West
frozen ground
s-wave = 1000 f/s
2800
5300
5300
3000
approximate p-wave
depth of investigation
per SEISOPT2D
1200
1400
s-wave = 430 f/s
MSW
Basalt
~3300
s-wave = 2300 f/s
depths and distances are in feet
velocities are in feet per second
topography, where shown, is approximate
p-wave interpretation is by time-intercept method
s-wave interpretation (dashed) is by refraction
microtremor method
Relative depth, feet
10
0
-10
-20
-30
-40
-50
-60
-70
0
30
60
90
120
150
180
210
240
Distance, feet

Line 10

Time-Distance Plots with Interpreted Velocities (ft/sec) & Depths (ft)

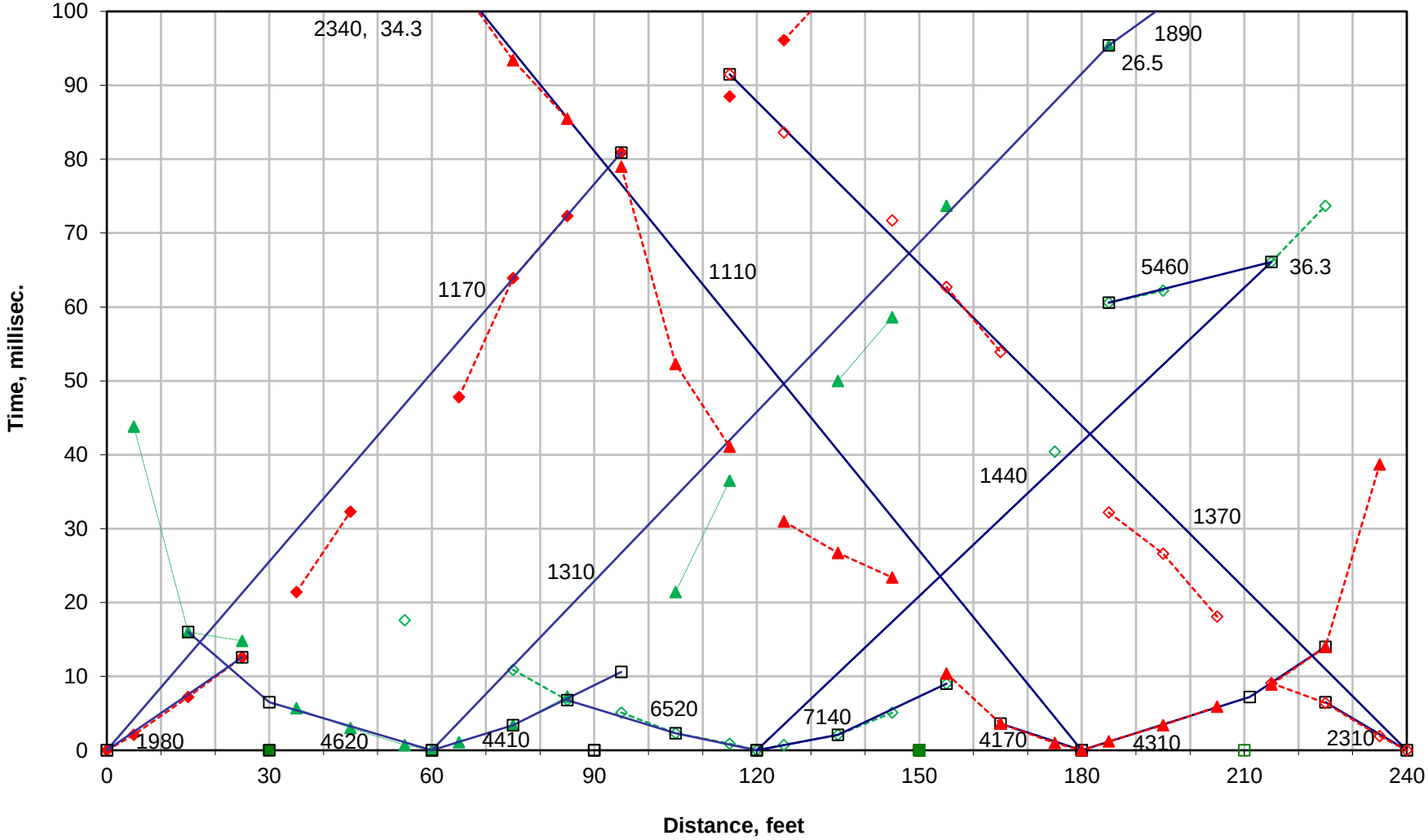

Line 11

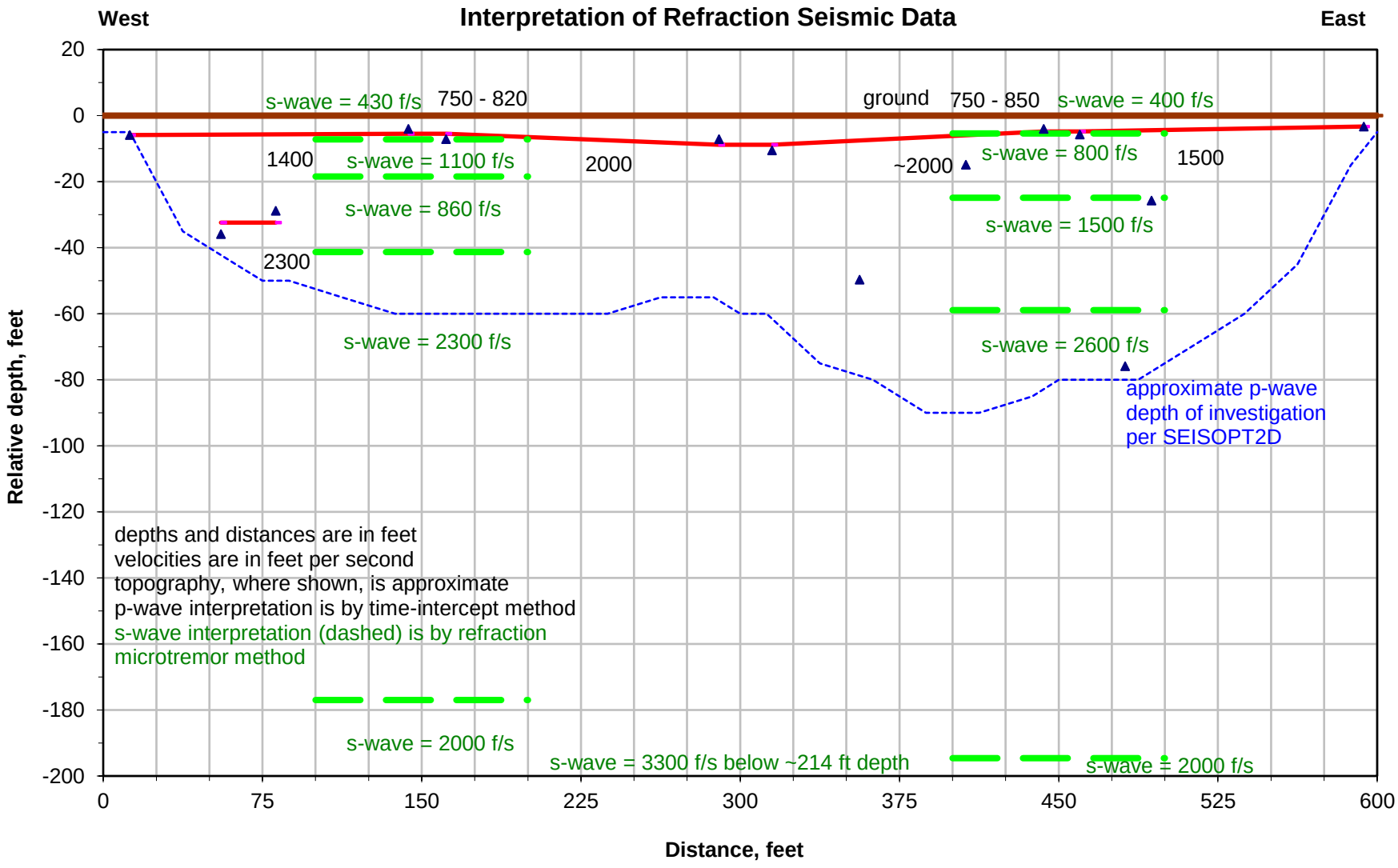
West
Interpretation of Refraction Seismic Data
East
s-wave = 430 f/s
750 - 820
ground
750 - 850
s-wave = 400 f/s
1400
s-wave = 1100 f/s
2000
~2000
s-wave = 800 f/s
1500
s-wave = 860 f/s
s-wave = 1500 f/s
2300
s-wave = 2300 f/s
s-wave = 2600 f/s
approximate p-wave
depth of investigation
per SEISOPT2D
depths and distances are in feet
velocities are in feet per second
topography, where shown, is approximate
p-wave interpretation is by time-intercept method
s-wave interpretation (dashed) is by refraction
microtremor method
s-wave = 2000 f/s
s-wave = 3300 f/s below ~214 ft depth
s-wave = 2000 f/s
Relative depth, feet
Distance, feet
20
0
-20
-40
-60
-80
-100
-120
-140
-160
-180
-200
0
75
150
225
300
375
450
525
600

Line 11

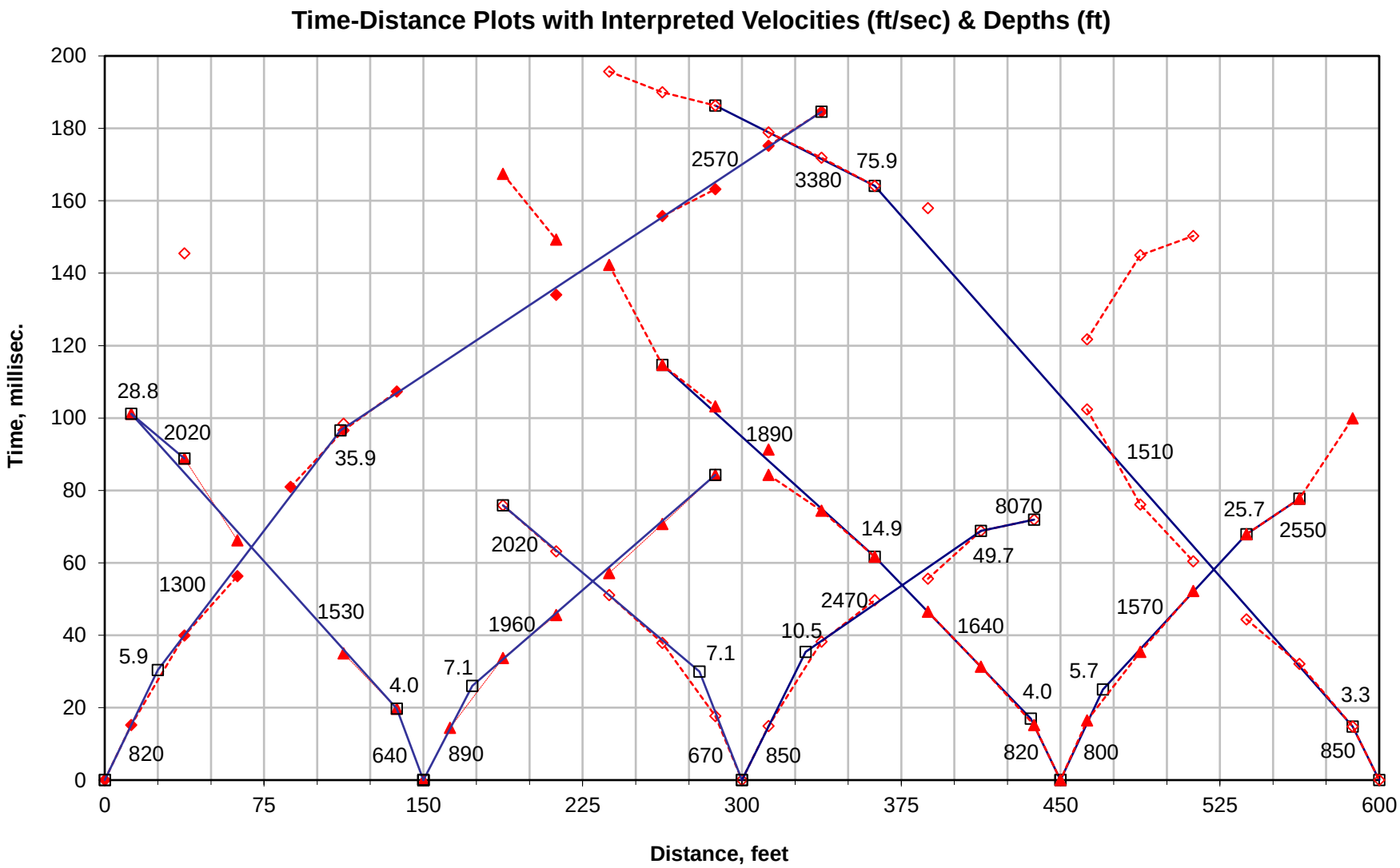
Time-Distance Plots with Interpreted Velocities (ft/sec) & Depths (ft)
Time, millisec.
Distance, feet
0
20
40
60
80
100
120
140
160
180
200
0
75
150
225
300
375
450
525
600
28.8
2020
5.9
1300
820
35.9
2570
1530
4.0
640
7.1
1960
890
2020
7.1
670
1890
14.9
2470
10.5
850
75.9
3380
1640
8070
49.7
4.0
820
1510
5.7
1570
800
25.7
2550
3.3
850

Line 12

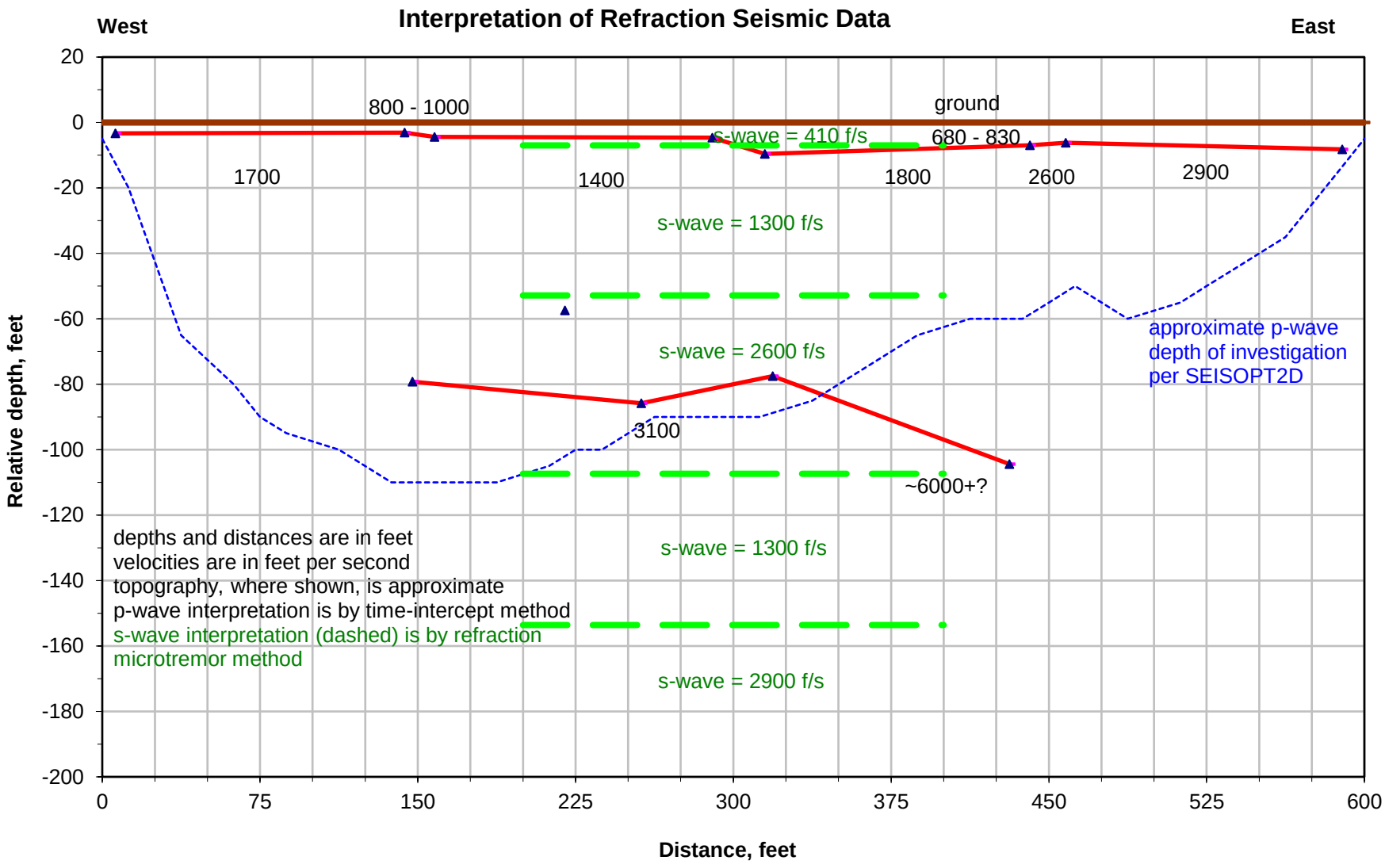
Interpretation of Refraction Seismic Data
West
East
Relative depth, feet
Distance, feet
20
0
-20
-40
-60
-80
-100
-120
-140
-160
-180
-200
0
75
150
225
300
375
450
525
600
800 - 1000
ground
s-wave = 410 f/s
680 - 830
1700
1400
1800
2600
2900
s-wave = 1300 f/s
s-wave = 2600 f/s
approximate p-wave
depth of investigation
per SEISOPT2D
3100
~6000+?
s-wave = 1300 f/s
s-wave = 2900 f/s
depths and distances are in feet
velocities are in feet per second
topography, where shown, is approximate
p-wave interpretation is by time-intercept method
s-wave interpretation (dashed) is by refraction
microtremor method

Line 12

Time-Distance Plots with Interpreted Velocities (ft/sec) & Depths (ft)

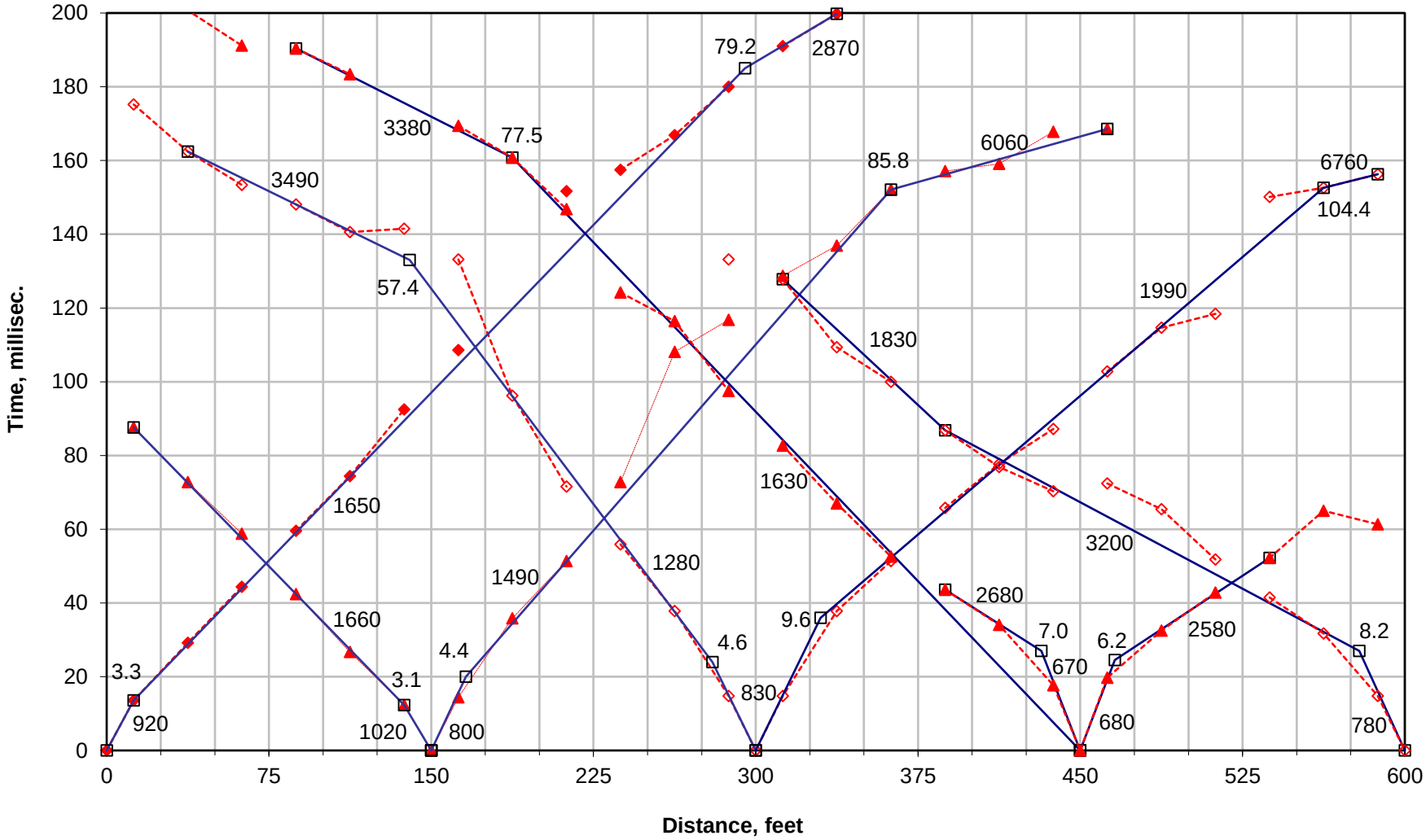

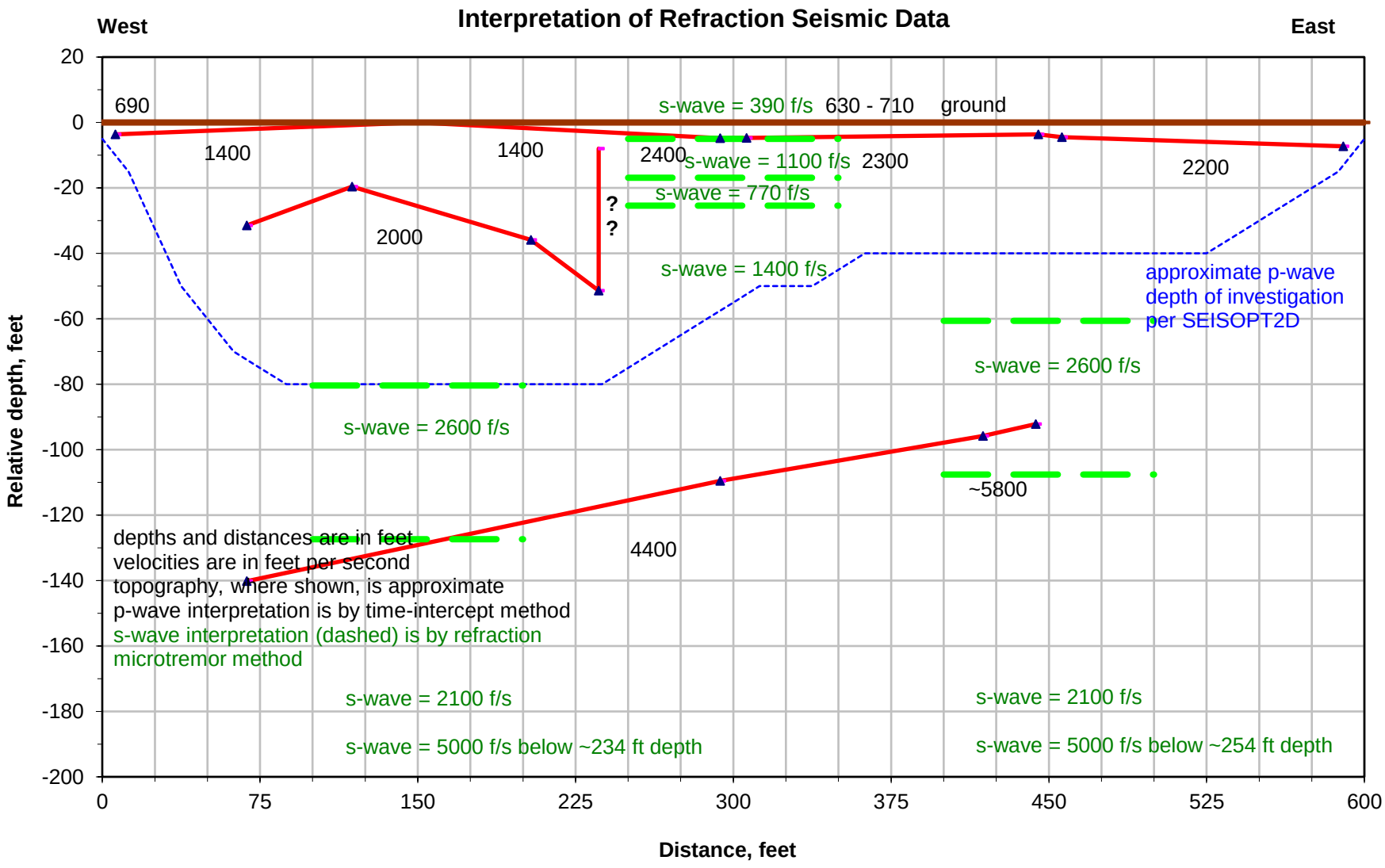
Interpretation of Refraction Seismic Data
West
East
690
s-wave = 390 f/s
630 - 710
ground
1400
1400
2400
s-wave = 1100 f/s
2300
2200
s-wave = 770 f/s
?
?
2000
s-wave = 1400 f/s
approximate p-wave
depth of investigation
per SEISOPT2D
s-wave = 2600 f/s
s-wave = 2600 f/s
~5800
4400
depths and distances are in feet
velocities are in feet per second
topography, where shown, is approximate
p-wave interpretation is by time-intercept method
s-wave interpretation (dashed) is by refraction
microtremor method
s-wave = 2100 f/s
s-wave = 2100 f/s
s-wave = 5000 f/s below ~234 ft depth
s-wave = 5000 f/s below ~254 ft depth
Relative depth, feet
Distance, feet
20
0
-20
-40
-60
-80
-100
-120
-140
-160
-180
-200
0
75
150
225
300
375
450
525
600

Line 13

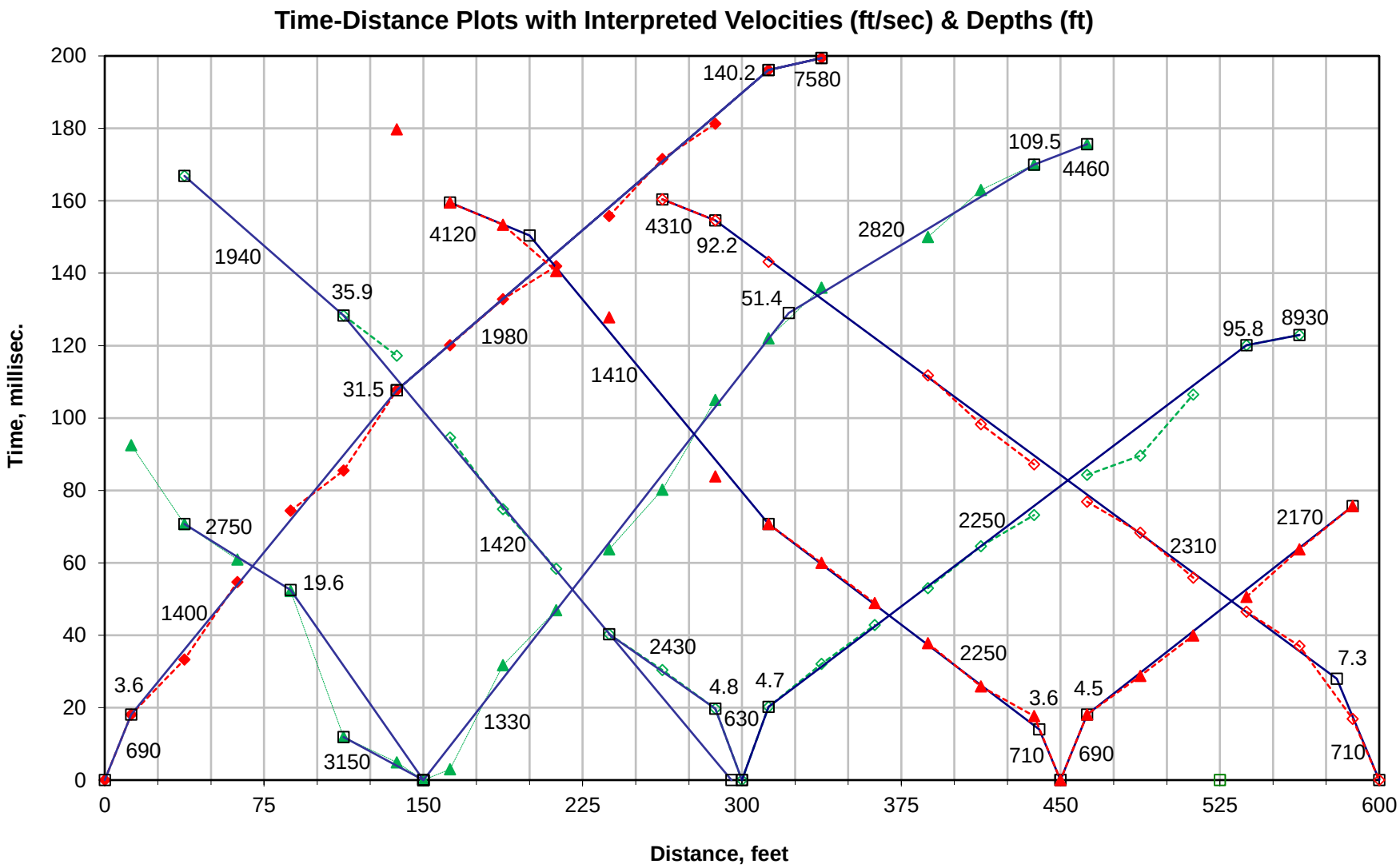
Time-Distance Plots with Interpreted Velocities (ft/sec) & Depths (ft)
Time, millisec.
Distance, feet
0
20
40
60
80
100
120
140
160
180
200
0
75
150
225
300
375
450
525
600
140.2
7580
109.5
4460
4120
4310
92.2
2820
1940
35.9
51.4
95.8
8930
1980
1410
31.5
2750
2250
2170
1420
2310
19.6
1400
2430
2250
7.3
3.6
4.8
4.7
4.5
3.6
1330
630
690
3150
710
690
710

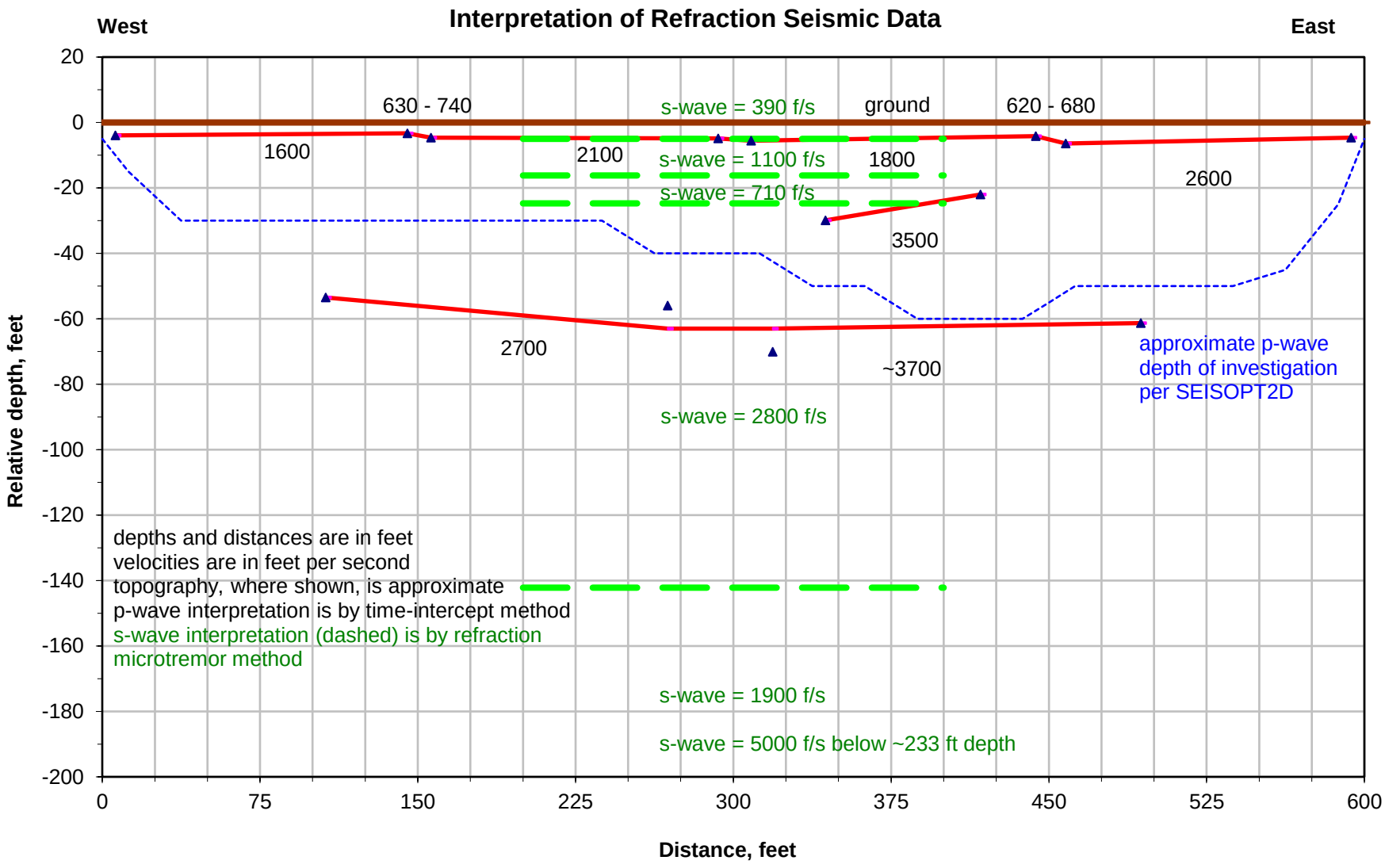
Interpretation of Refraction Seismic Data
West
East
630 - 740
s-wave = 390 f/s
ground
620 - 680
1600
2100
s-wave = 1100 f/s
1800
2600
s-wave = 710 f/s
3500
2700
~3700
approximate p-wave
depth of investigation
per SEISOPT2D
s-wave = 2800 f/s
depths and distances are in feet
velocities are in feet per second
topography, where shown, is approximate
p-wave interpretation is by time-intercept method
s-wave interpretation (dashed) is by refraction
microtremor method
s-wave = 1900 f/s
s-wave = 5000 f/s below ~233 ft depth
Relative depth, feet
20
0
-20
-40
-60
-80
-100
-120
-140
-160
-180
-200
0
75
150
225
300
375
450
525
600
Distance, feet

Line 14

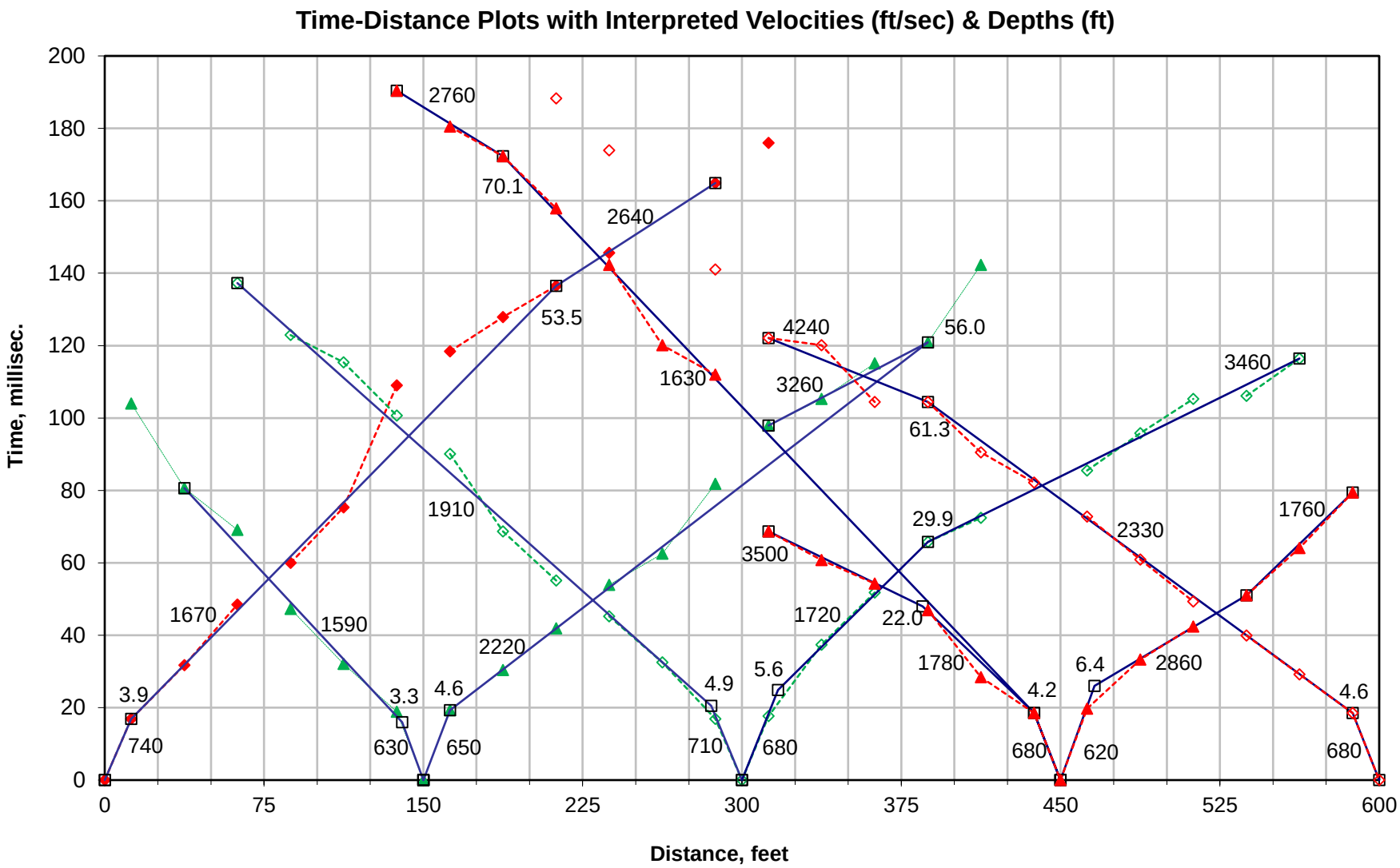
Time-Distance Plots with Interpreted Velocities (ft/sec) & Depths (ft)
Time, millisec.
Distance, feet
0
20
40
60
80
100
120
140
160
180
200
0
75
150
225
300
375
450
525
600
2760
70.1
2640
53.5
1630
4240
56.0
3260
61.3
3460
1910
29.9
2330
1760
3500
1670
1590
1720
22.0
2220
1780
6.4
2860
5.6
4.9
4.2
4.6
3.9
3.3
4.6
740
630
650
710
680
680
620
680

Line 15

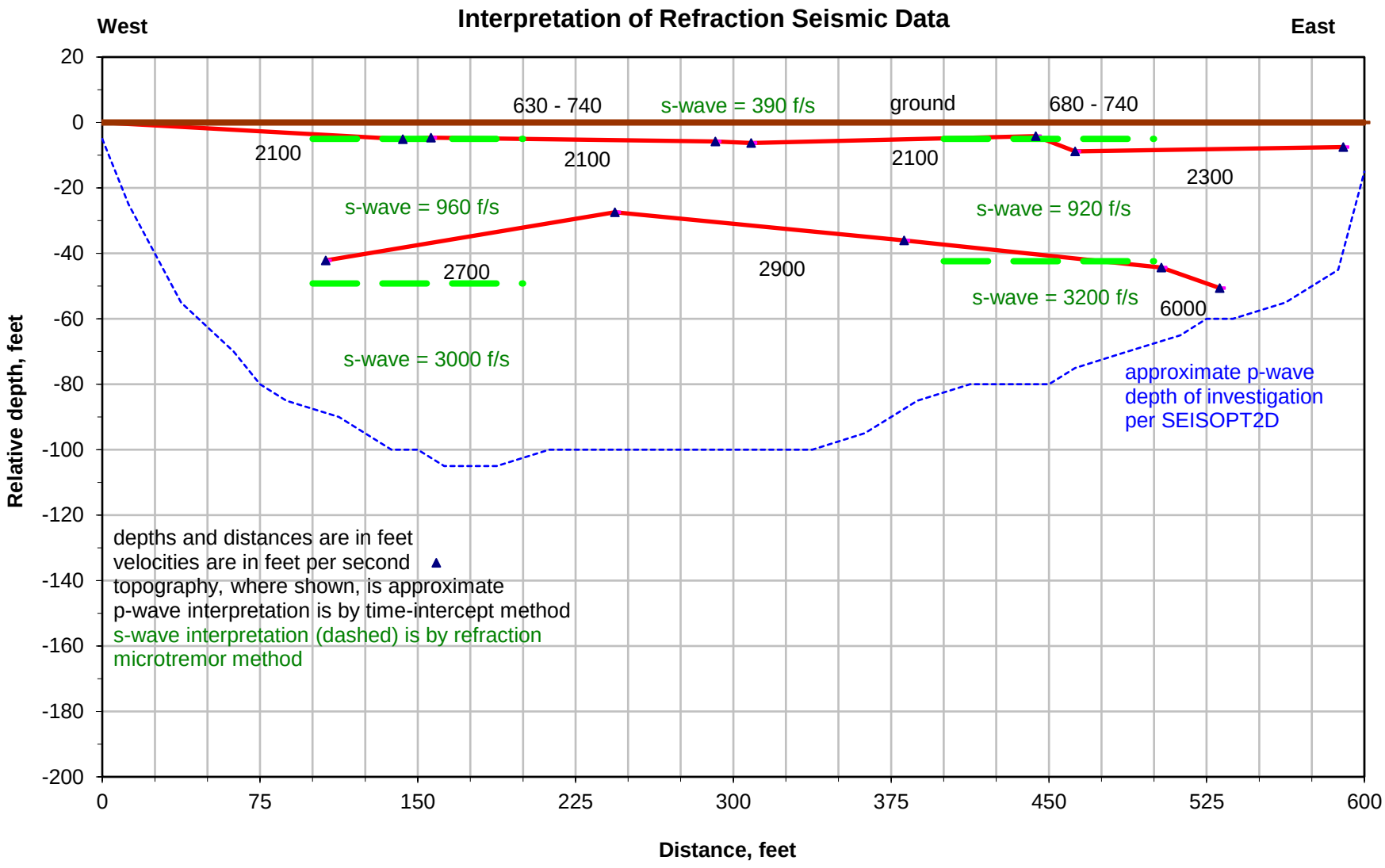
Interpretation of Refraction Seismic Data
West
East
630 - 740
s-wave = 390 f/s
ground
680 - 740
2100
2100
2100
2300
s-wave = 960 f/s
s-wave = 920 f/s
2700
2900
s-wave = 3200 f/s
6000
s-wave = 3000 f/s
approximate p-wave
depth of investigation
per SEISOPT2D
depths and distances are in feet
velocities are in feet per second
topography, where shown, is approximate
p-wave interpretation is by time-intercept method
s-wave interpretation (dashed) is by refraction
microtremor method
Relative depth, feet
Distance, feet
20
0
-20
-40
-60
-80
-100
-120
-140
-160
-180
-200
0
75
150
225
300
375
450
525
600

Time-Distance Plots with Interpreted Velocities (ft/sec) & Depths (ft)

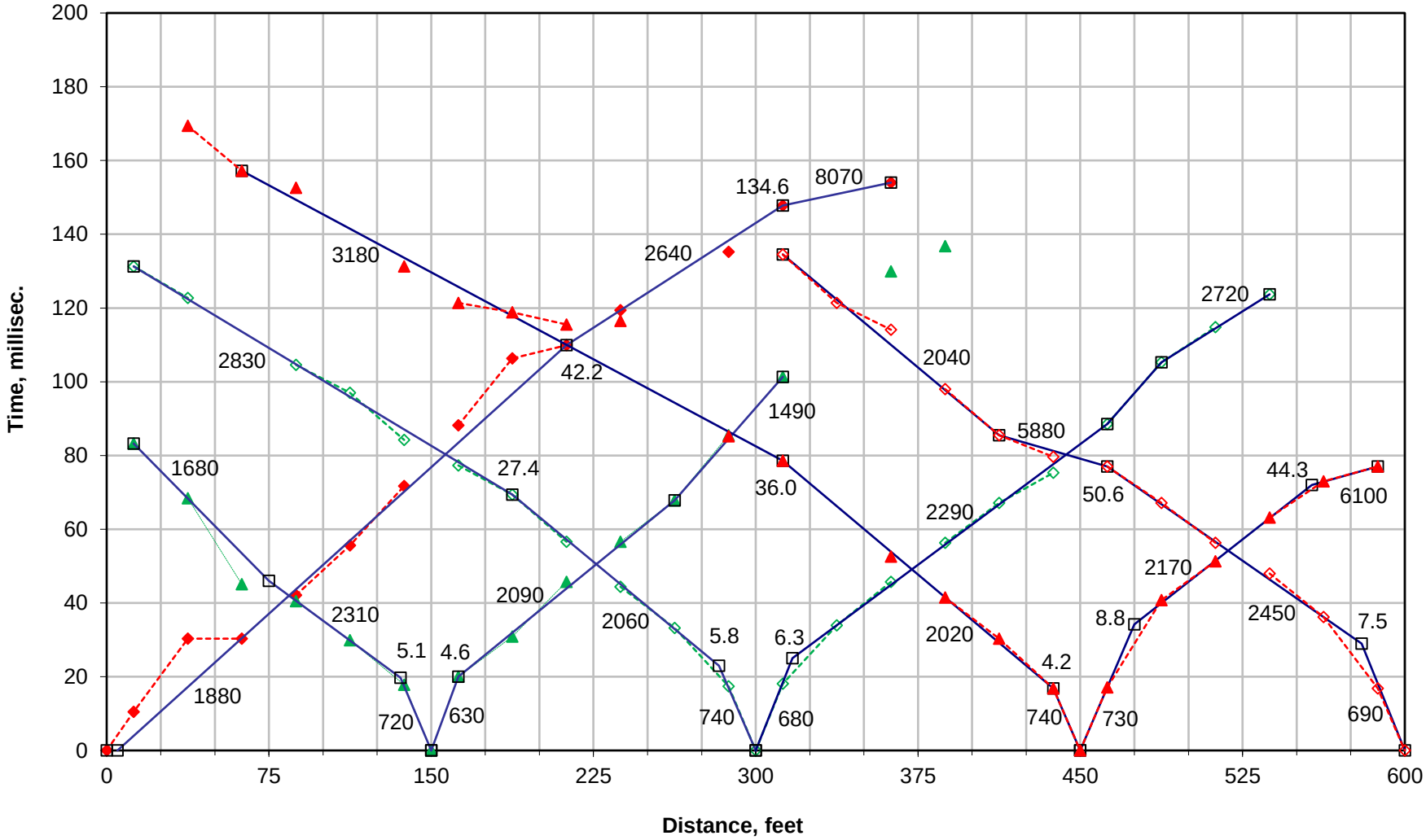

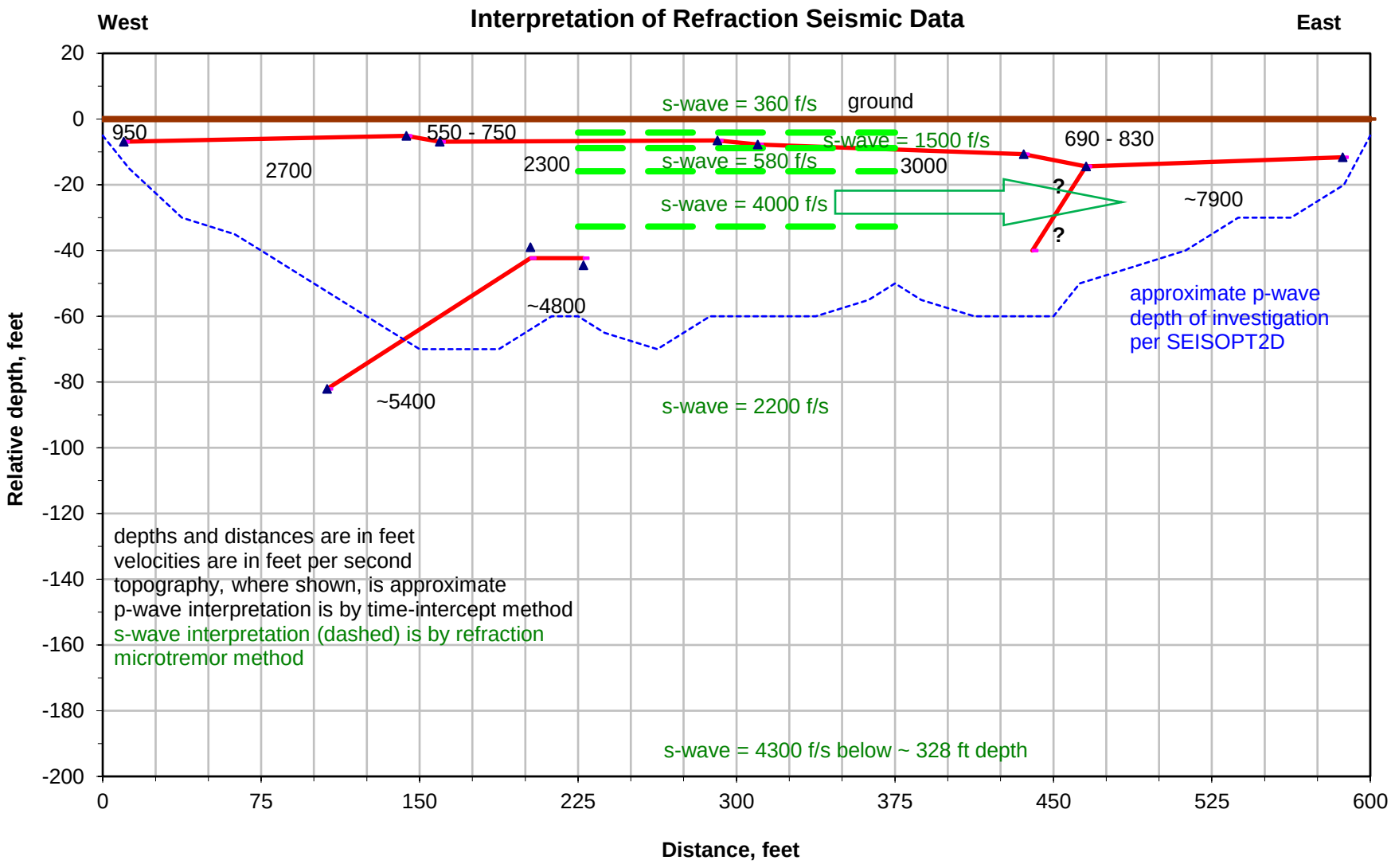
Interpretation of Refraction Seismic Data
West
East
Relative depth, feet
Distance, feet
20
0
-20
-40
-60
-80
-100
-120
-140
-160
-180
-200
0
75
150
225
300
375
450
525
600
ground
s-wave = 360 f/s
s-wave = 1500 f/s
s-wave = 580 f/s
s-wave = 4000 f/s
s-wave = 2200 f/s
s-wave = 4300 f/s below ~ 328 ft depth
950
2700
550 - 750
2300
3000
690 - 830
~7900
~4800
~5400
?
?
approximate p-wave
depth of investigation
per SEISOPT2D
depths and distances are in feet
velocities are in feet per second
topography, where shown, is approximate
p-wave interpretation is by time-intercept method
s-wave interpretation (dashed) is by refraction
microtremor method

Time-Distance Plots with Interpreted Velocities (ft/sec) & Depths (ft)

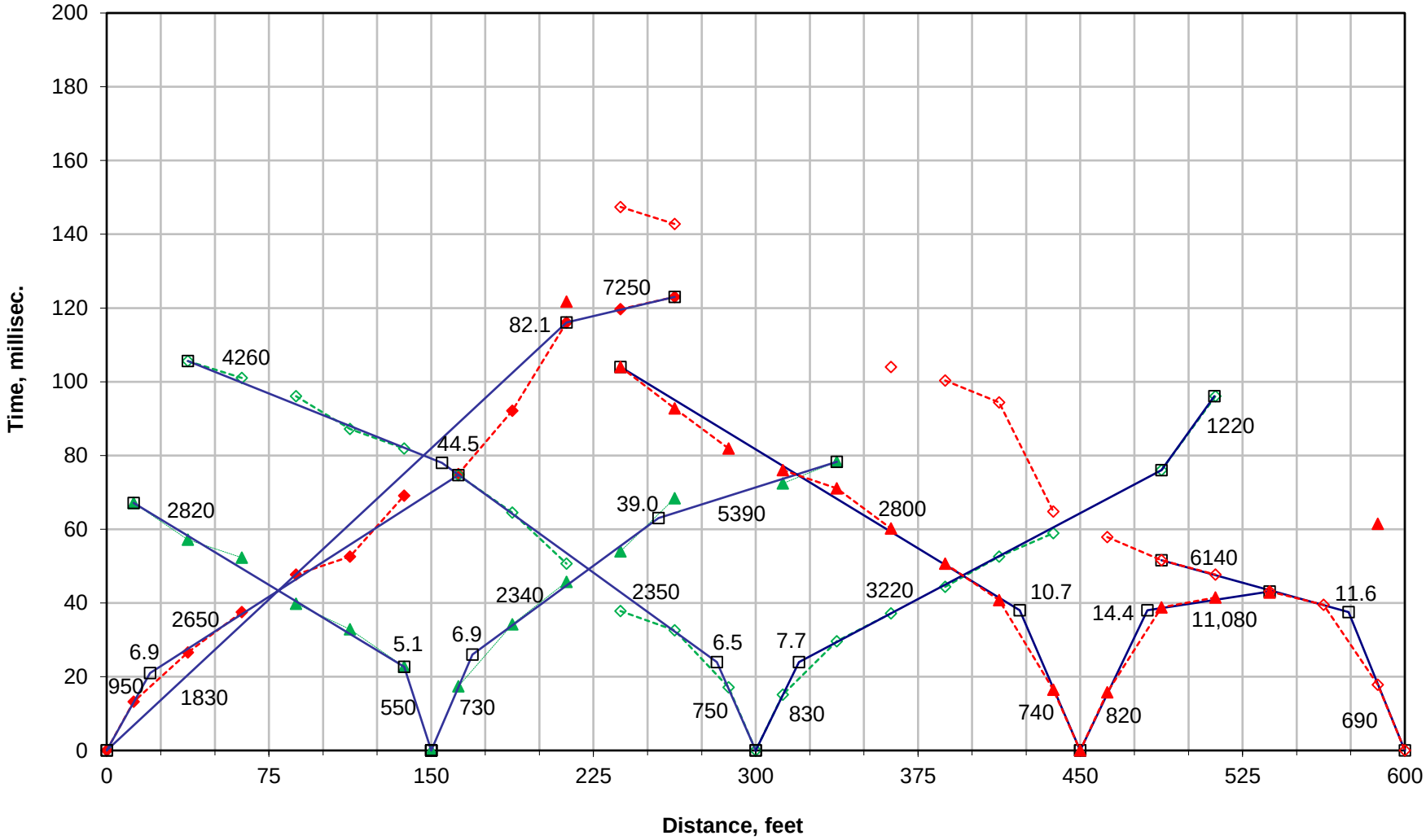

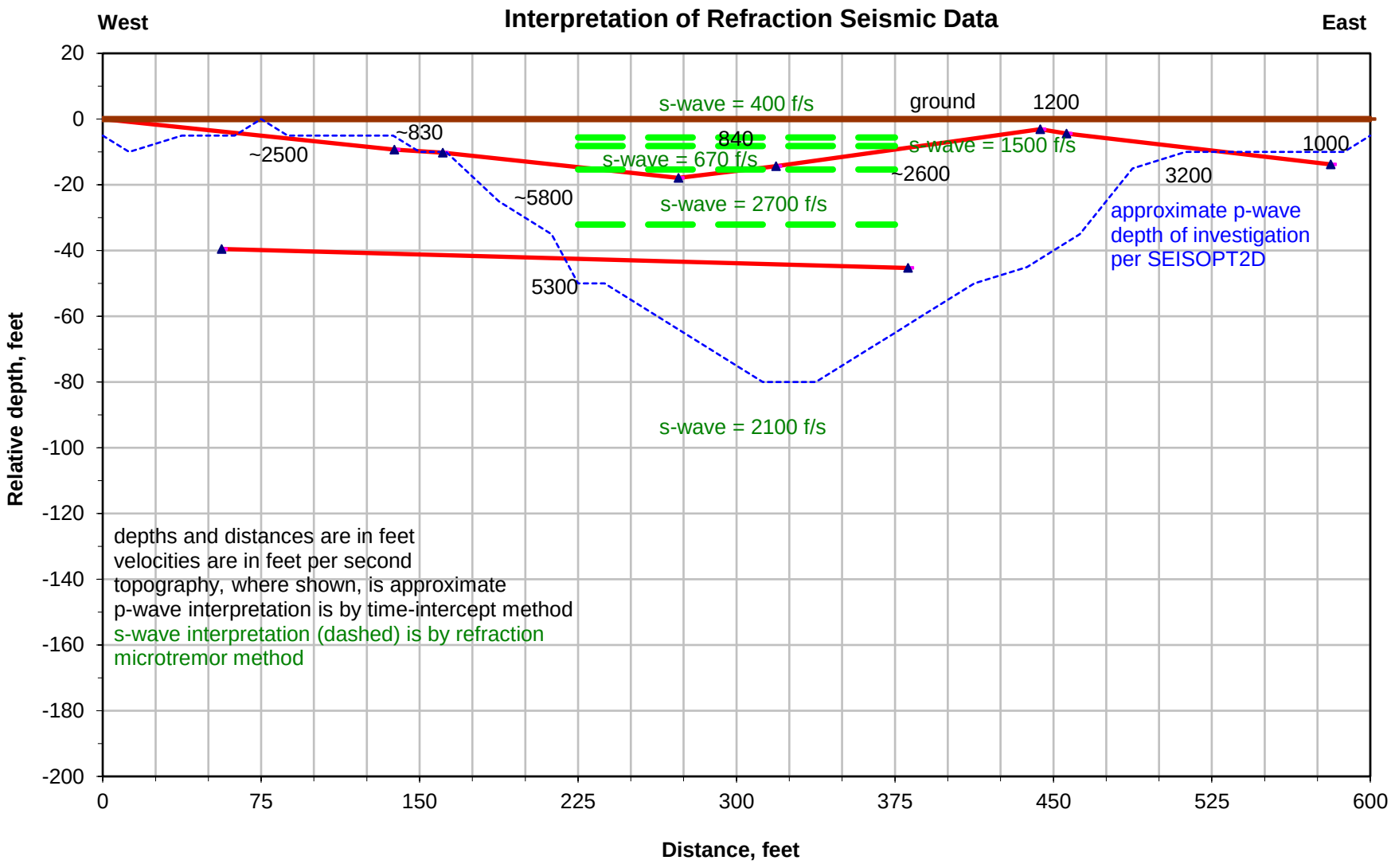
Interpretation of Refraction Seismic Data
West
East
s-wave = 400 f/s
ground
1200
~830
840
s-wave = 1500 f/s
1000
~2500
s-wave = 670 f/s
~2600
3200
~5800
s-wave = 2700 f/s
approximate p-wave
depth of investigation
per SEISOPT2D
5300
s-wave = 2100 f/s
depths and distances are in feet
velocities are in feet per second
topography, where shown, is approximate
p-wave interpretation is by time-intercept method
s-wave interpretation (dashed) is by refraction
microtremor method
Relative depth, feet
20
0
-20
-40
-60
-80
-100
-120
-140
-160
-180
-200
0
75
150
225
300
375
450
525
600
Distance, feet

Line 17

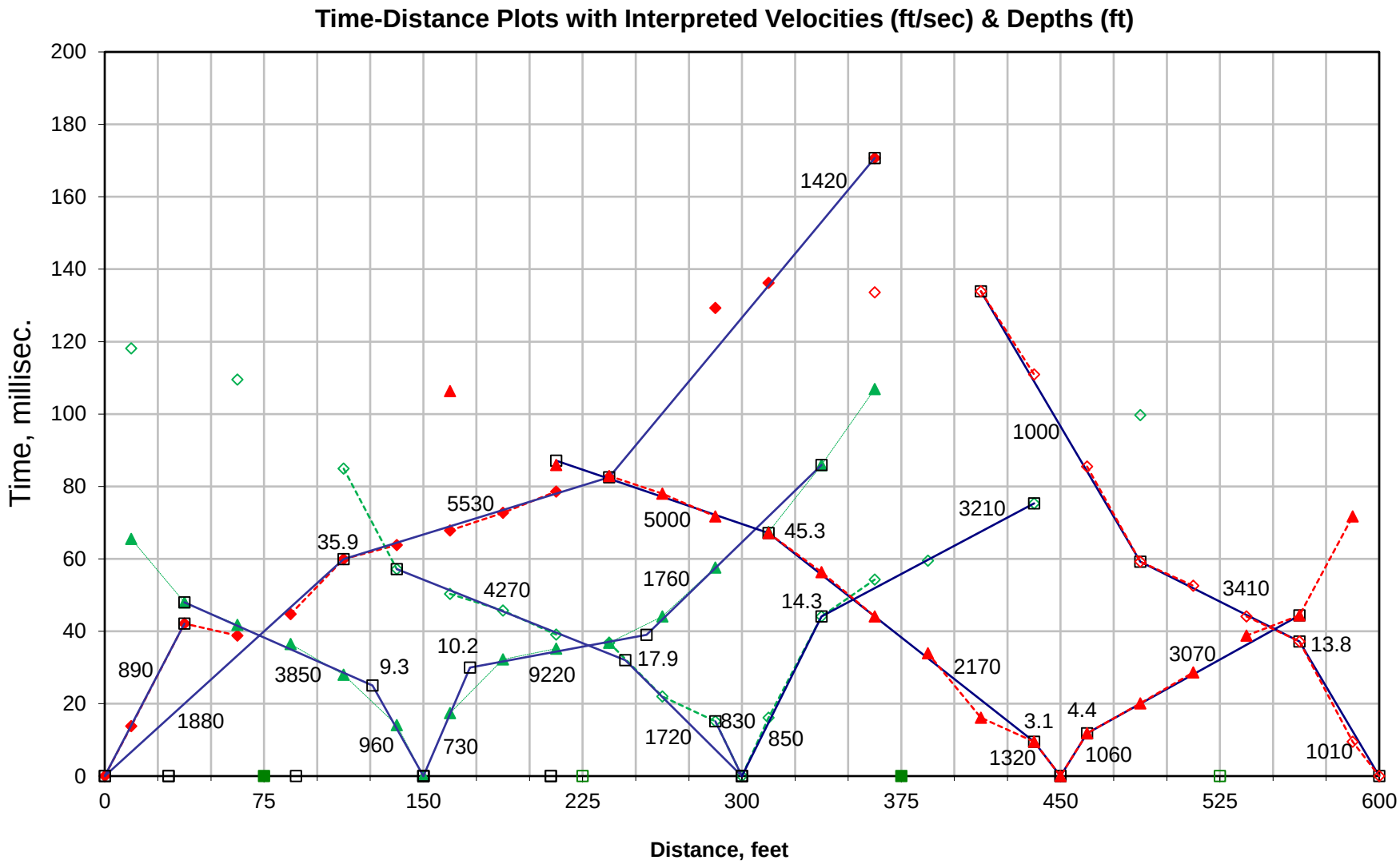
Time-Distance Plots with Interpreted Velocities (ft/sec) & Depths (ft)
Time, millisec.
Distance, feet
0
20
40
60
80
100
120
140
160
180
200
0
75
150
225
300
375
450
525
600
1420
1000
5530
5000
45.3
3210
35.9
4270
1760
14.3
3410
10.2
9.3
17.9
890
3850
9220
2170
3070
13.8
1880
830
4.4
3.1
960
730
1720
850
1320
1060
1010

Line 18

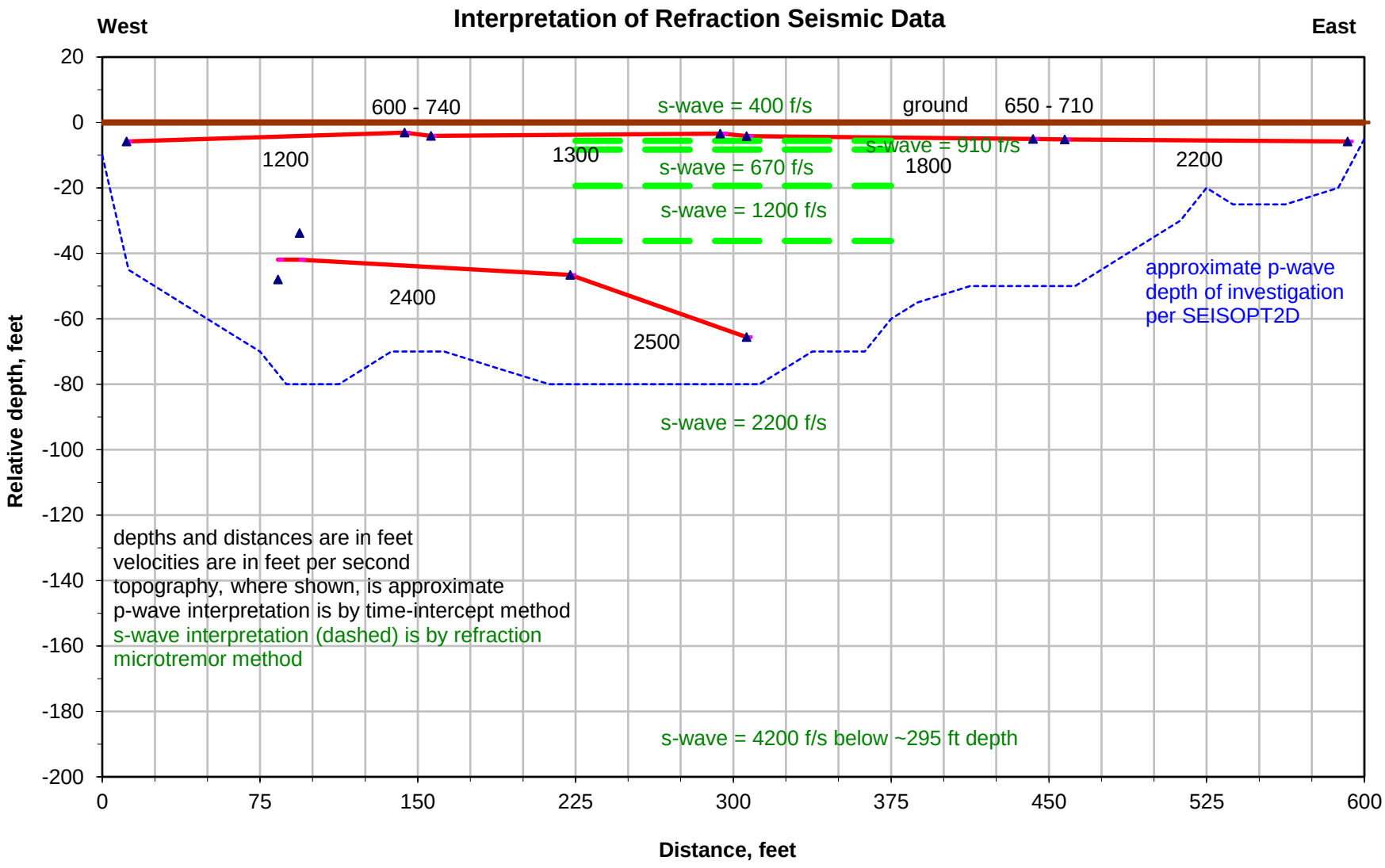
Interpretation of Refraction Seismic Data
West
East
Relative depth, feet
Distance, feet
20
0
-20
-40
-60
-80
-100
-120
-140
-160
-180
-200
0
75
150
225
300
375
450
525
600
600 - 740
s-wave = 400 f/s
ground
650 - 710
1200
1300
s-wave = 910 f/s
1800
2200
s-wave = 670 f/s
s-wave = 1200 f/s
2400
2500
approximate p-wave
depth of investigation
per SEISOPT2D
s-wave = 2200 f/s
depths and distances are in feet
velocities are in feet per second
topography, where shown, is approximate
p-wave interpretation is by time-intercept method
s-wave interpretation (dashed) is by refraction
microtremor method
s-wave = 4200 f/s below ~295 ft depth

Line 18

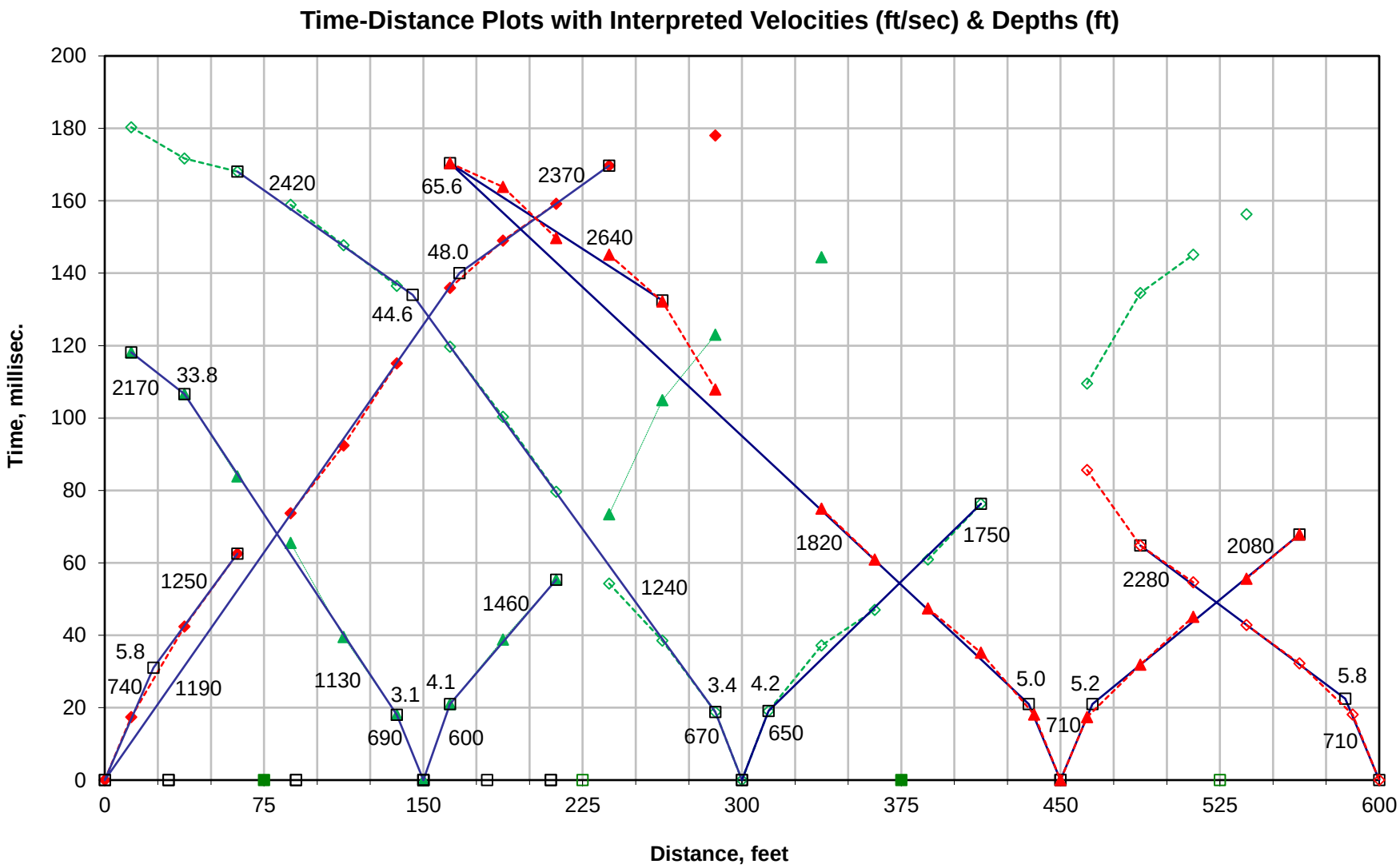
Time-Distance Plots with Interpreted Velocities (ft/sec) & Depths (ft)
Time, millisec.
Distance, feet
0
20
40
60
80
100
120
140
160
180
200
0
75
150
225
300
375
450
525
600
2420
65.6
2370
2640
48.0
44.6
2170
33.8
1250
5.8
740
1190
1130
3.1
690
4.1
600
1460
1240
3.4
670
4.2
650
1750
1820
5.0
710
5.2
2280
2080
5.8
710

Line 19

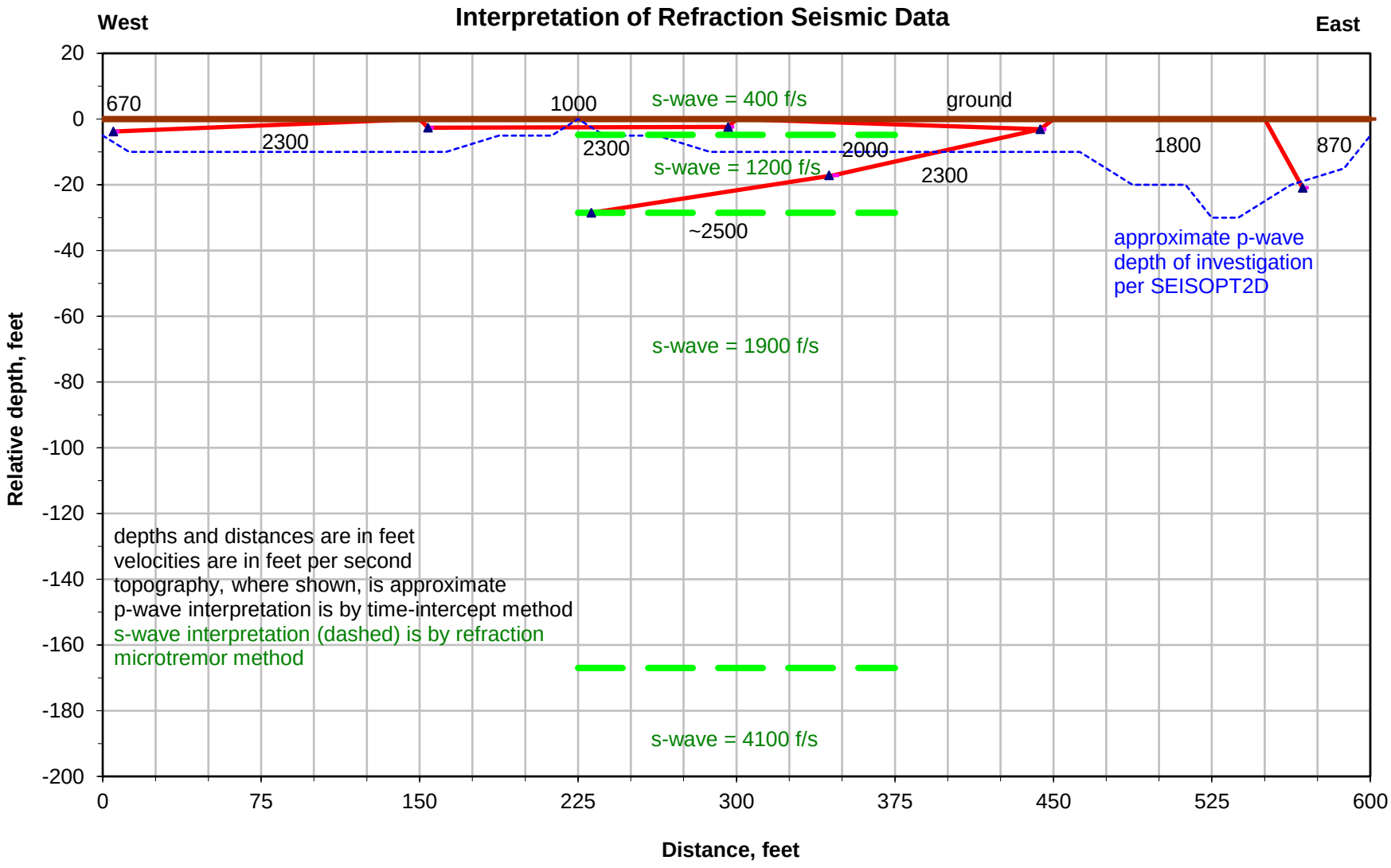
Interpretation of Refraction Seismic Data
West
East
670
1000
s-wave = 400 f/s
ground
2300
2300
2000
1800
870
s-wave = 1200 f/s
2300
~2500
approximate p-wave
depth of investigation
per SEISOPT2D
s-wave = 1900 f/s
depths and distances are in feet
velocities are in feet per second
topography, where shown, is approximate
p-wave interpretation is by time-intercept method
s-wave interpretation (dashed) is by refraction
microtremor method
s-wave = 4100 f/s
Relative depth, feet
20
0
-20
-40
-60
-80
-100
-120
-140
-160
-180
-200
0
75
150
225
300
375
450
525
600
Distance, feet

Time-Distance Plots with Interpreted Velocities (ft/sec) & Depths (ft)

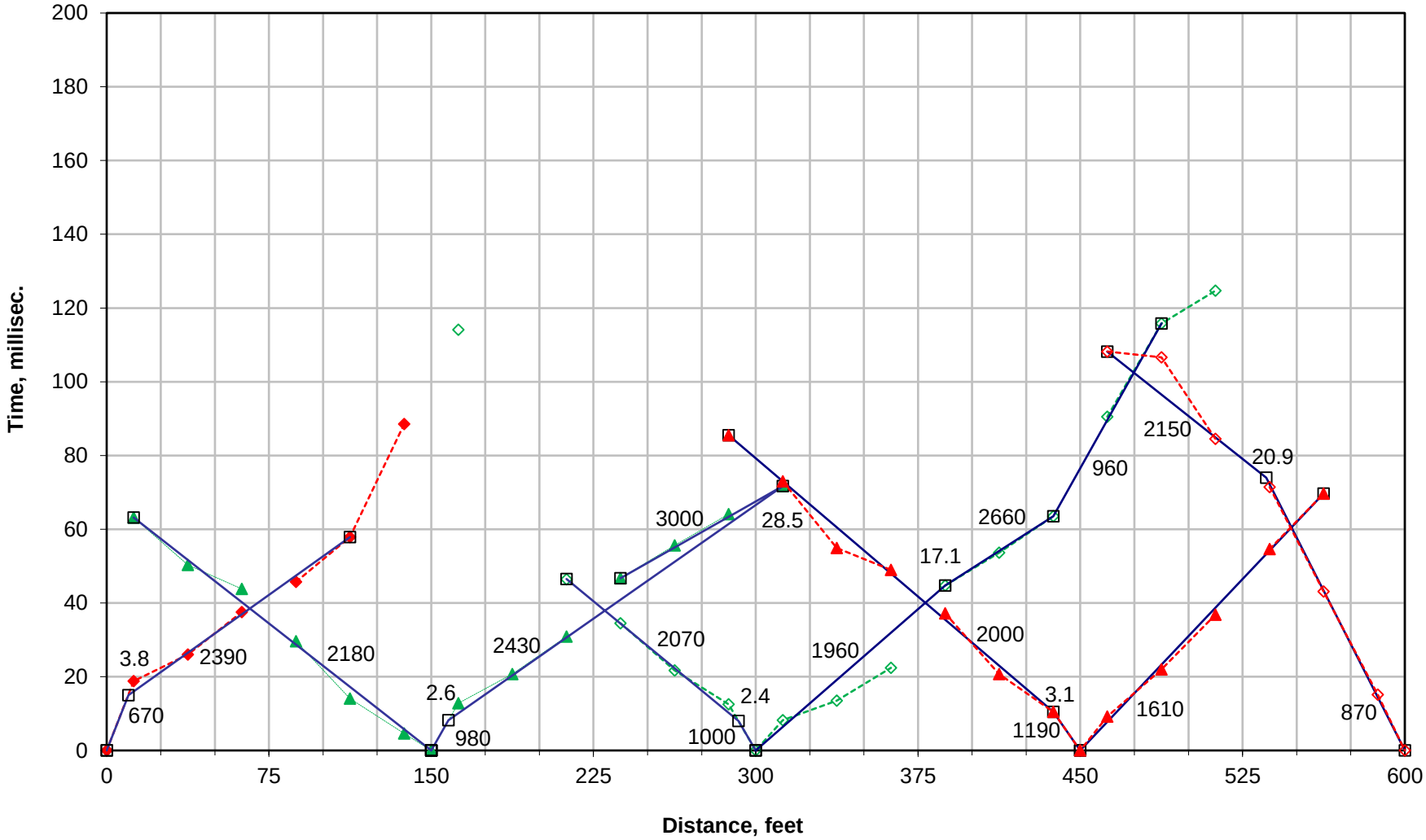

Line 20

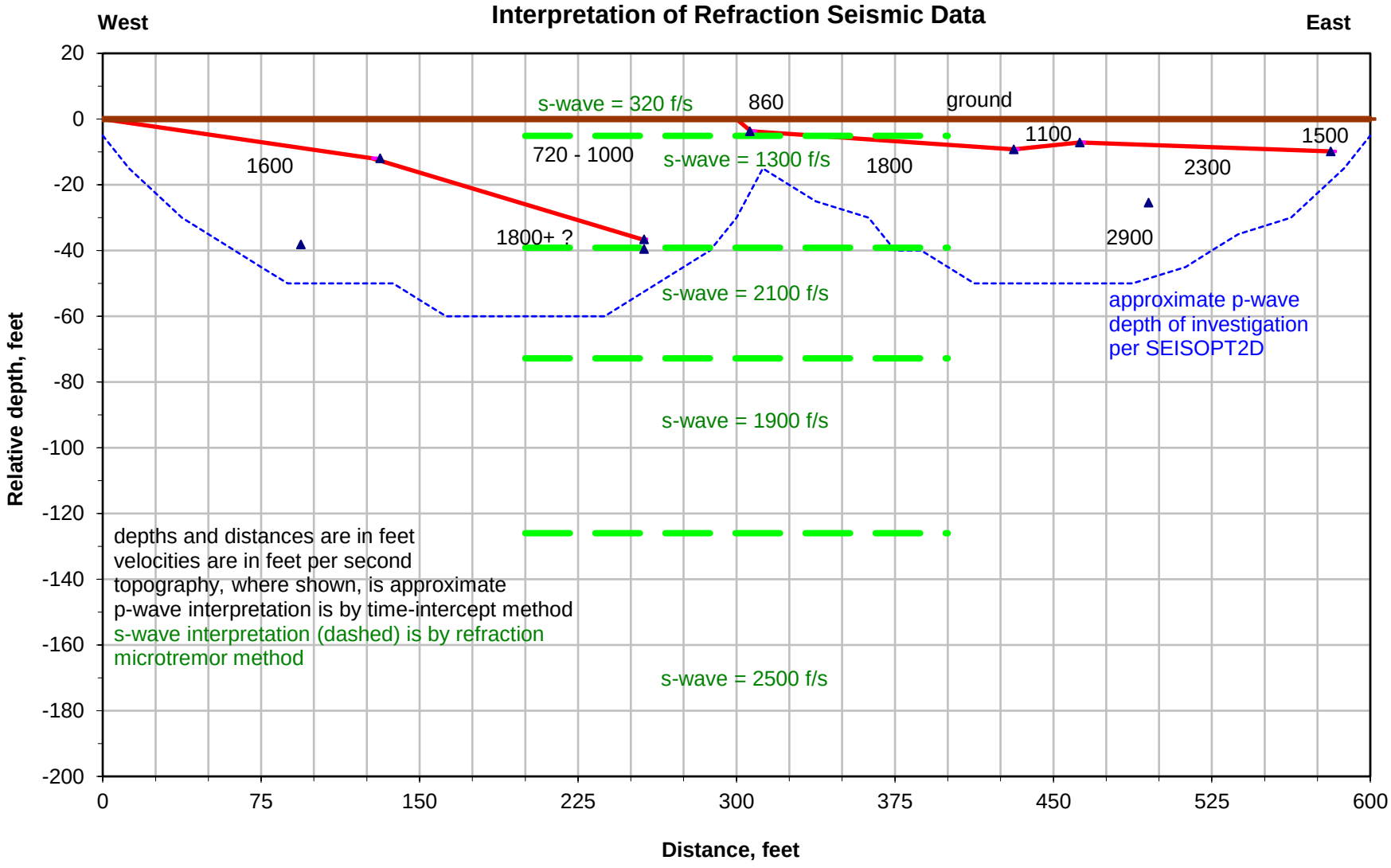
Interpretation of Refraction Seismic Data
West
East
s-wave = 320 f/s
860
ground
720 - 1000
s-wave = 1300 f/s
1600
1800
1100
1500
2300
1800+ ?
2900
s-wave = 2100 f/s
approximate p-wave
depth of investigation
per SEISOPT2D
s-wave = 1900 f/s
depths and distances are in feet
velocities are in feet per second
topography, where shown, is approximate
p-wave interpretation is by time-intercept method
s-wave interpretation (dashed) is by refraction
microtremor method
s-wave = 2500 f/s
Relative depth, feet
20
0
-20
-40
-60
-80
-100
-120
-140
-160
-180
-200
0
75
150
225
300
375
450
525
600
Distance, feet

Line 20

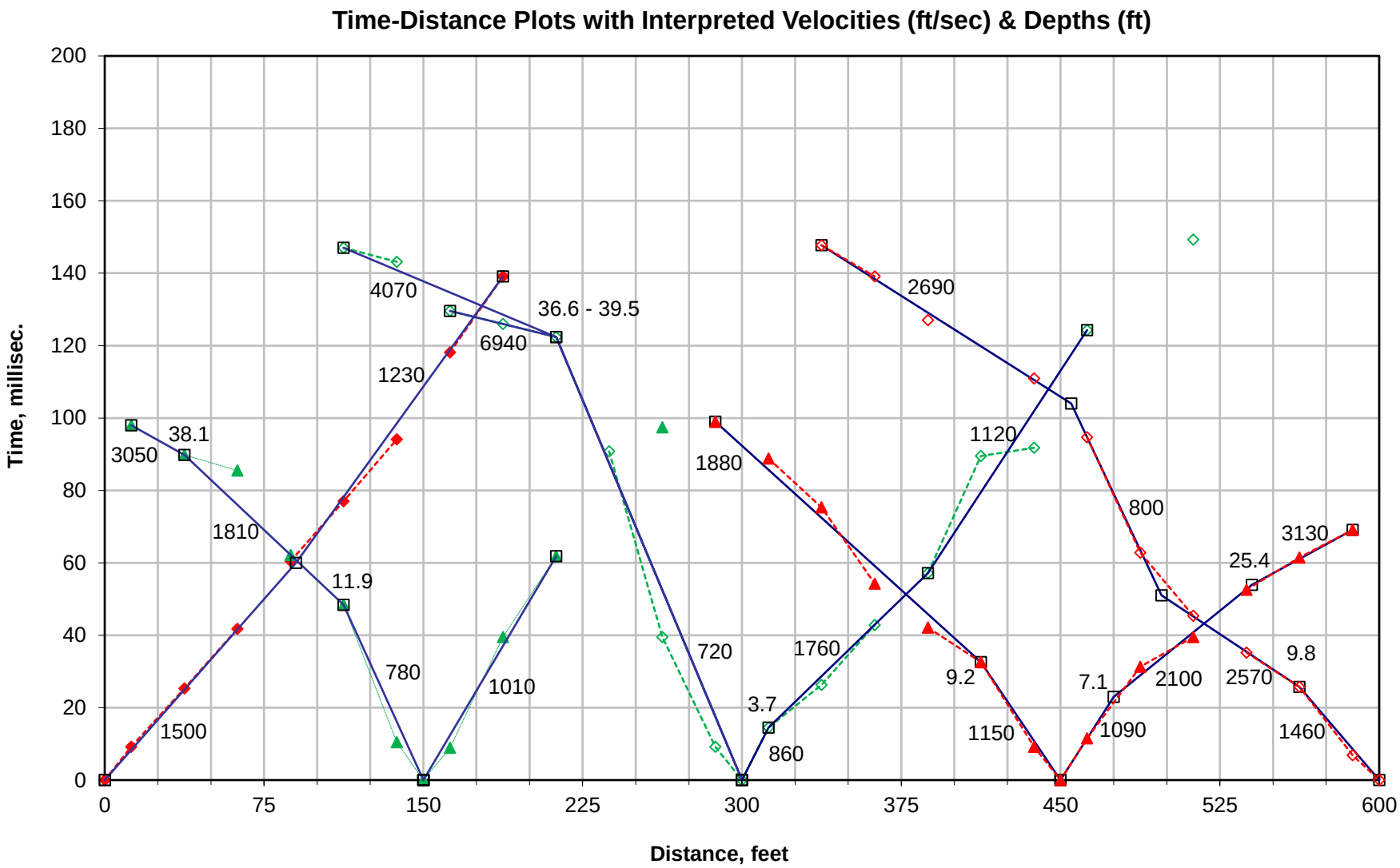
Time-Distance Plots with Interpreted Velocities (ft/sec) & Depths (ft)
Time, millisec.
Distance, feet
0
20
40
60
80
100
120
140
160
180
200
0
75
150
225
300
375
450
525
600
4070
36.6 - 39.5
6940
1230
38.1
3050
1810
11.9
780
1010
1500
720
1880
3.7
860
1760
1120
2690
9.2
1150
7.1
1090
800
2100
25.4
3130
2570
9.8
1460

Refraction Microtremor S-wave Interpretation **Line 1** Amec Foster Wheeler Job No. 17-2015-4061

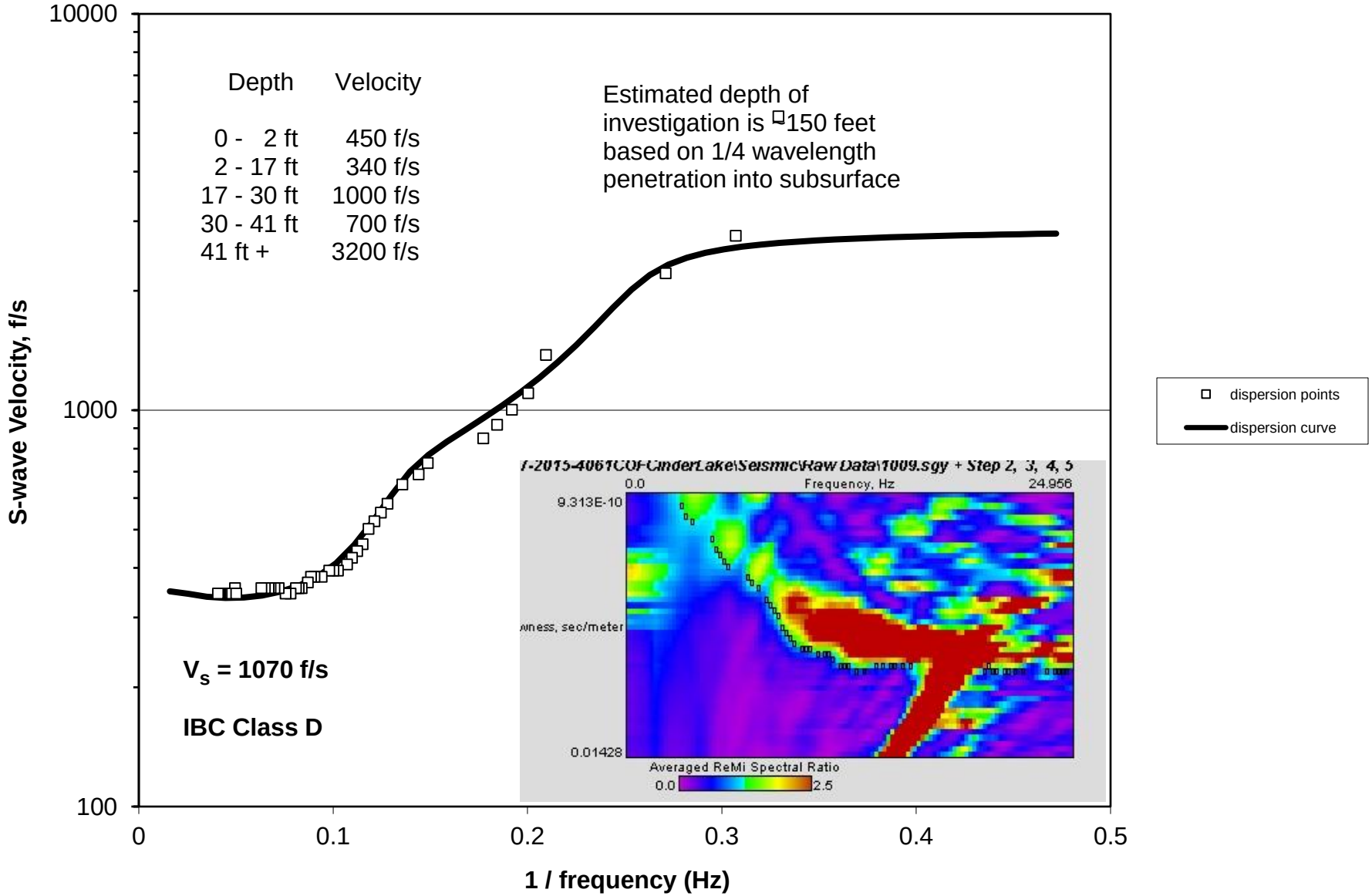

Refraction Microtremor S-wave Interpretation **Line 2** Amec Foster Wheeler Job No. 17-2015-4061

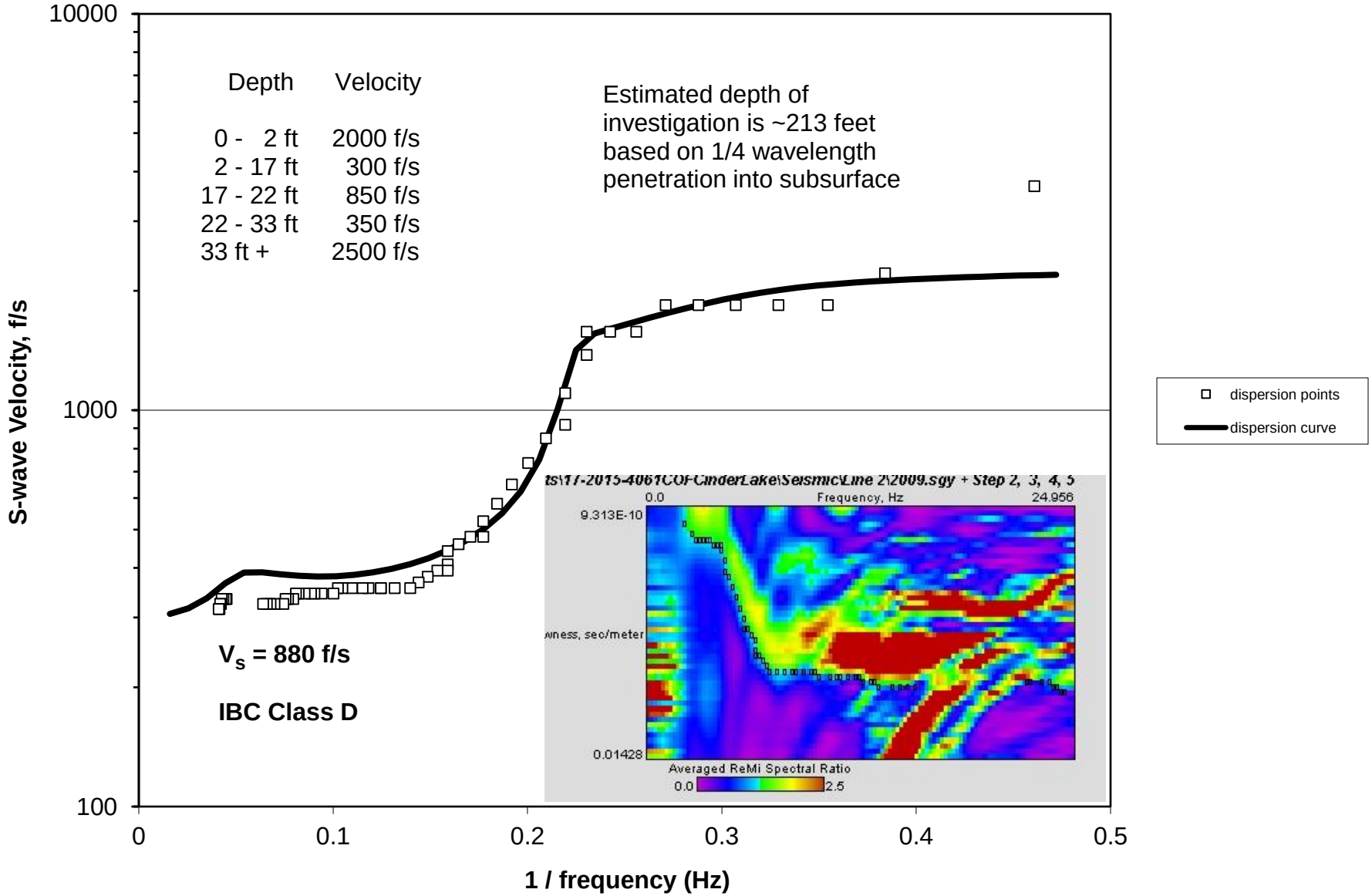

Refraction Microtremor S-wave Interpretation **Line 3A** Amec Foster Wheeler Job No. 17-2015-4061

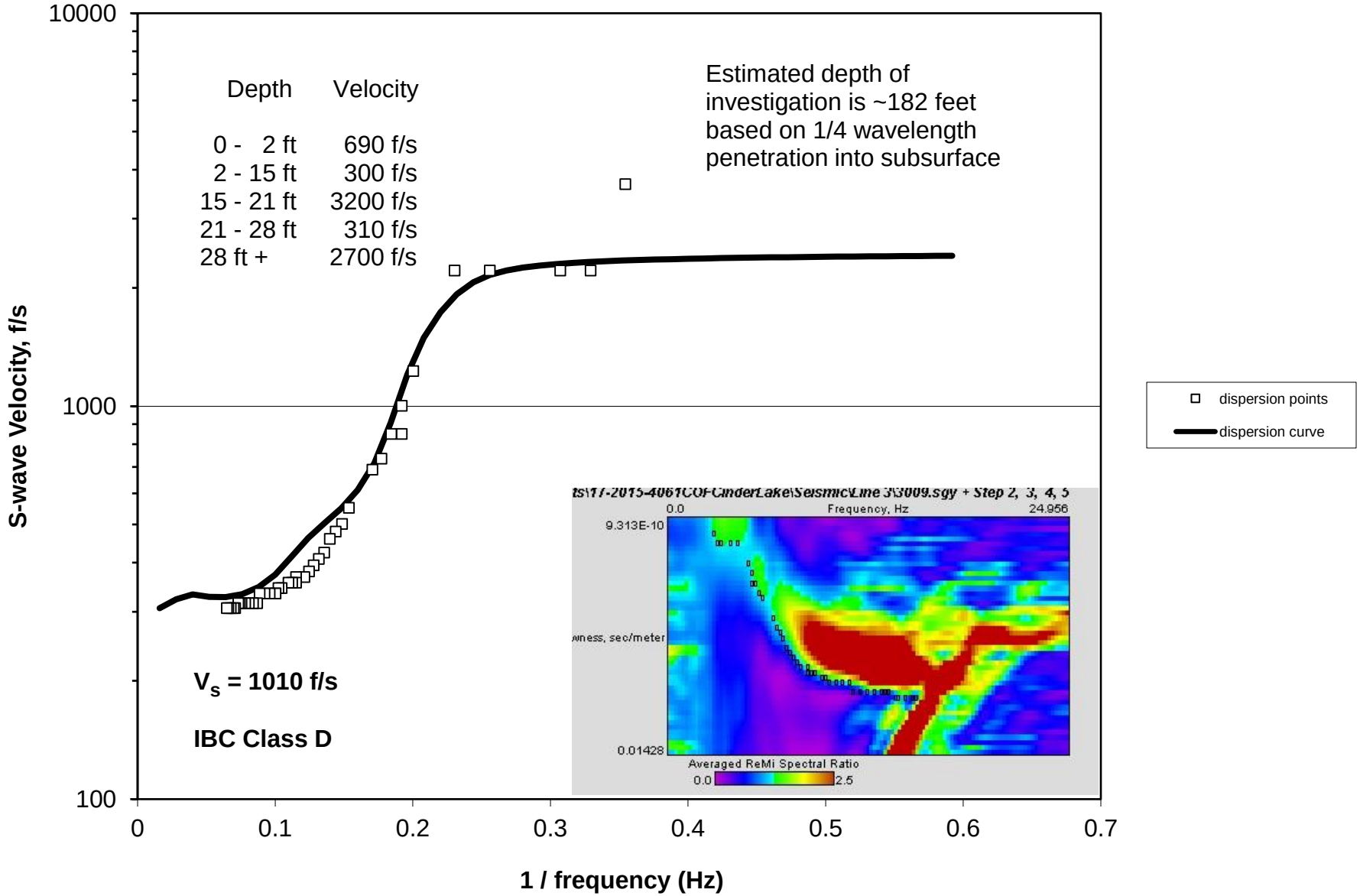

Refraction Microtremor S-wave Interpretation **Line 3B** Amec Foster Wheeler Job No. 17-2015-4061

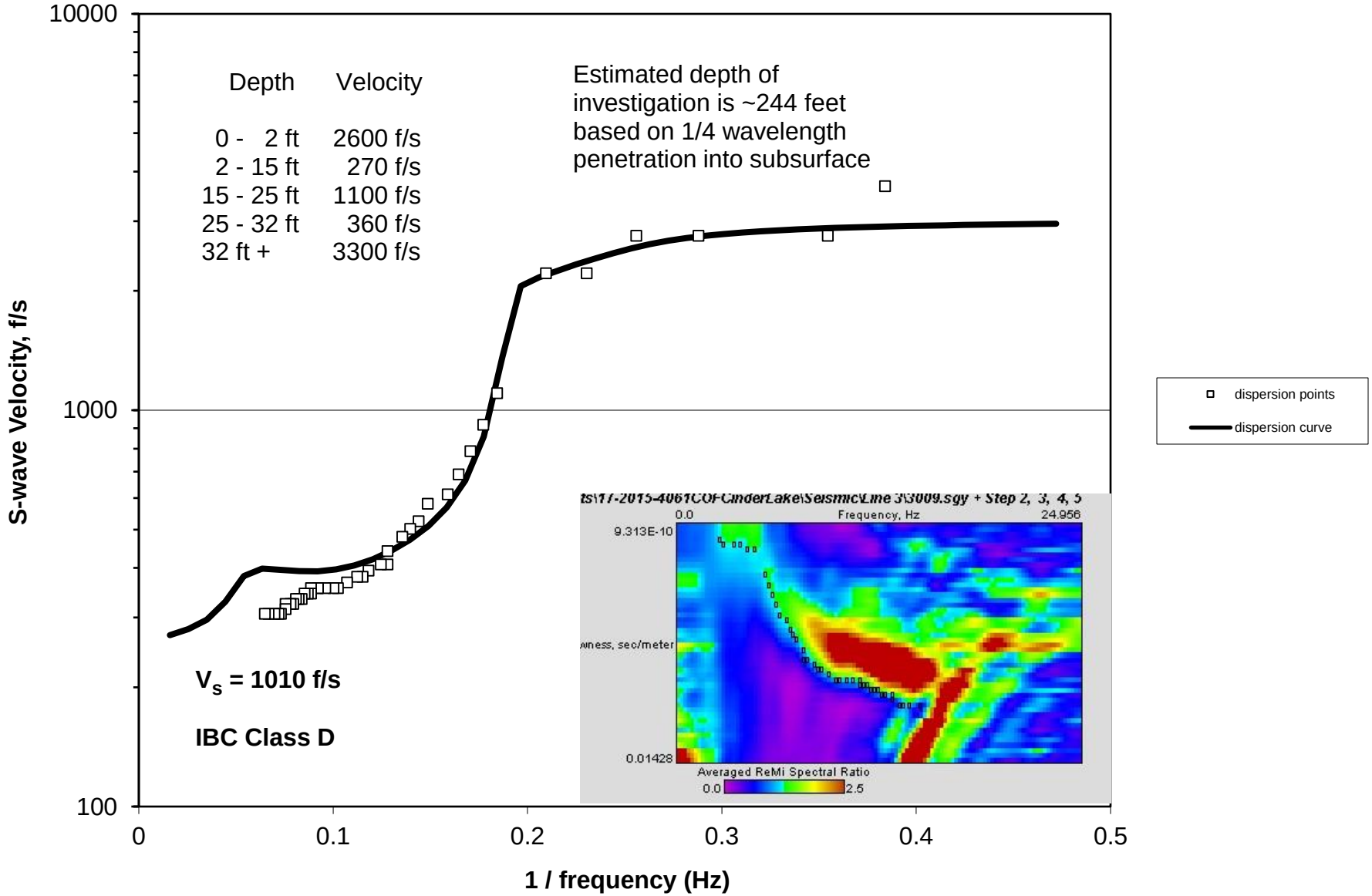

Refraction Microtremor S-wave Interpretation **Line 4** Amec Foster Wheeler Job No. 17-2015-4061

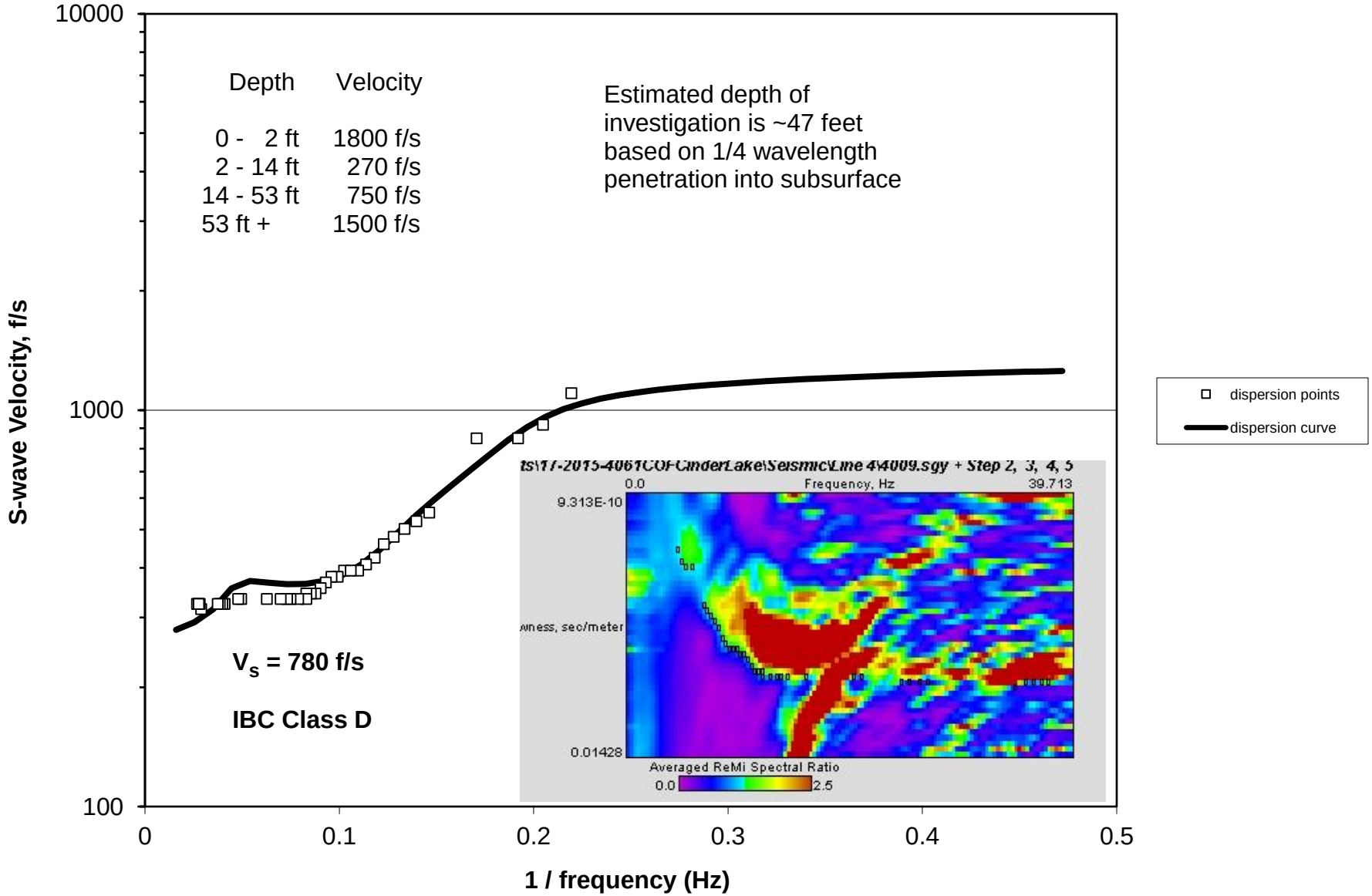

Refraction Microtremor S-wave Interpretation **Line 5B A** Amec Foster Wheeler Job No. 17-2015-4061

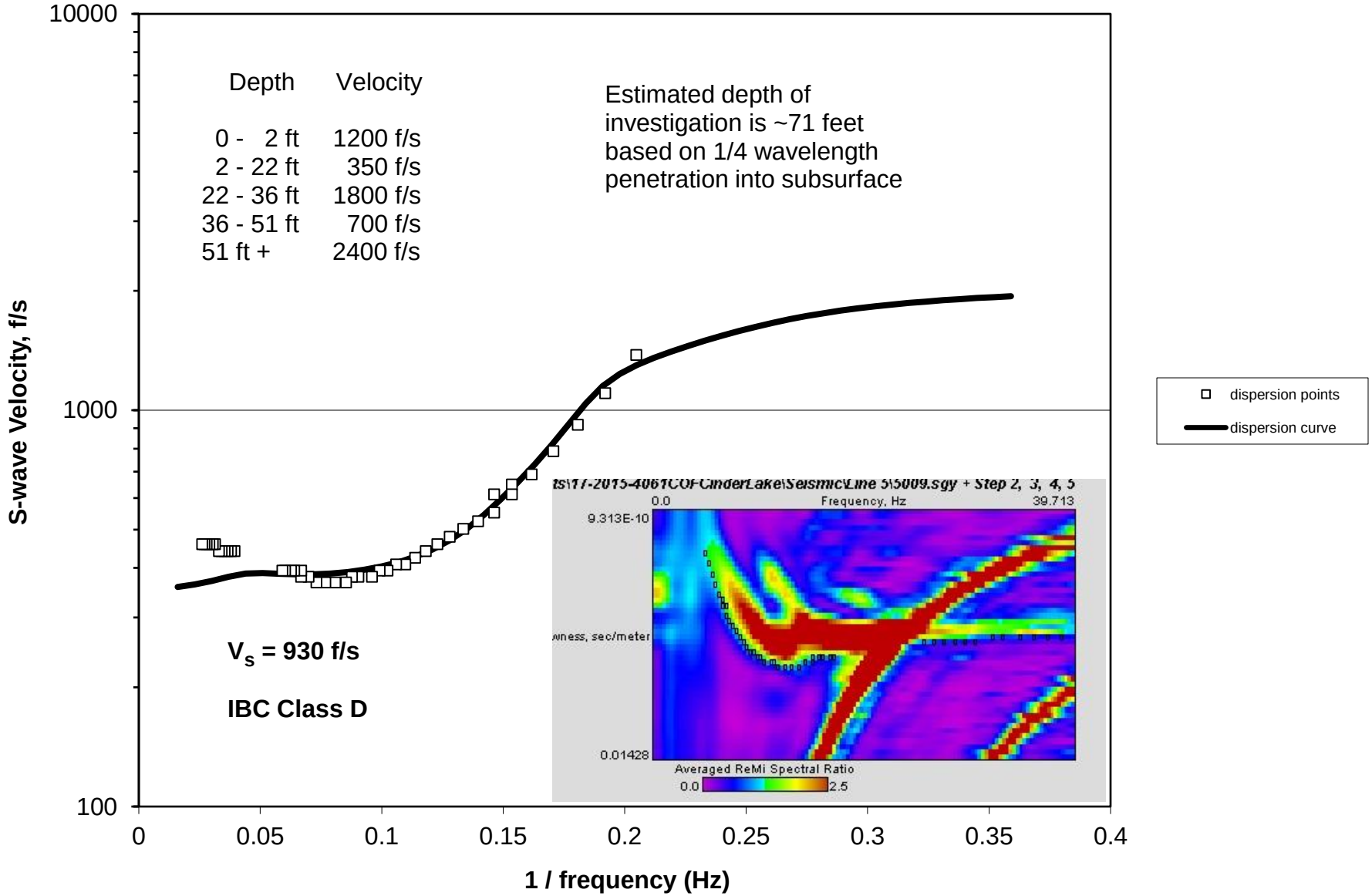

Refraction Microtremor S-wave Interpretation **Line 5B B** Amec Foster Wheeler Job No. 17-2015-4061

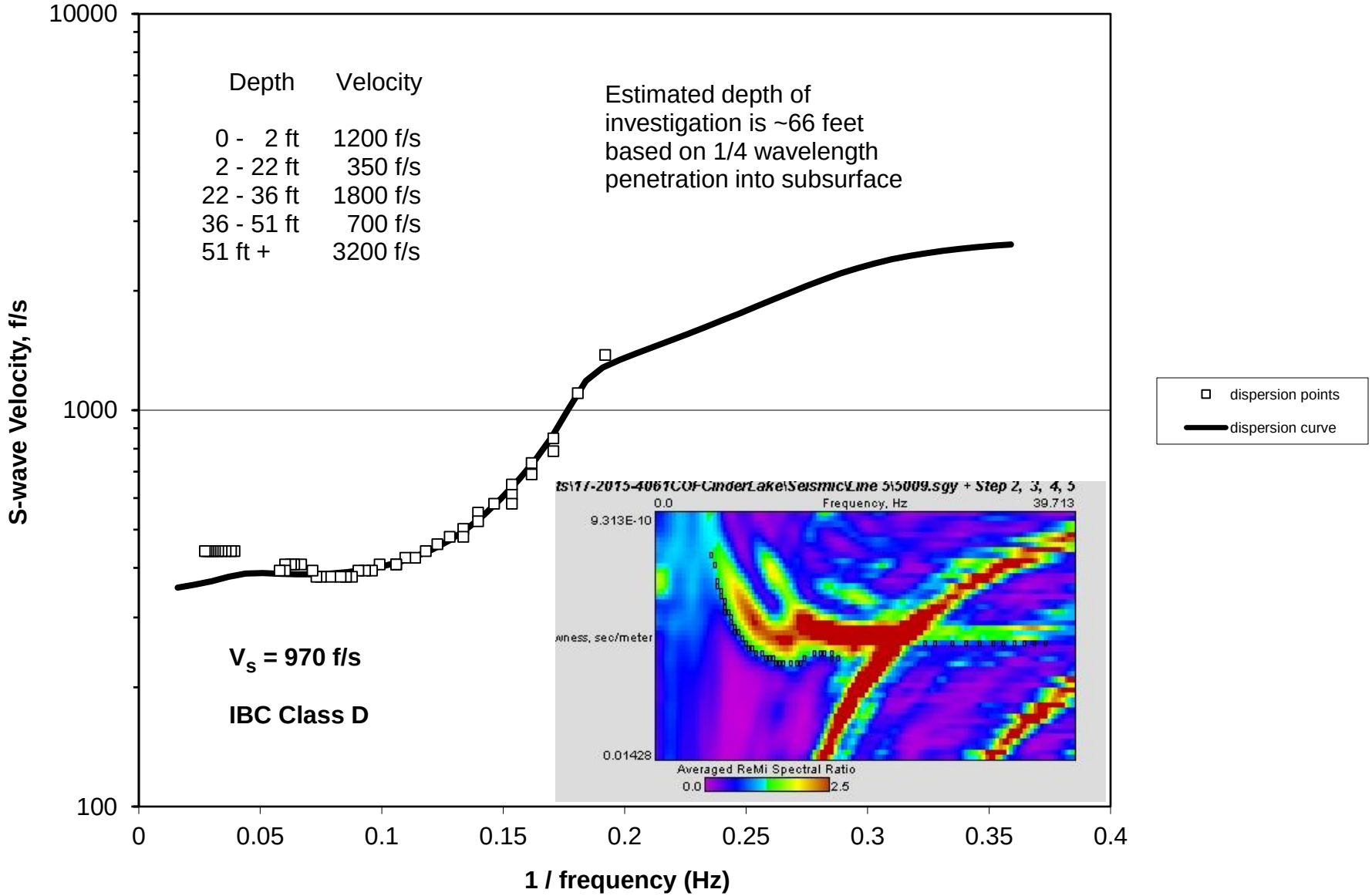

Refraction Microtremor S-wave Interpretation **Line 6** Amec Foster Wheeler Job No. 17-2015-4061

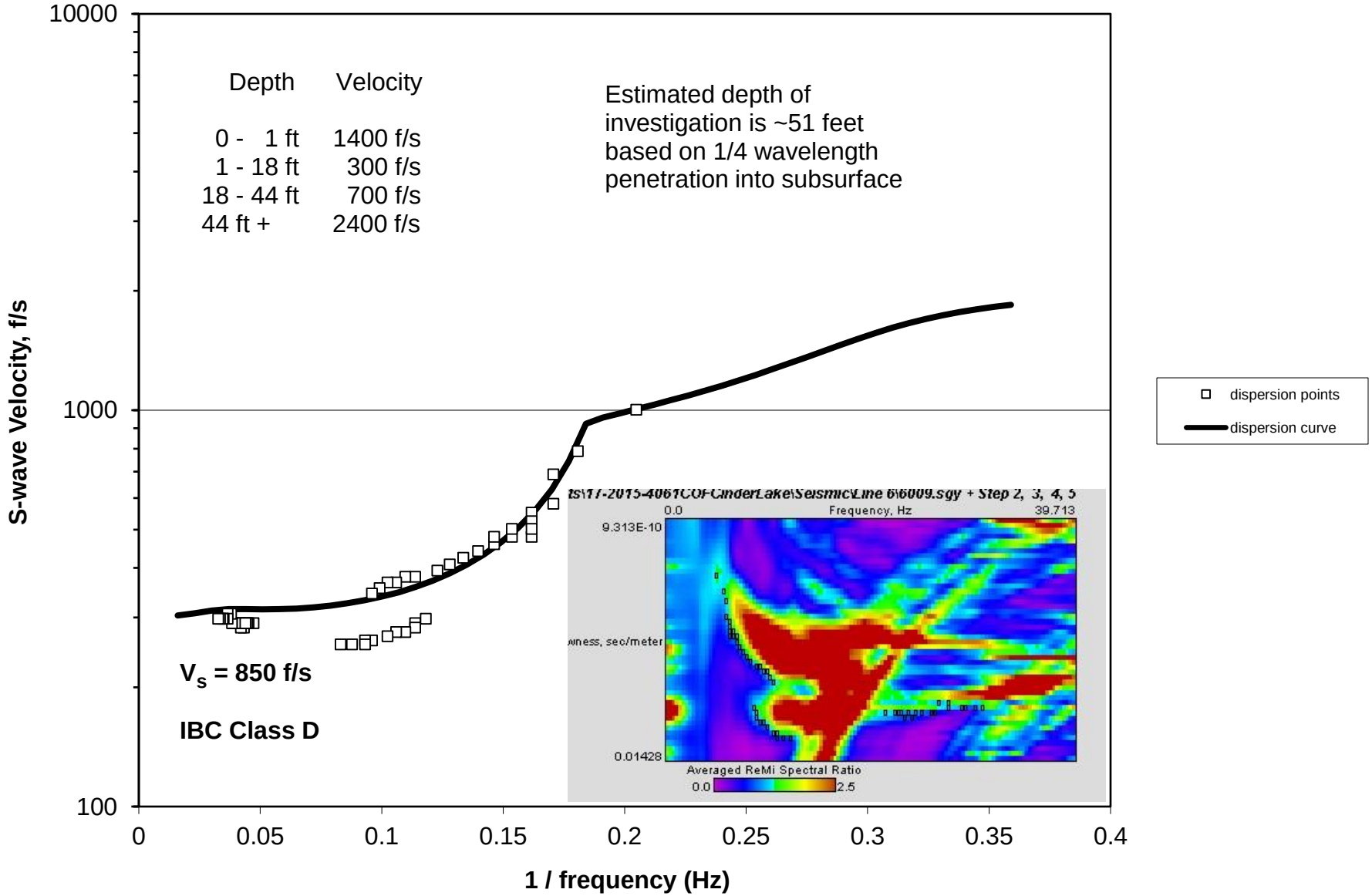

Refraction Microtremor S-wave Interpretation **Line 7** Amec Foster Wheeler Job No. 17-2015-4061

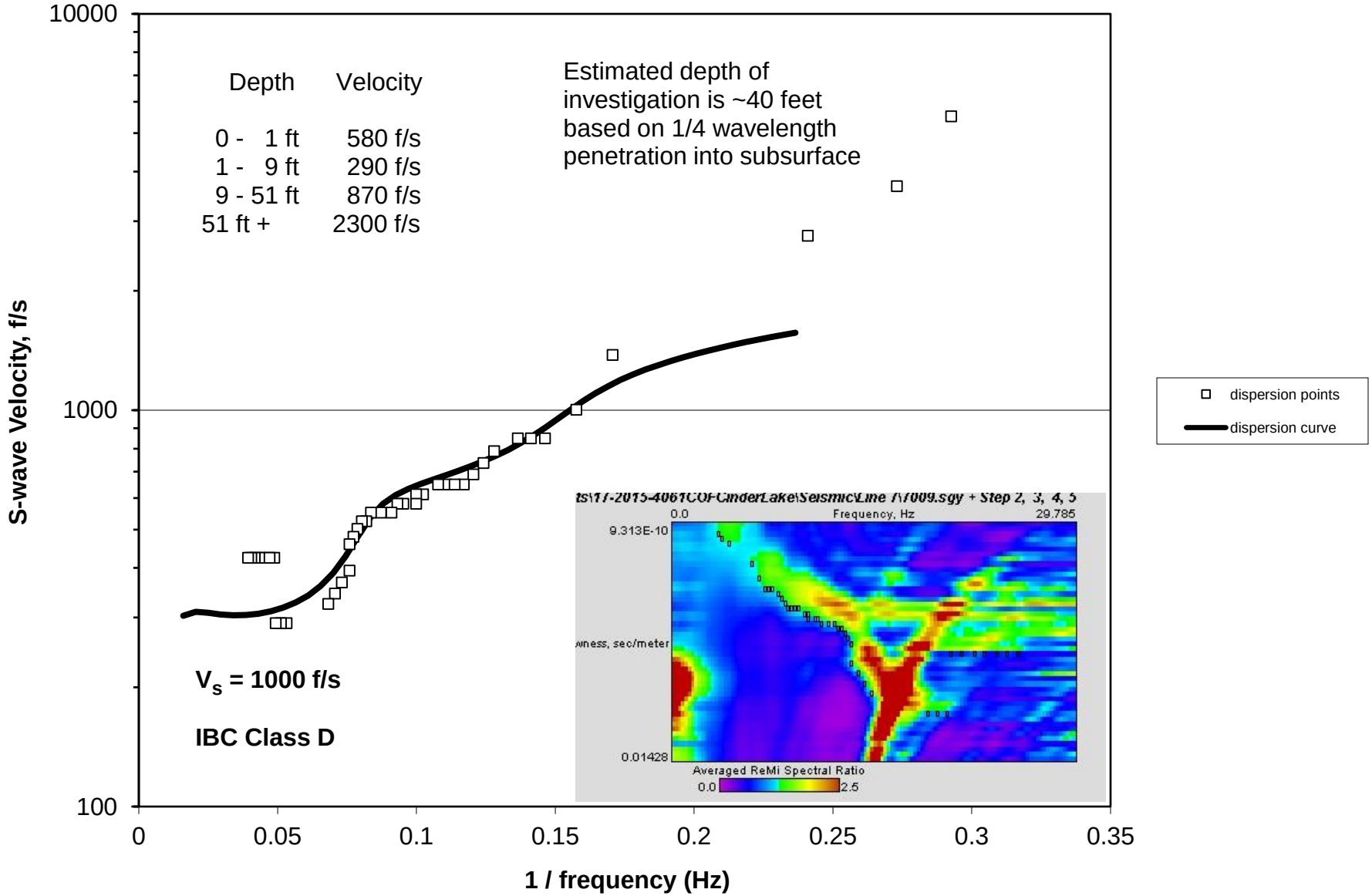

Refraction Microtremor S-wave Interpretation **Line 7 Alternative** Amec Foster Wheeler Job No. 17-2015-4061

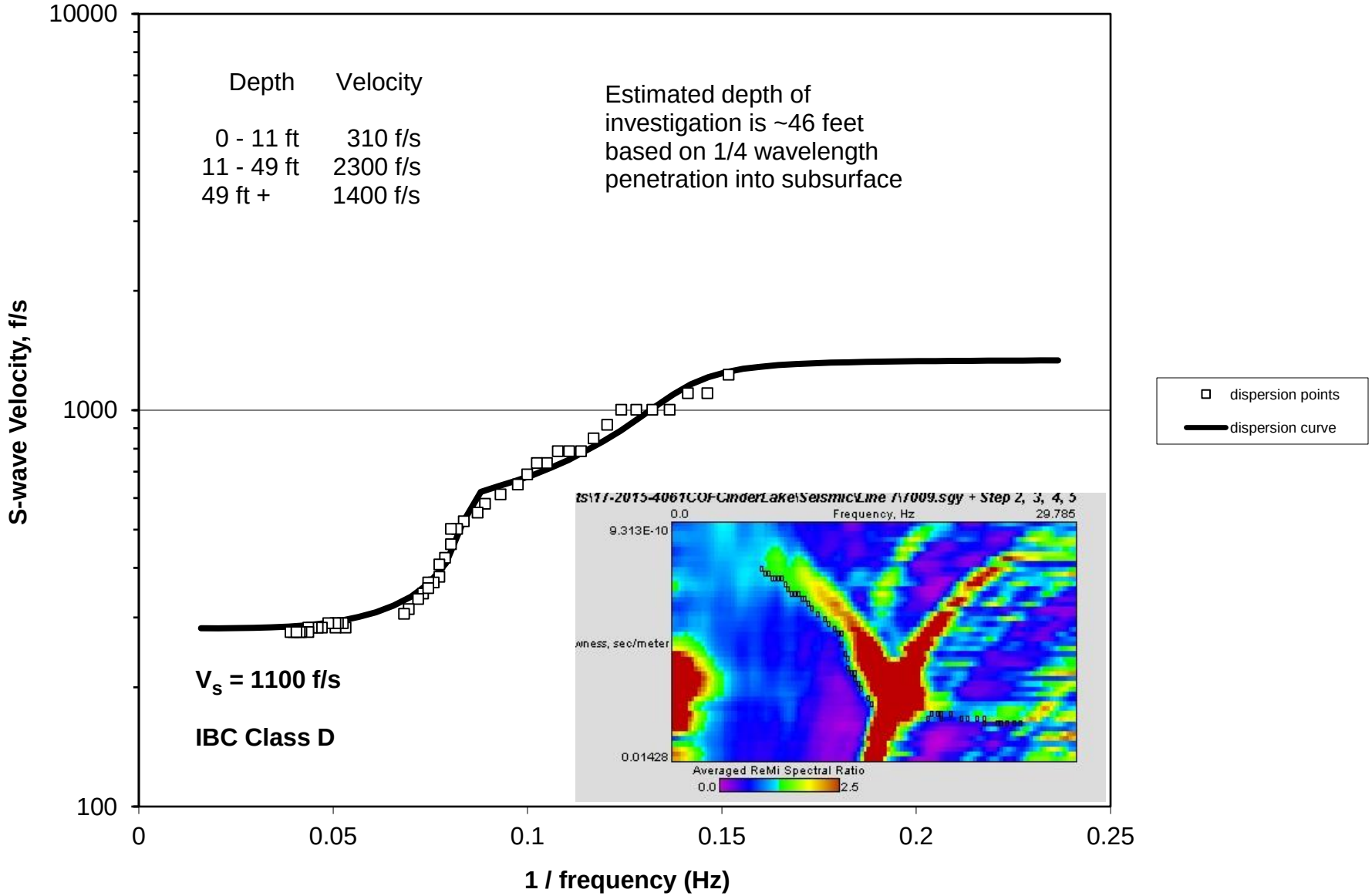

Refraction Microtremor S-wave Interpretation **Line 8** Amec Foster Wheeler Job No. 17-2015-4061

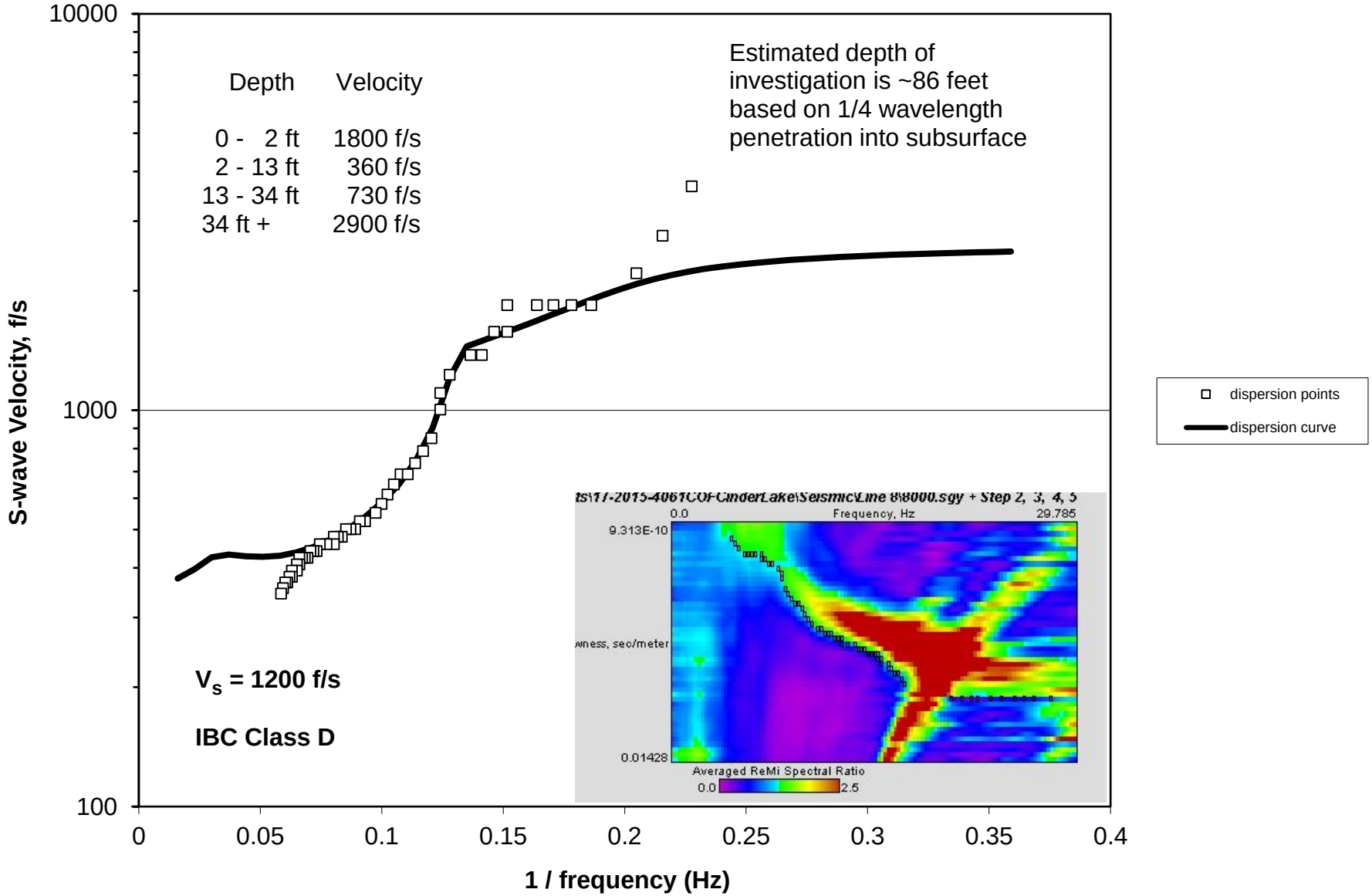

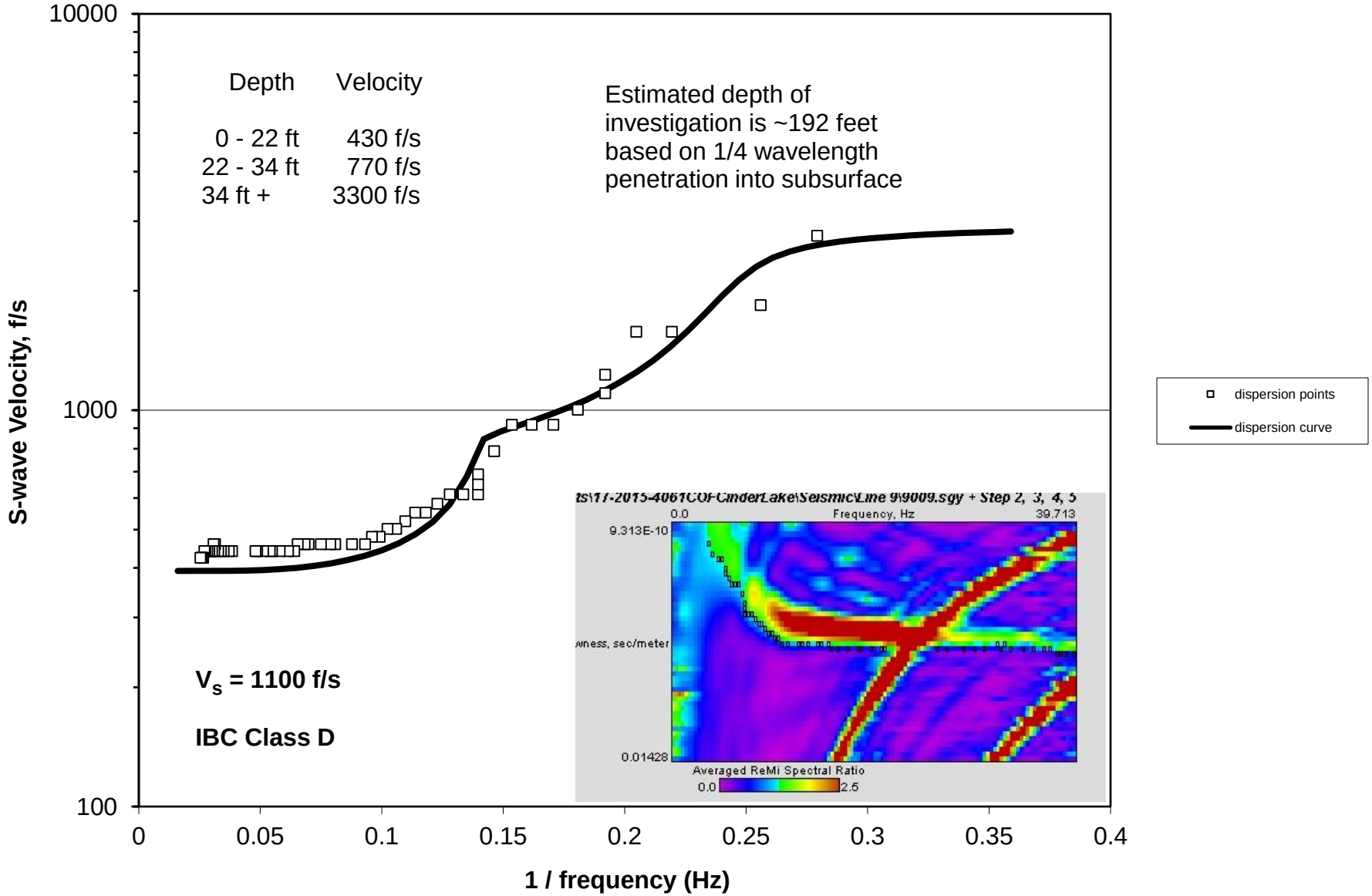
10000
1000
100
S-wave Velocity, f/s
0
0.05
0.1
0.15
0.2
0.25
0.3
0.35
0.4
1 / frequency (Hz)
Depth Velocity
0 - 22 ft 430 f/s
22 - 34 ft 770 f/s
34 ft + 3300 f/s
Estimated depth of investigation is ~192 feet based on 1/4 wavelength penetration into subsurface
V_S = 1100 f/s
IBC Class D
dispersion points
dispersion curve
0.0
Frequency, Hz
39.713
9.313E-10
0.01428
Averaged ReMi Spectral Ratio
0.0
2.5

Refraction Microtremor S-wave Interpretation **Line 9 Alternative** Amec Foster Wheeler Job No. 17-2015-4061

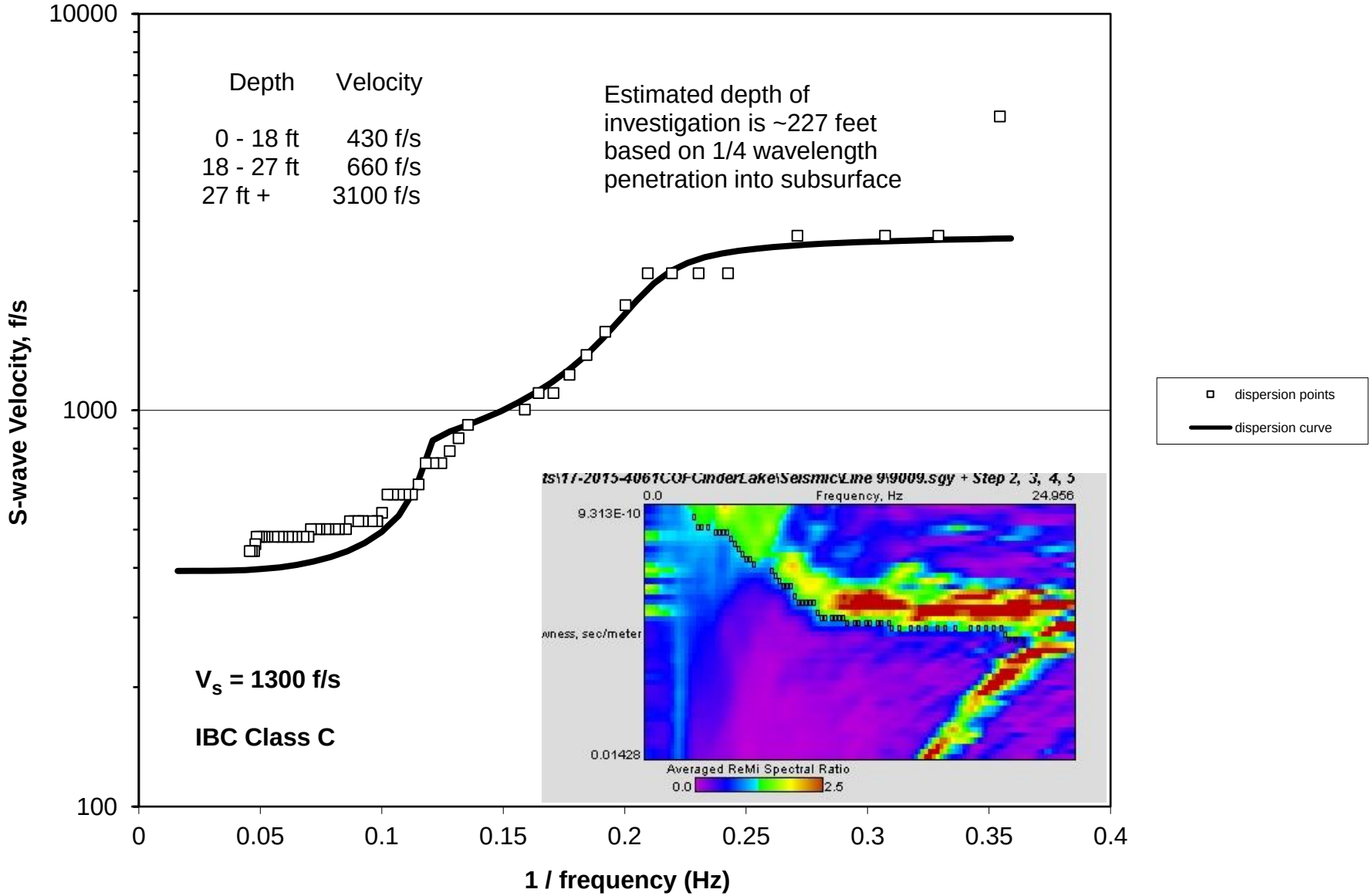

Refraction Microtremor S-wave Interpretation **Line 10** Amec Foster Wheeler Job No. 17-2015-4061

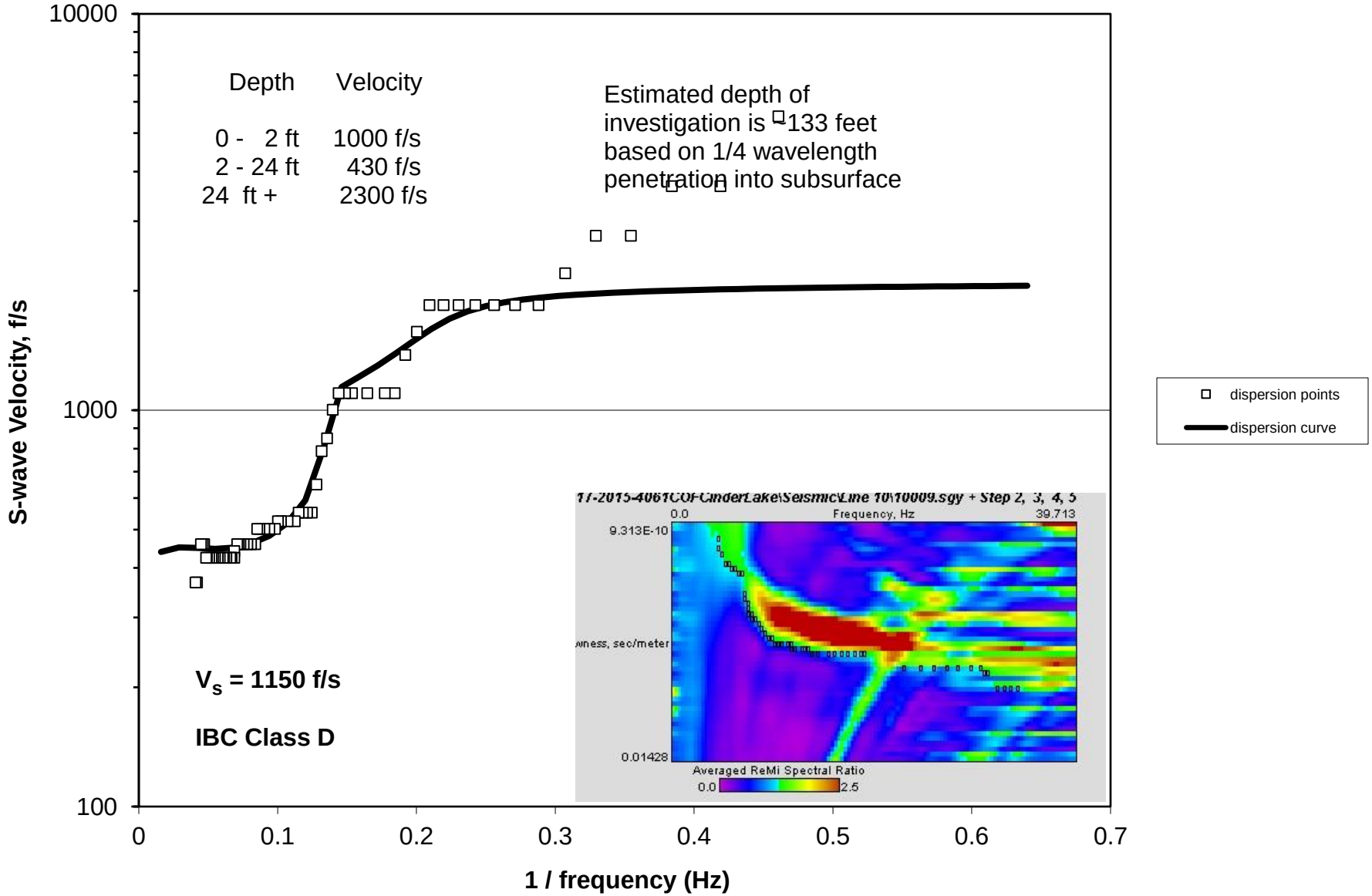

Refraction Microtremor S-wave Interpretation **Line 11A** Amec Foster Wheeler Job No. 17-2015-4061

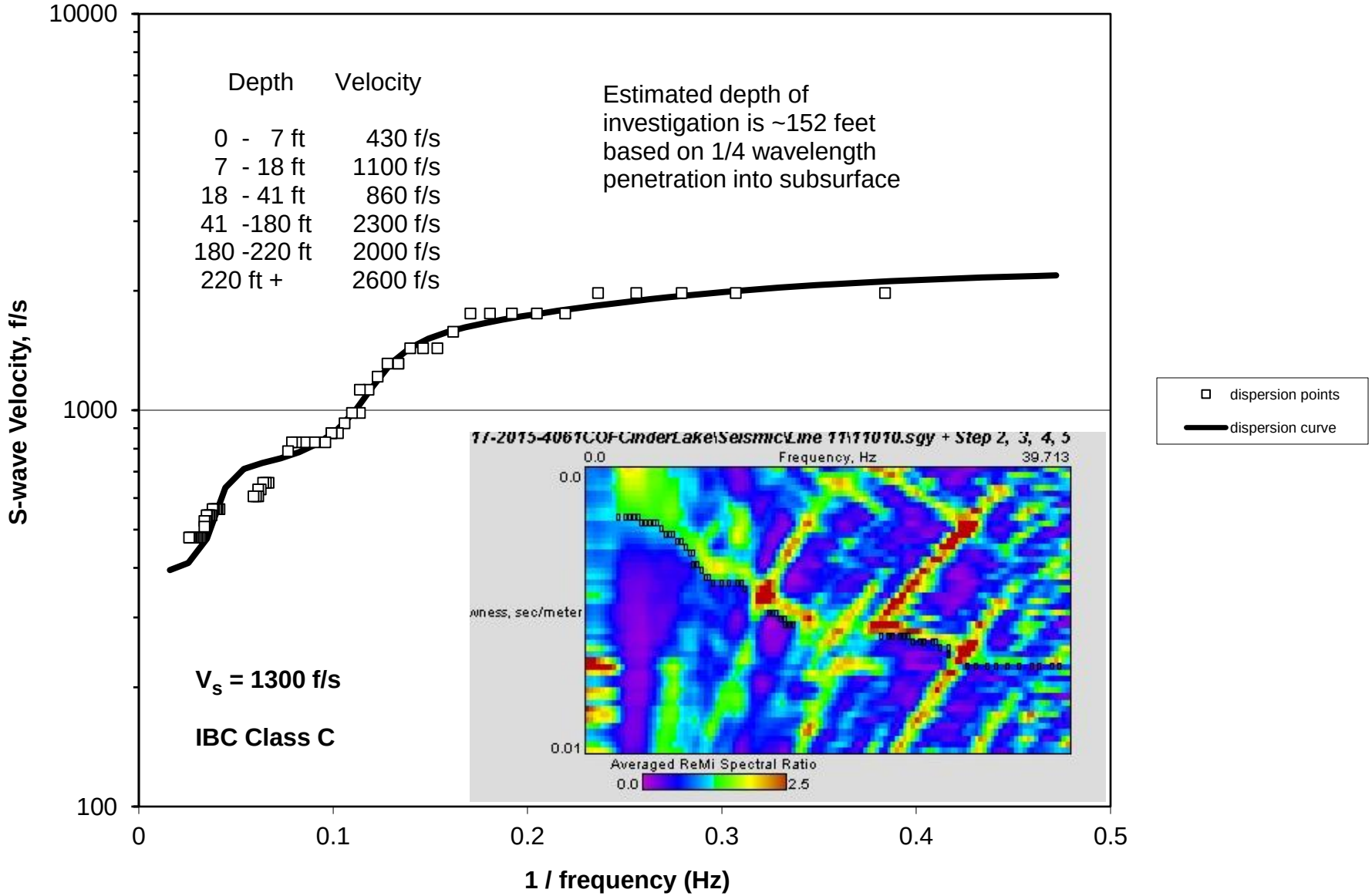

Refraction Microtremor S-wave Interpretation **Line 11B** Amec Foster Wheeler Job No. 17-2015-4061

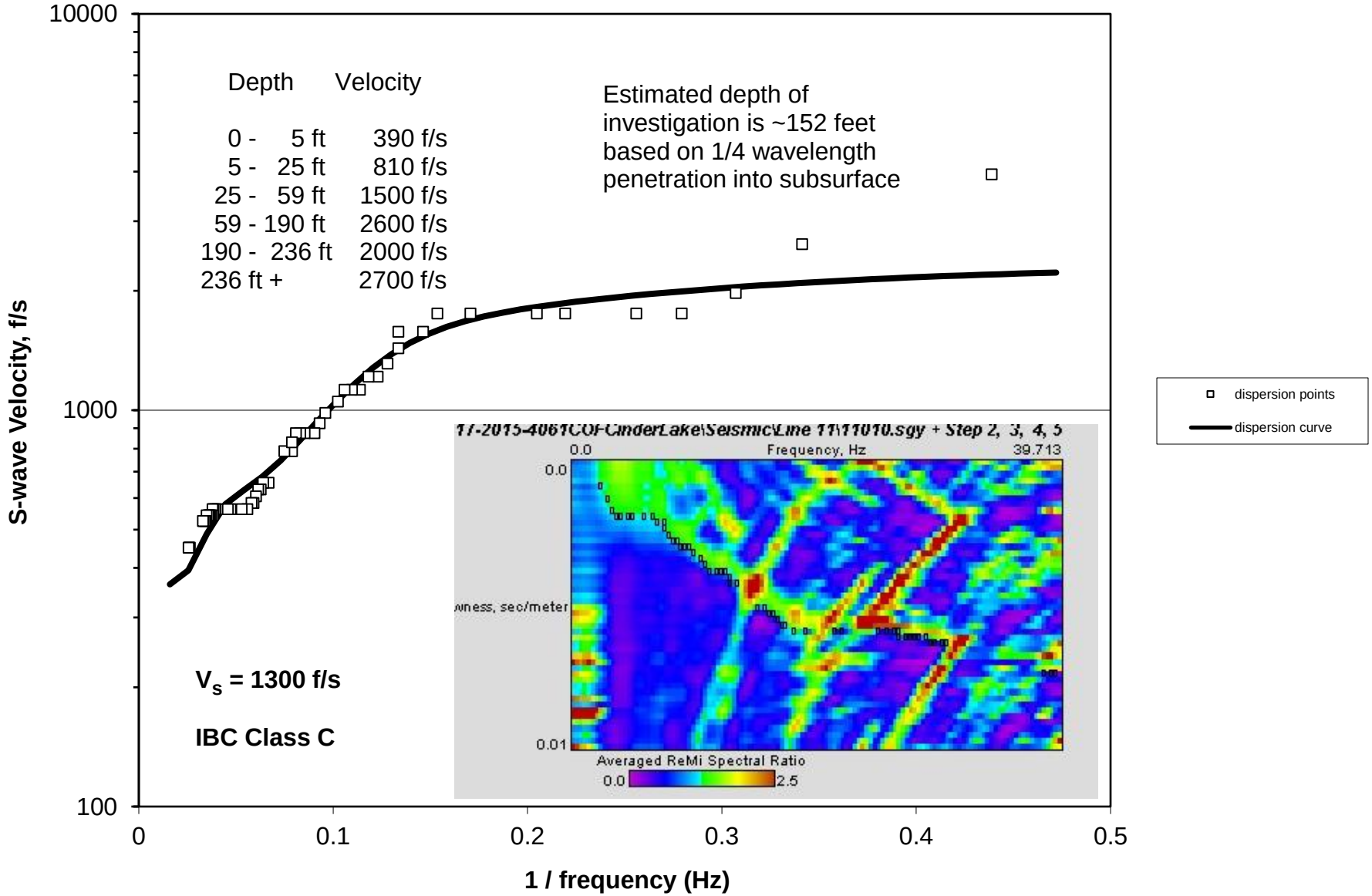

Refraction Microtremor S-wave Interpretation **Line 11C** Amec Foster Wheeler Job No. 17-2015-4061

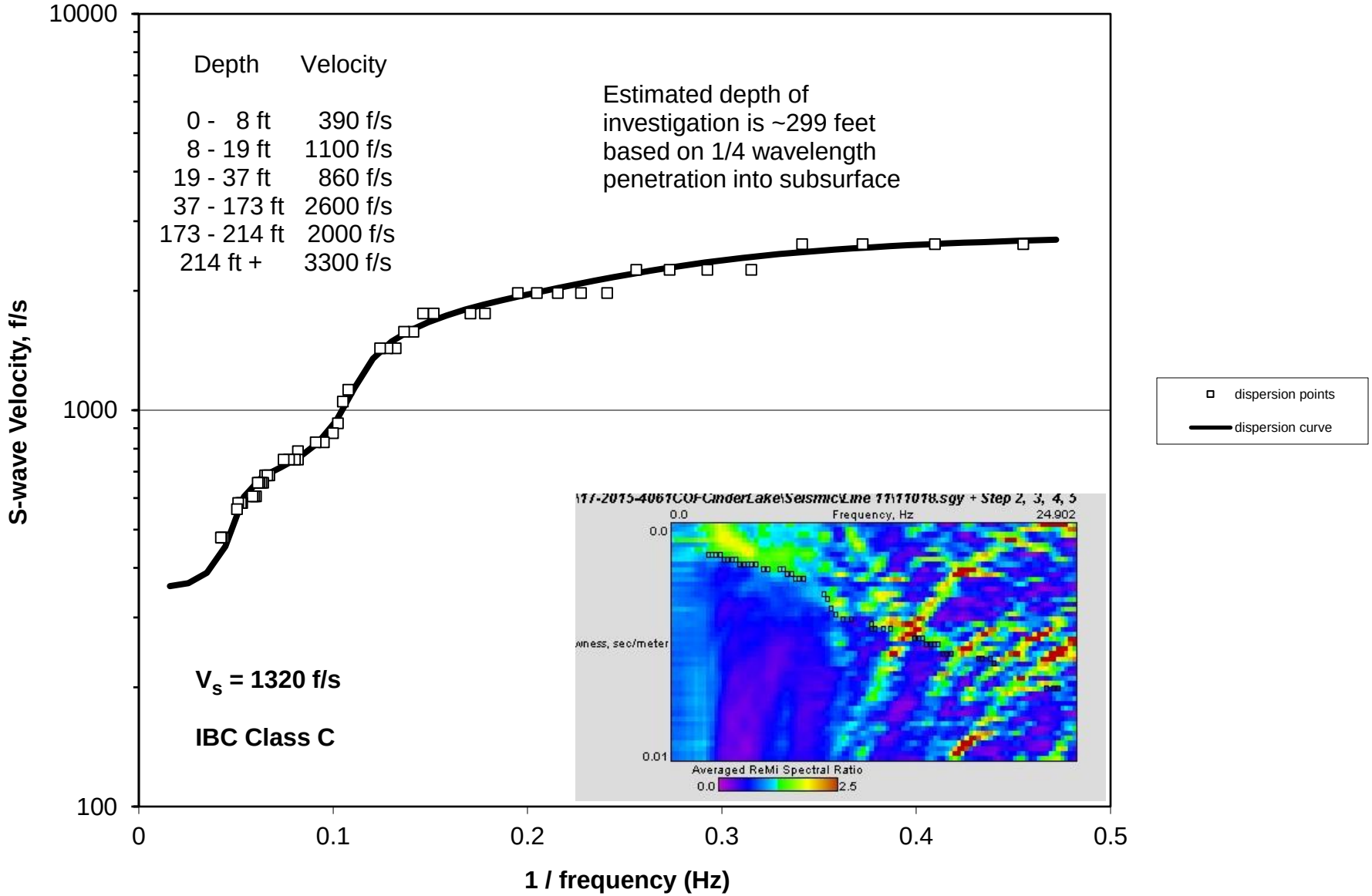

Refraction Microtremor S-wave Interpretation **Line 12** Amec Foster Wheeler Job No. 17-2015-4061

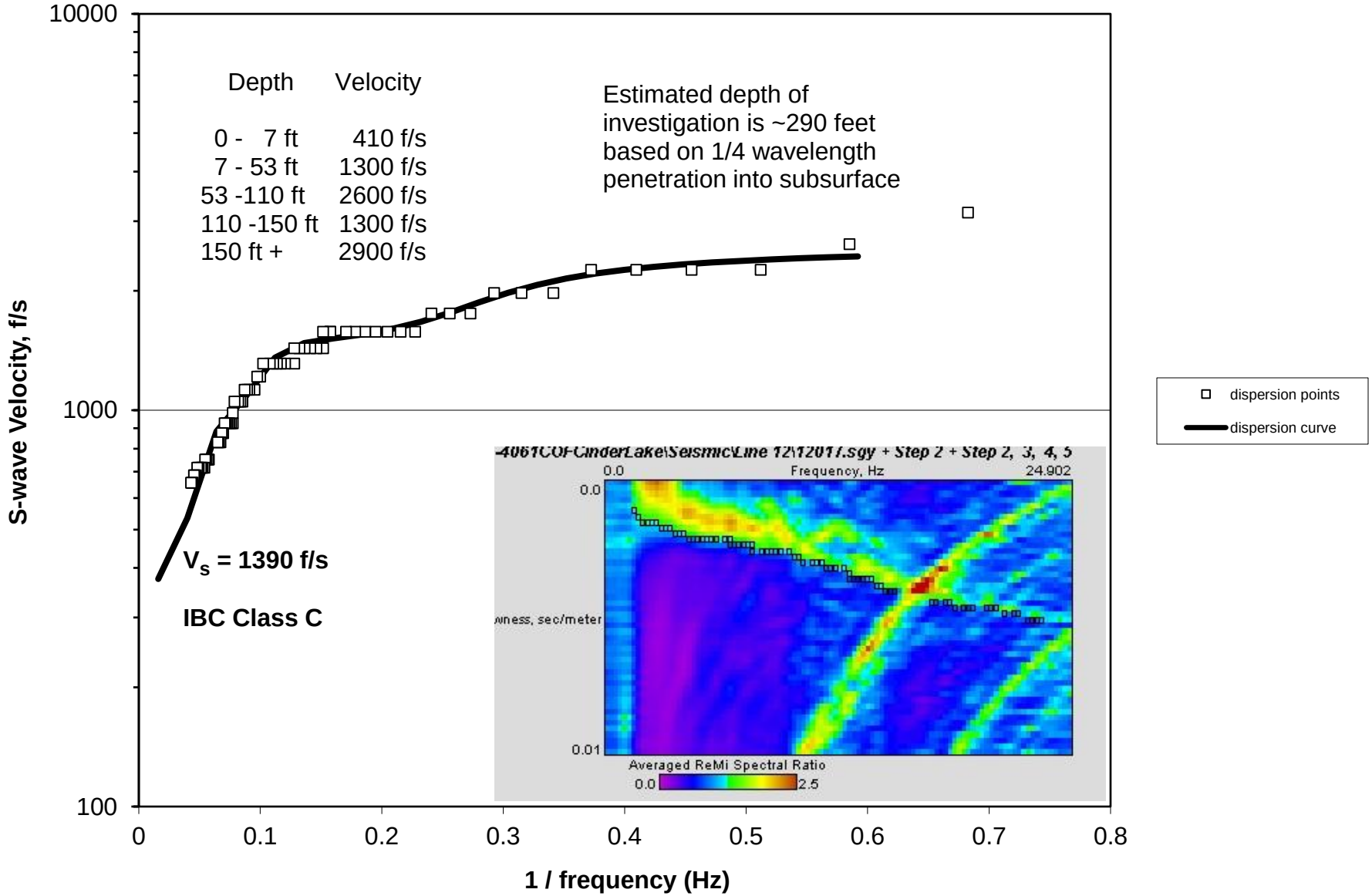

Refraction Microtremor S-wave Interpretation **Line 13A** Amec Foster Wheeler Job No. 17-2015-4061

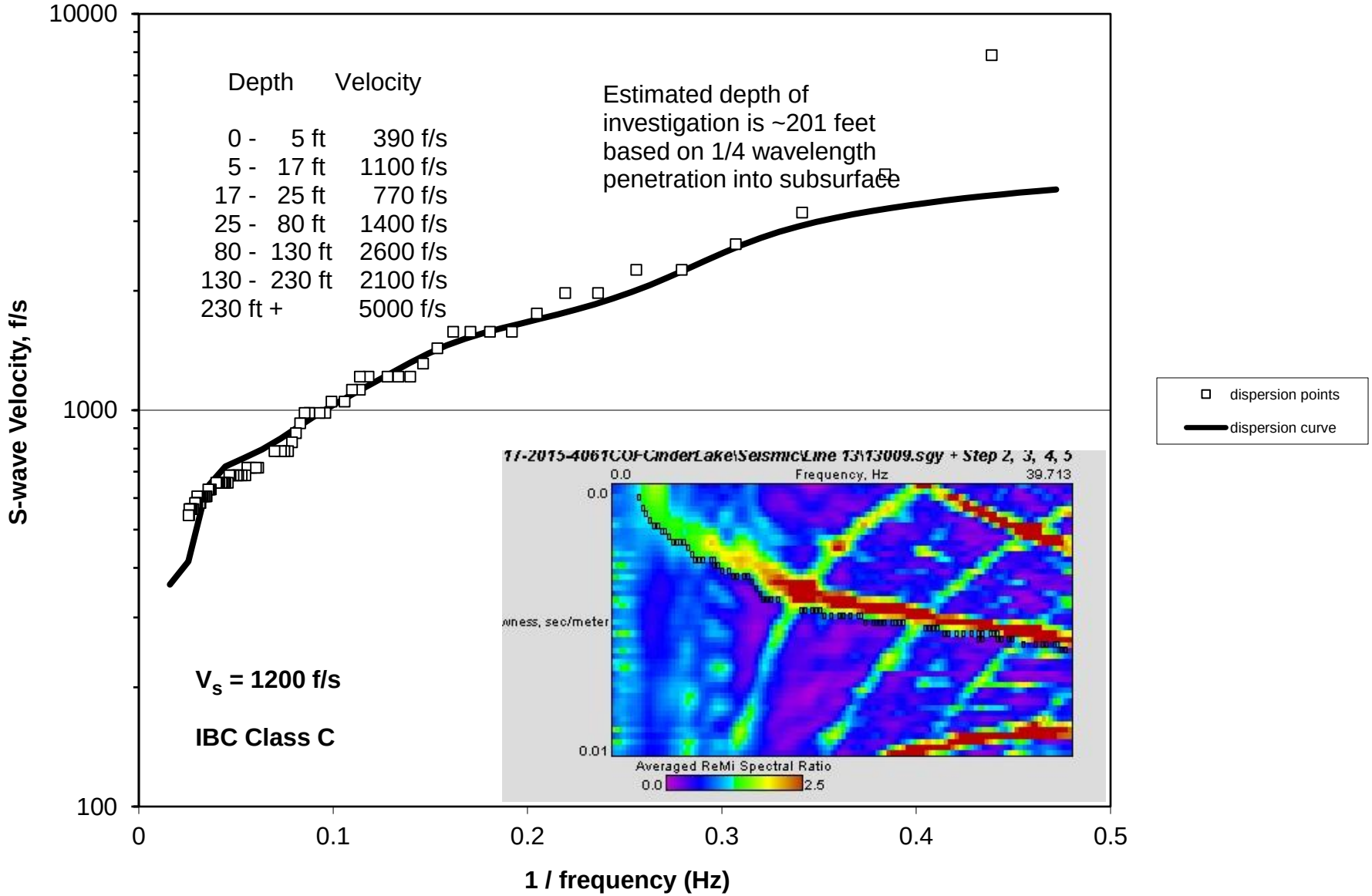

Refraction Microtremor S-wave Interpretation **Line 13B** Amec Foster Wheeler Job No. 17-2015-4061

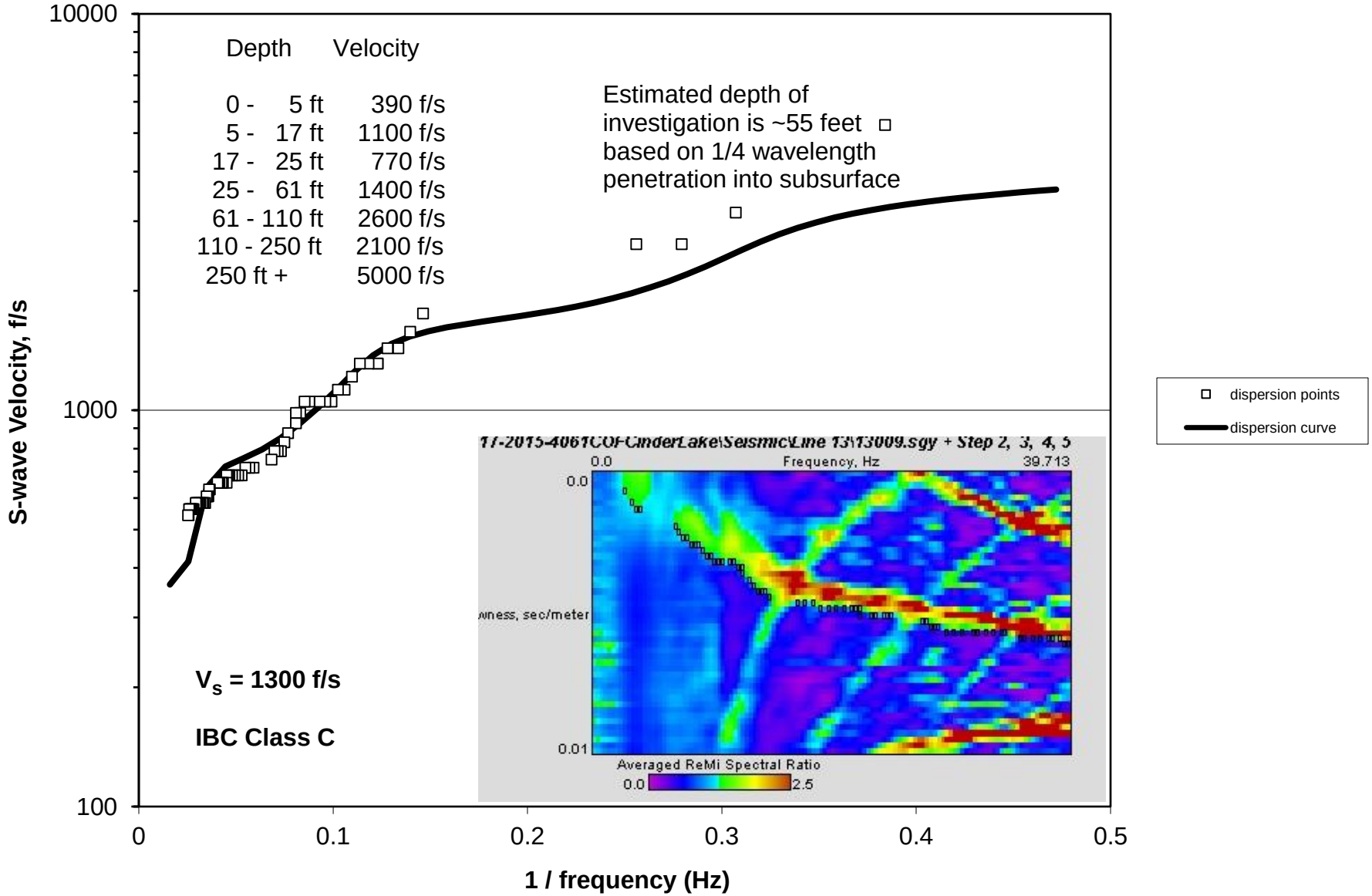

Refraction Microtremor S-wave Interpretation **Line 14** Amec Foster Wheeler Job No. 17-2015-4061

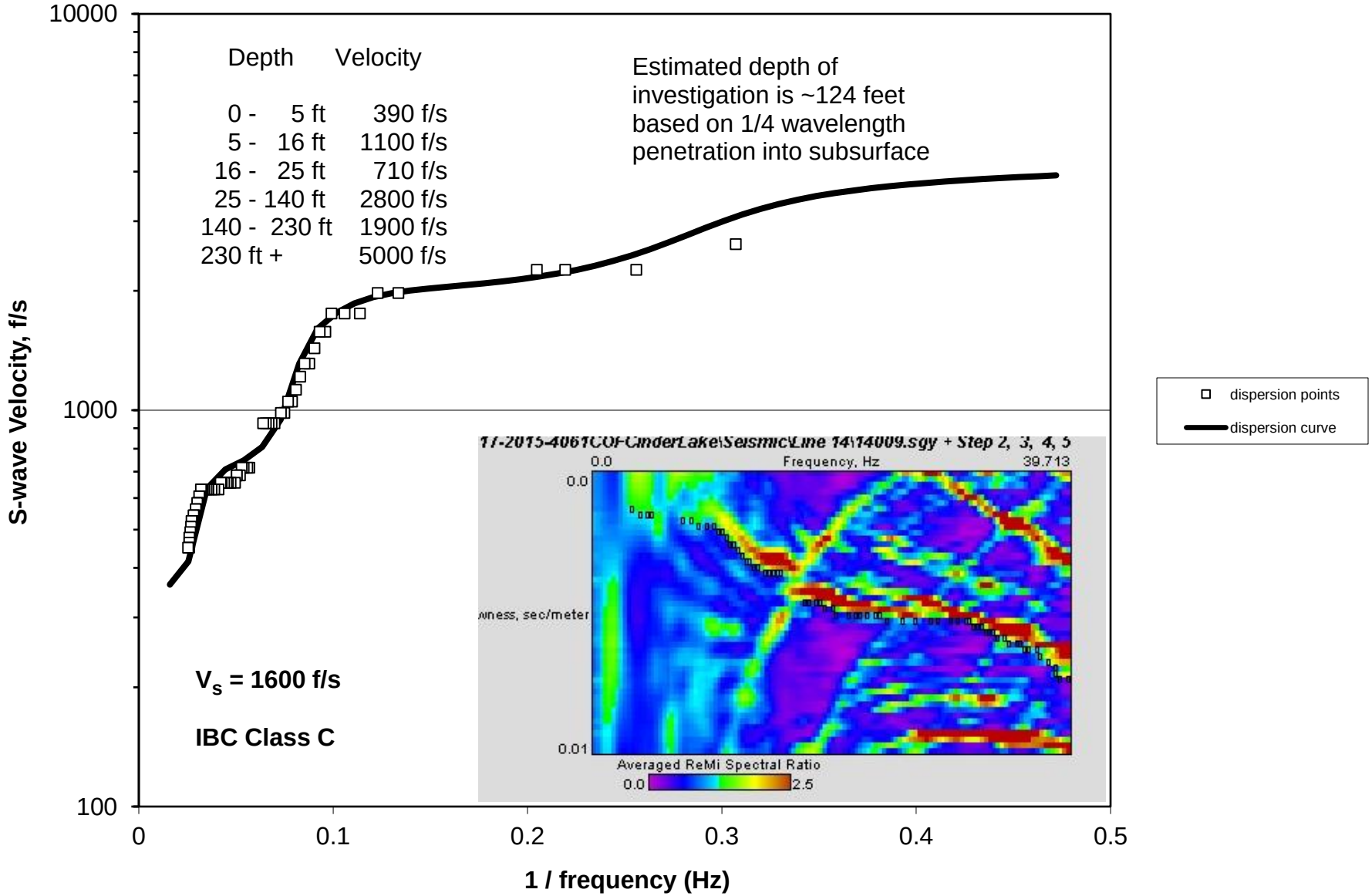

Refraction Microtremor S-wave Interpretation **Line 15A** Amec Foster Wheeler Job No. 17-2015-4061

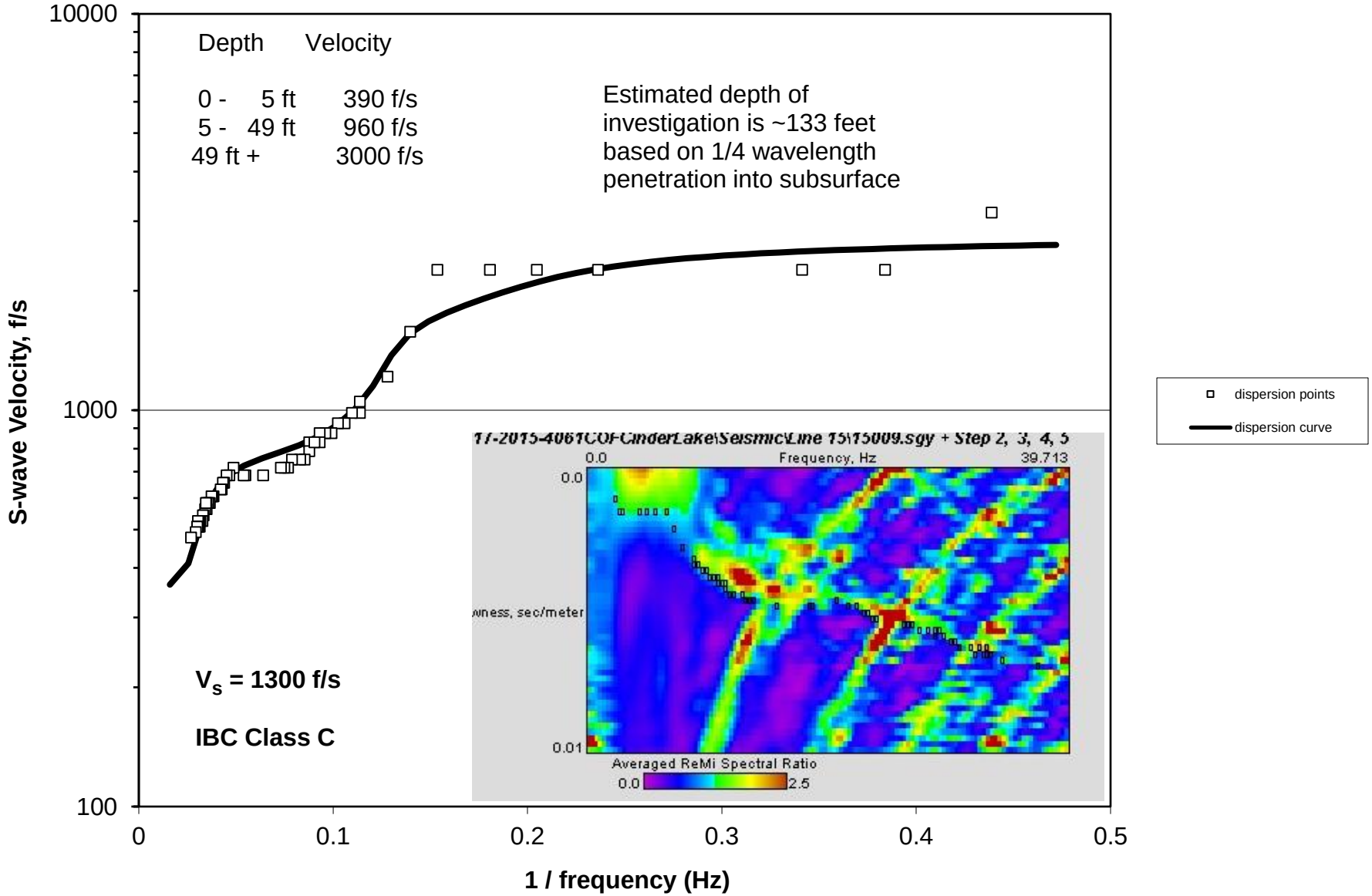

Refraction Microtremor S-wave Interpretation **Line 15B** Amec Foster Wheeler Job No. 17-2015-4061

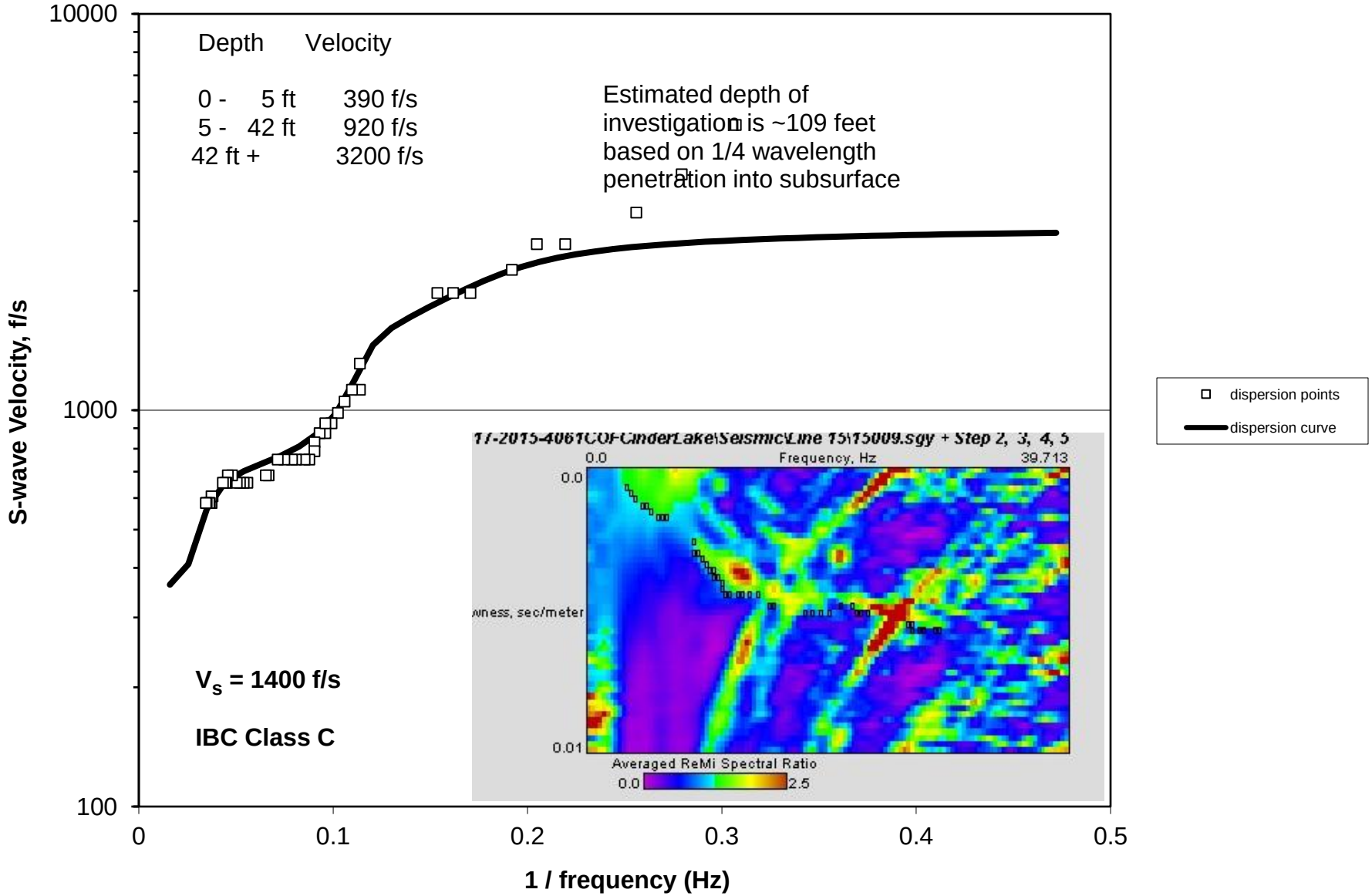

Refraction Microtremor S-wave Interpretation **Line 16** Amec Foster Wheeler Job No. 17-2015-4061

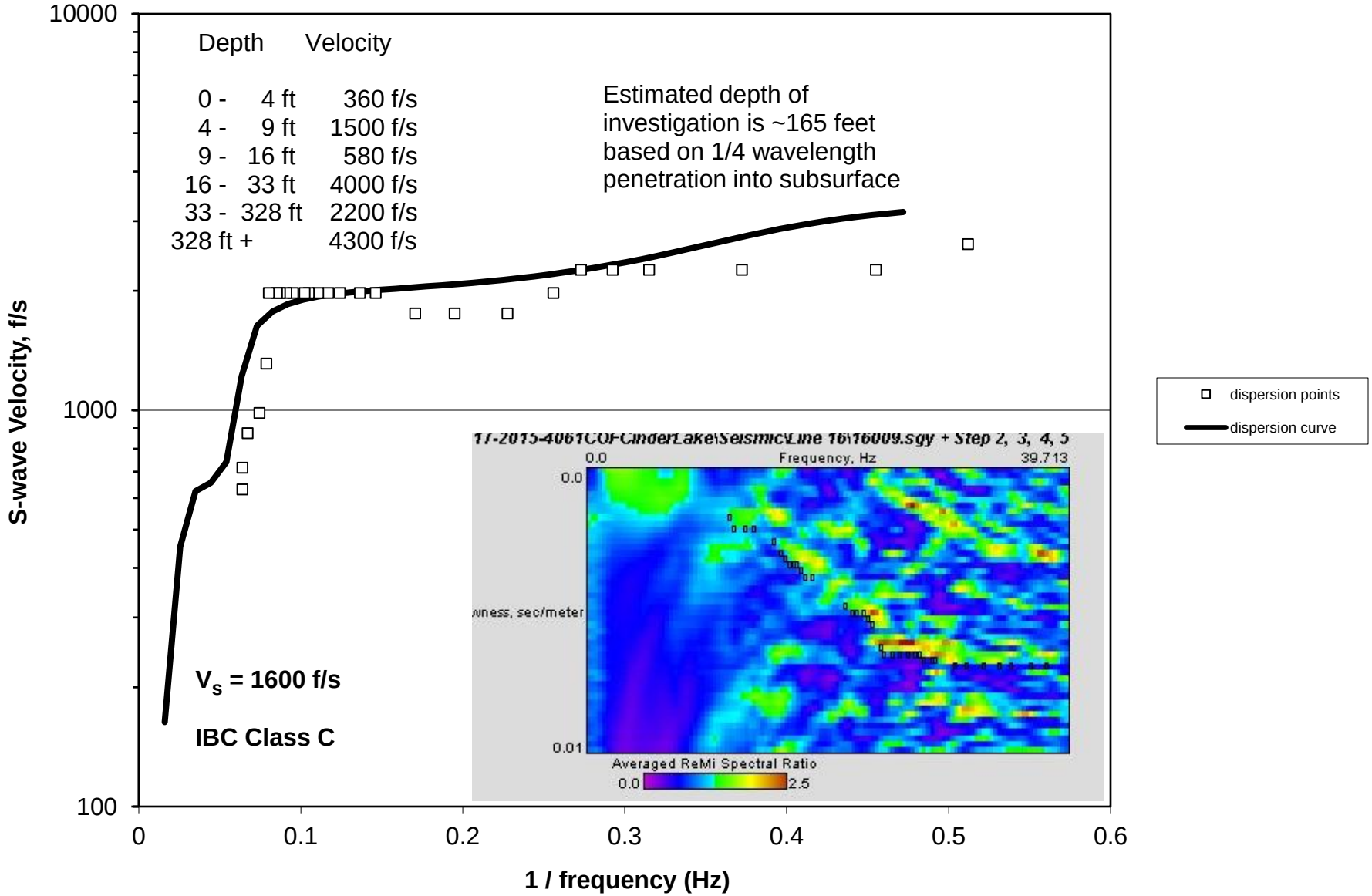

Refraction Microtremor S-wave Interpretation **Line 17** Amec Foster Wheeler Job No. 17-2015-4061

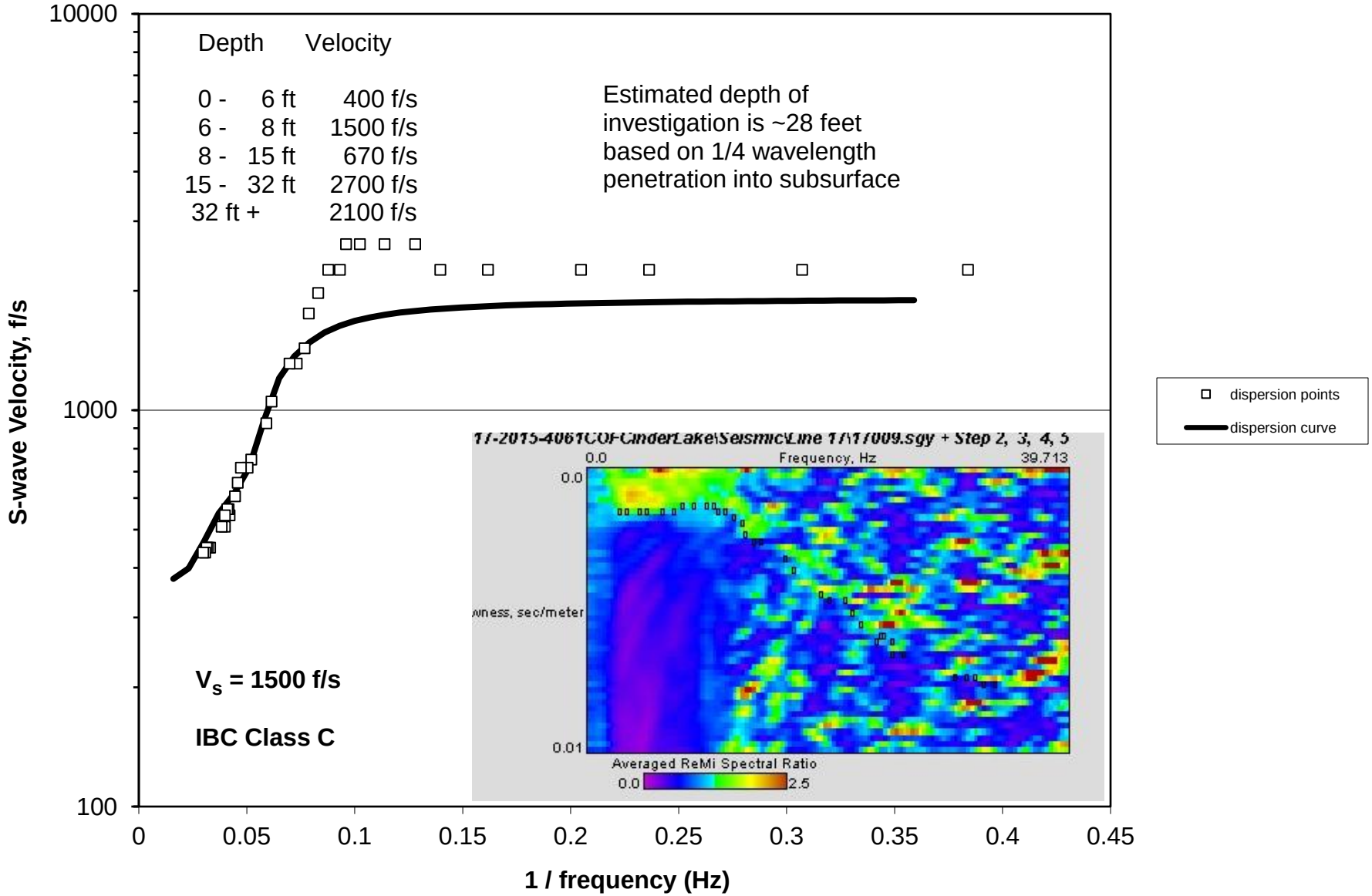

Refraction Microtremor S-wave Interpretation **Line 18** Amec Foster Wheeler Job No. 17-2015-4061

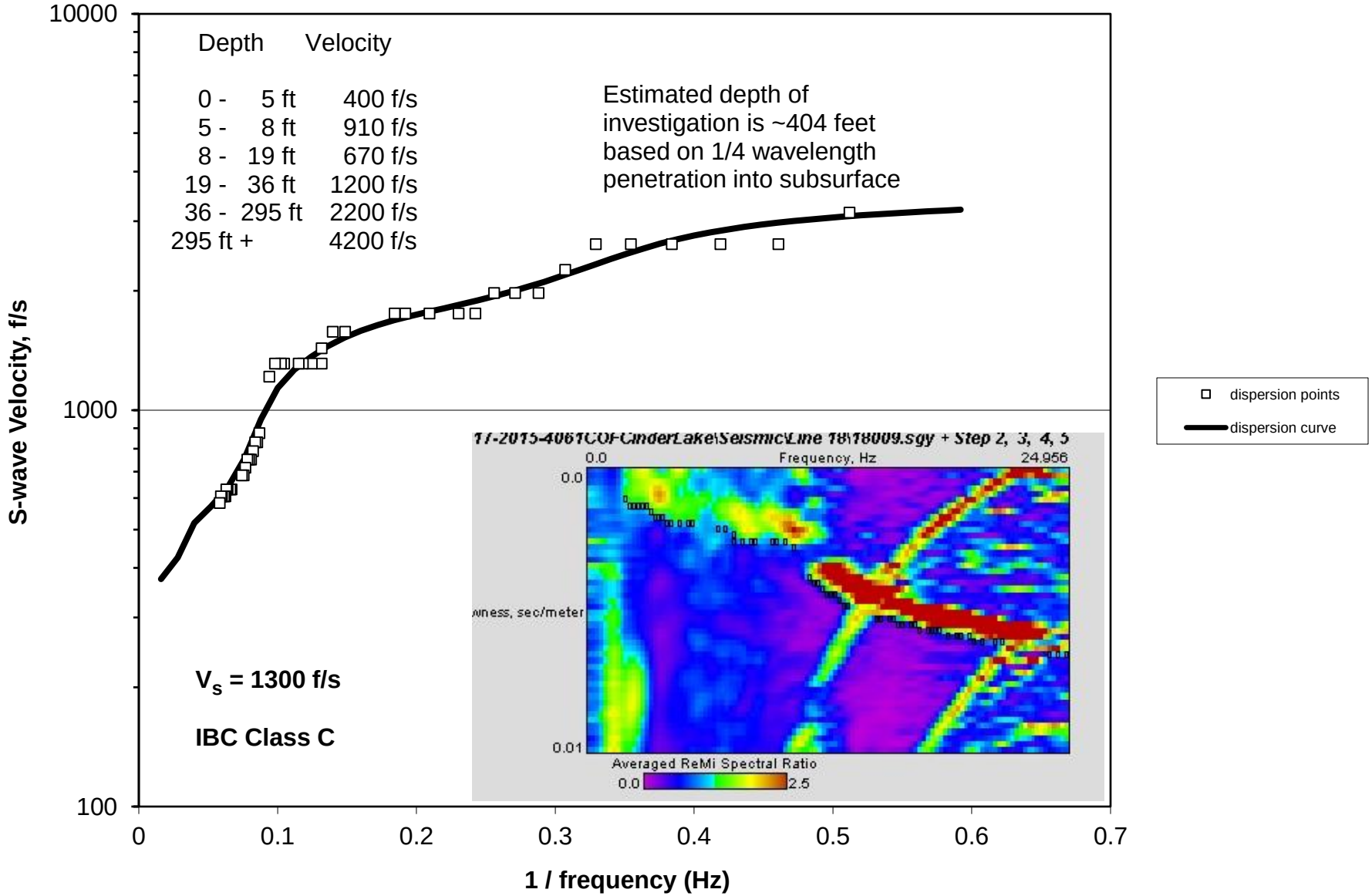

Refraction Microtremor S-wave Interpretation **Line 19** Amec Foster Wheeler Job No. 17-2015-4061

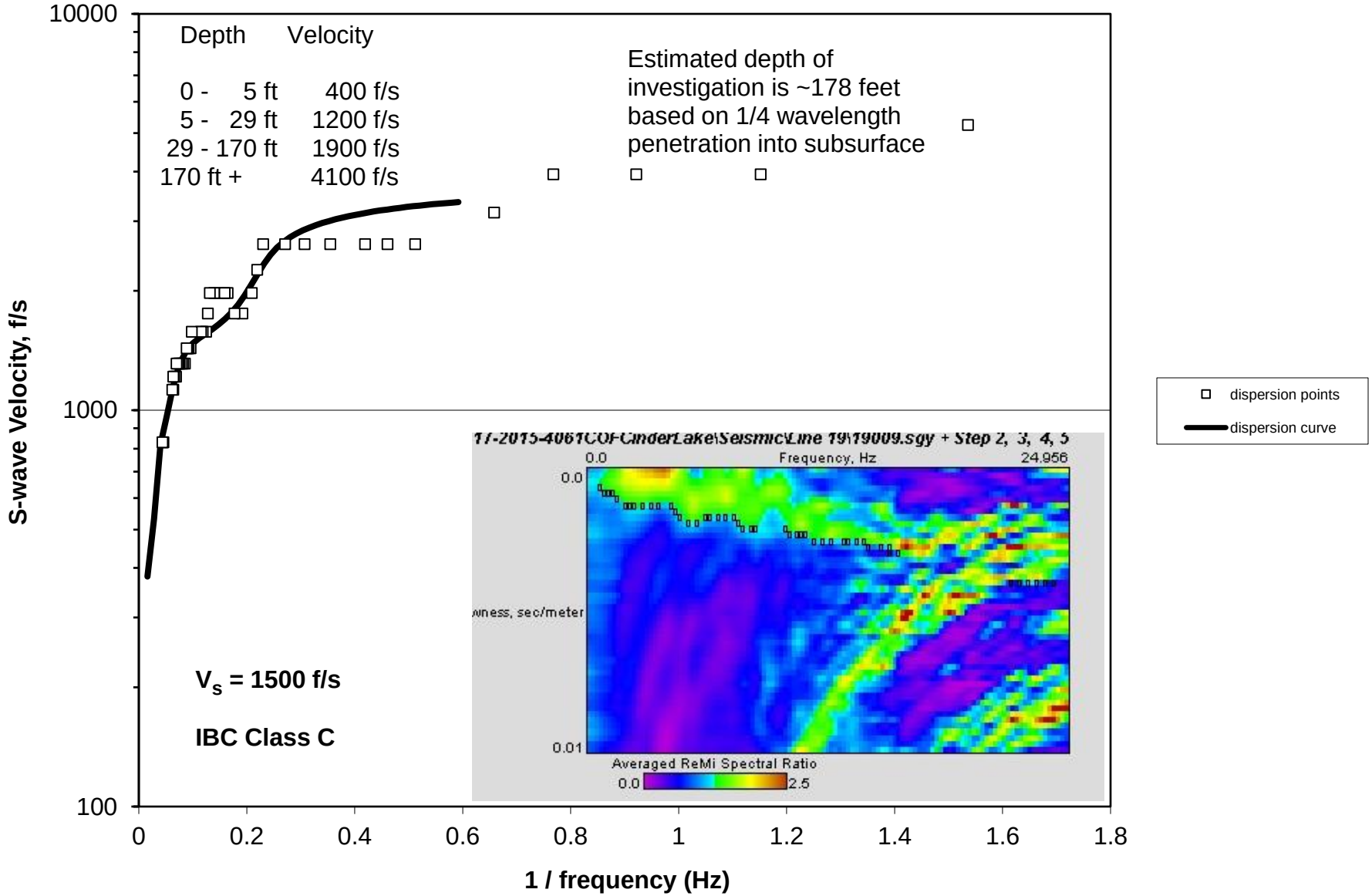

Refraction Microtremor S-wave Interpretation **Line 20** Amec Foster Wheeler Job No. 17-2015-4061

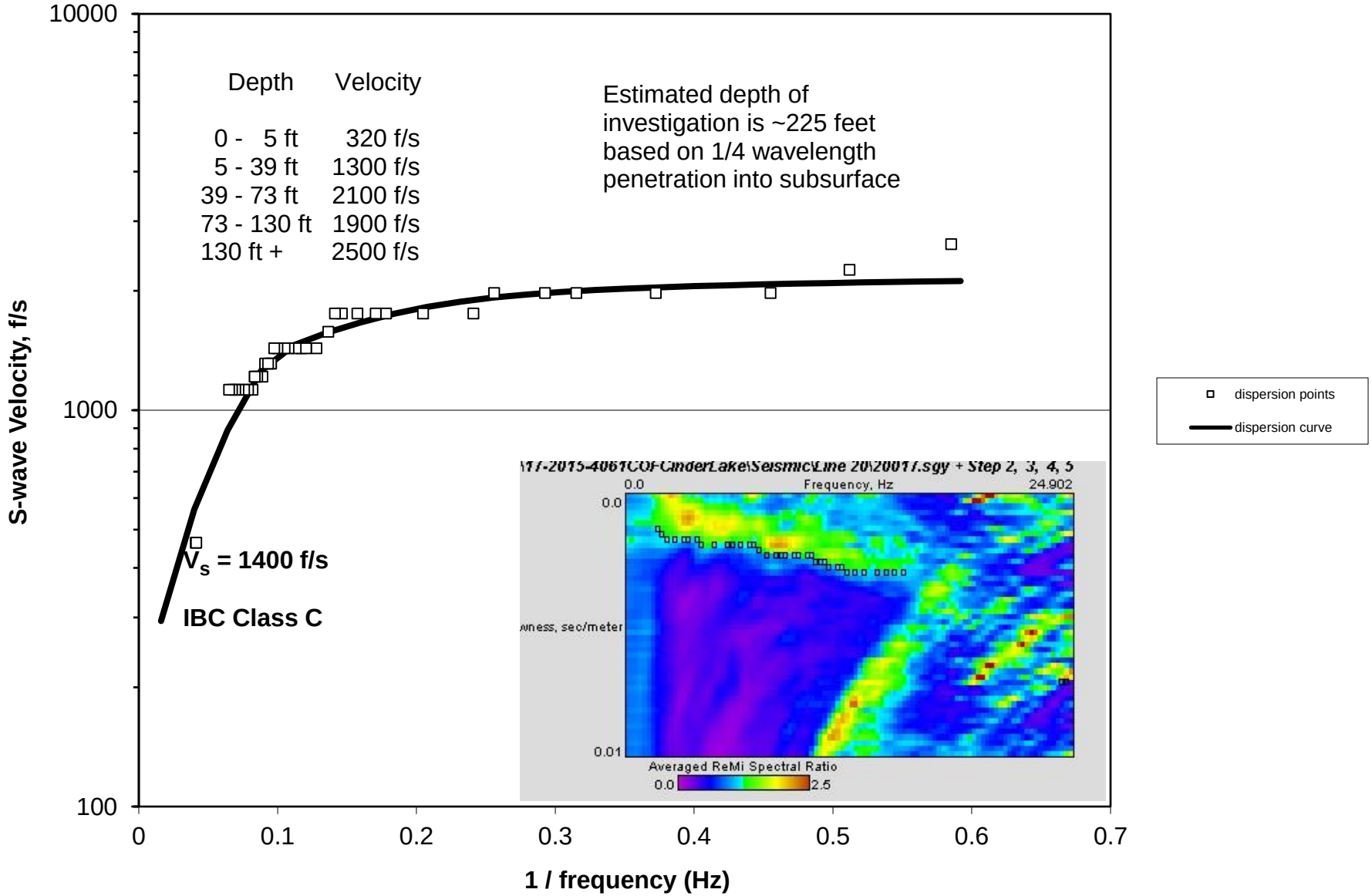

APPENDIX B

SEISMIC TABLES AND CHARTS

TABLE B-1
Approximate Excavatability of Materials
Using Various Ripping & Trenching Equipment

Material & Range of Marginal Rippability by Seismic Velocity (Cat, 1984; 1993; 2012)	Typical Bulldozer Used as Ripper (Cat, 1984; 1993; 2012)	Equivalent Backhoe (Kirsten, 1982; 1988)
"Caliche"		
4,000 – 6,000 fps	D7G, 200 HP	235
5,500 – 7,700 fps	D8R/T, 305-310 HP	-
6,300 – 8,600 fps	D8L, 335 HP	245
6,300 – 8,600 fps	D9R/T, 405-410 HP	-
6,300 – 8,700 fps	D9N, 370 HP	-
7,200 – 10,300 fps	D9L, 460 HP	RH 40
7,200 – 10,300 fps	D10T, 580 HP	-
7,200 – 10,300 fps	D10N, 520 HP	-
7,400 – 10,600 fps	D10, 700 HP	-
7,500 – 11,000 fps	D11T, 850 HP	-
7,600 – 11,000 fps	D11N, 770 HP	
Conglomerate		
4,600 – 5,700 fps	D7G, 200 HP	235
6,200 – 8,200 fps	D8R/T, 305-310 HP	-
7,600 – 9,300 fps	D8L, 335 HP	245
7,700 – 9,300 fps	D9R/T, 405-410 HP	-
7,600 – 9,300 fps	D9N, 370 HP	-
8,400 – 10,600 fps	D9L, 460 HP	RH 40
8,500 – 10,600 fps	D10T, 580 HP	-
8,400 – 10,600 fps	D10N, 520 HP	-
9,000 – 11,000 fps	D10, 700 HP	-
9,300 – 11,500 fps	D11T, 850 HP	
9,300 – 11,500 fps	D11N, 770 HP	
Basalt		
4,600 – 5,200 fps	D7G, 200 HP	235
7,600 – 8,600 fps	D8L, 335 HP	245
7,700 – 8,600 fps	D9N, 370 HP	-
8,000 – 8,900 fps	D9L, 460 HP	RH 40
8,000 – 8,900 fps	D10N, 520 HP	-
8,300 – 9,200 fps	D10, 700 HP	-
8,800 – 9,800 fps	D11N, 770 HP	-

Note: Bulldozer and backhoe power are presented by Kirsten (1982, 1988) as a measure of equivalent performance for excavation. The Caterpillar D6D bulldozer and 225 backhoe and D4E/D5B bulldozer and 215 backhoe are considered equivalent. Seismic velocities below marginal indicate that the material is rippable. Seismic velocities above marginal indicate that the material is non-rippable. All velocities are approximate and represent a typical range. See the Caterpillar Performance Handbook (Caterpillar, 1984, 1993, 2012 or current edition) for details on use of this information. Different model configurations include variations in weight and horsepower.

FIGURE B-1

Typical Excavatability Performance in Cemented Soils for Various Equipment Completing Test Pits in Salt River Valley Area

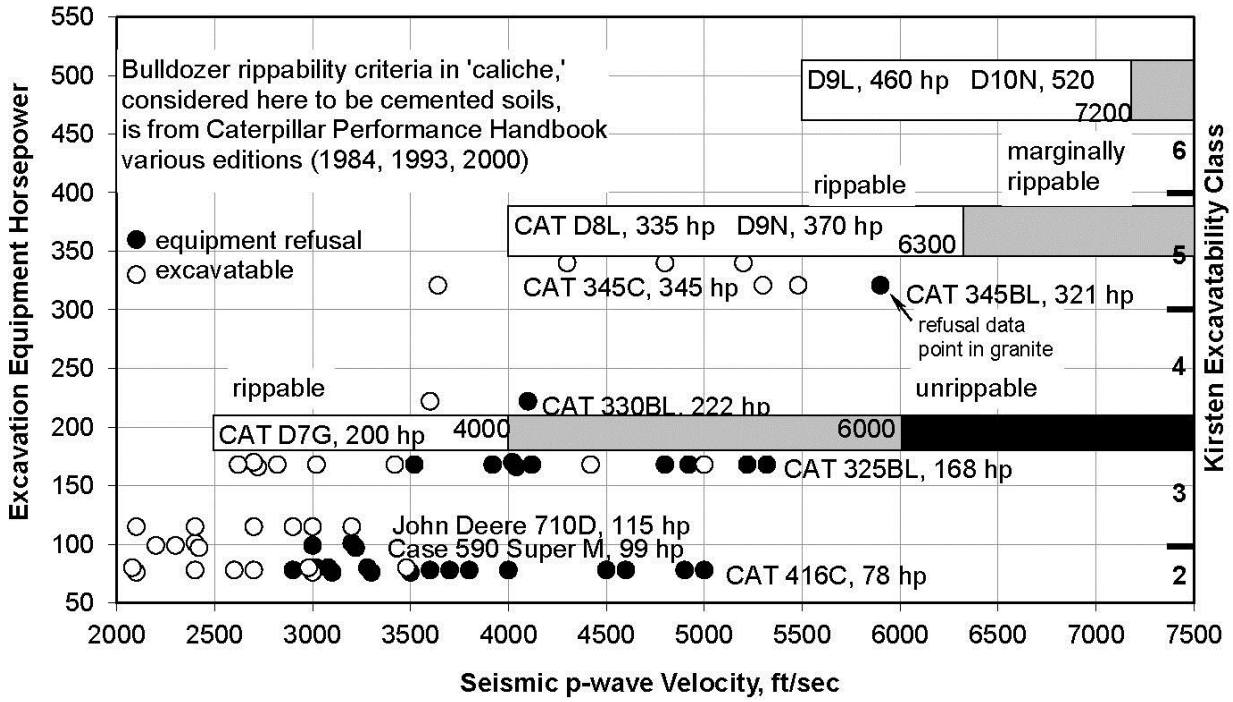

Note: From Rucker and Fergason, (2006; 2009). This chart documents typical backhoe and trackhoe excavation performance at lower seismic p-wave velocities than are presented in the Caterpillar Rippability Charts (CAT 1981, 1993, 2000). These correlations were developed in cemented materials as a function of subsurface material p-wave seismic velocity and equipment horsepower using data from test pits with overlapping seismic lines in the Salt River Valley, Arizona area. Although there are anticipated to be differences between cemented soils and highly weathered to decomposed granites, this chart shows a general trend of increasing p-wave velocities indicating more power required for excavation.

FIGURE B-2

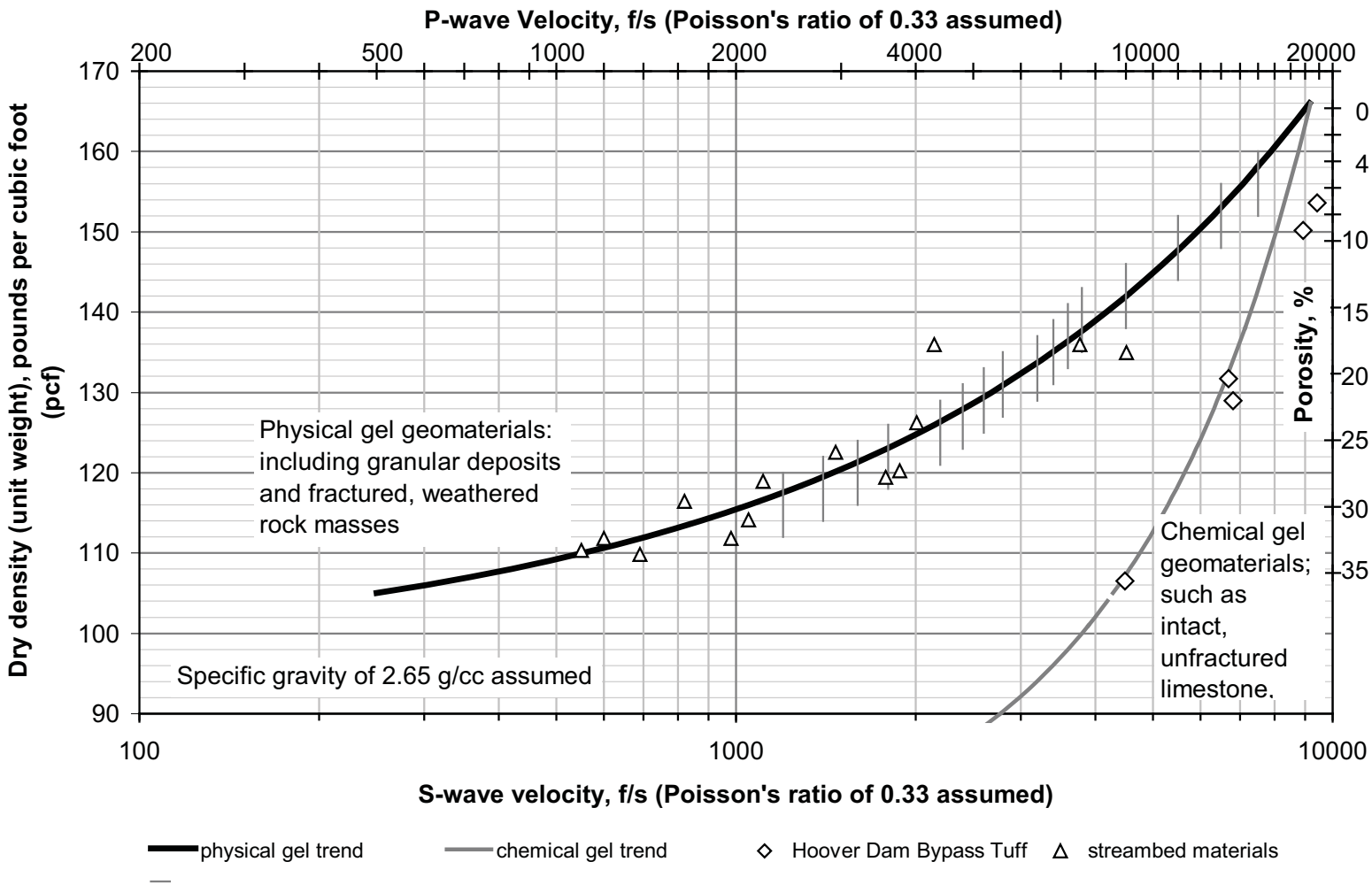
P-wave Velocity, f/s (Poisson's ratio of 0.33 assumed)
200
500
1000
2000
4000
10000
20000
Dry density (unit weight), pounds per cubic foot (pcf)
170
160
150
140
130
120
110
100
90
Porosity, %
0
4
10
15
20
25
30
35
Physical gel geomaterials: including granular deposits and fractured, weathered rock masses
Specific gravity of 2.65 g/cc assumed
Chemical gel geomaterials; such as intact, unfractured limestone.
100
1000
10000
S-wave velocity, f/s (Poisson's ratio of 0.33 assumed)
physical gel trend
chemical gel trend
Hoover Dam Bypass Tuff
streambed materials

FIGURE B-3

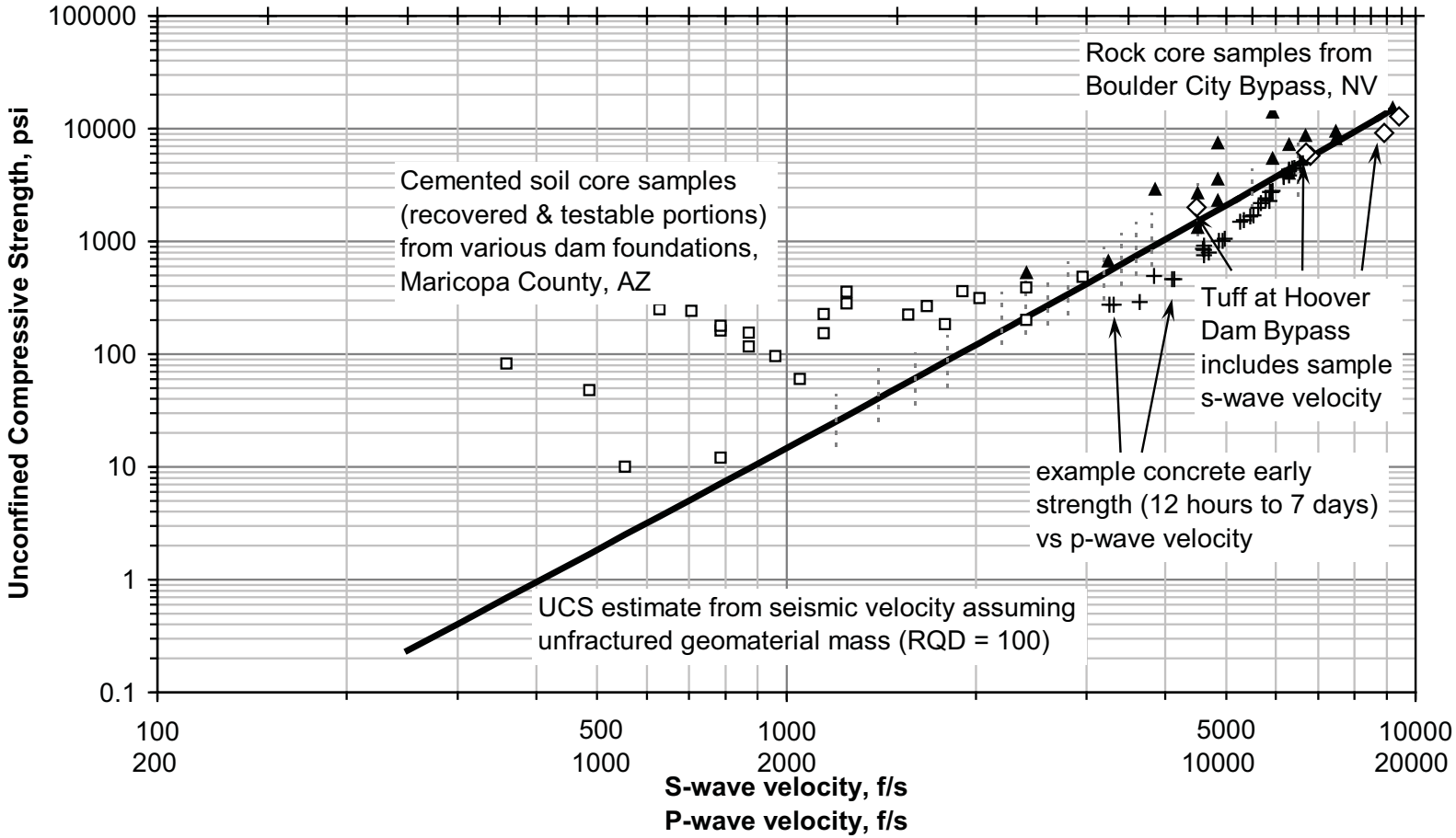

Note that this method assumes an unfractured geo-material mass (RQD = 100). Since fracturing tends to reduce seismic velocity, this method should typically underestimate UCS in fractured rock masses.

FIGURE B-4

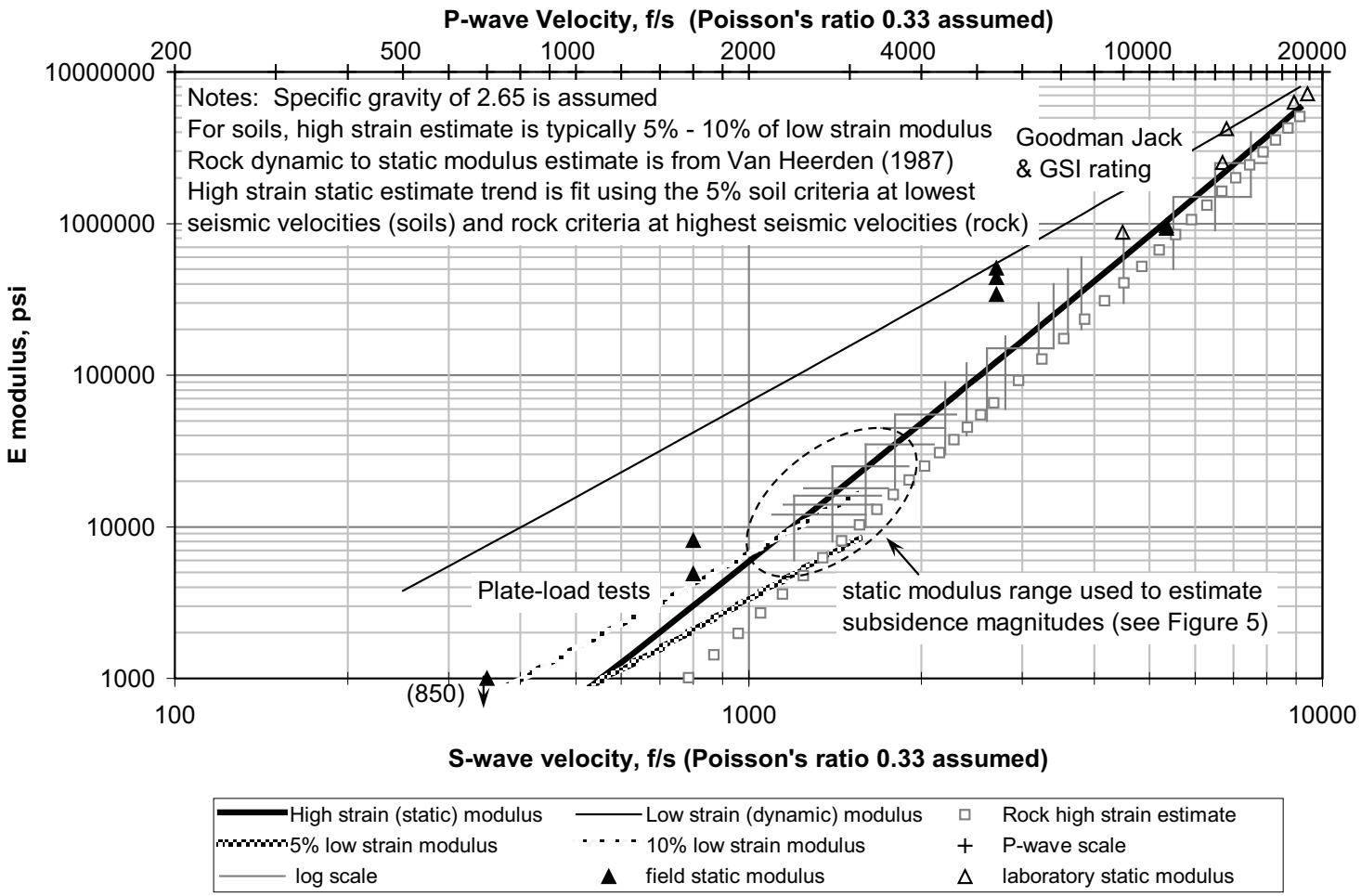
P-wave Velocity, f/s (Poisson's ratio 0.33 assumed)
200
500
1000
2000
4000
10000
20000
10000000
1000000
100000
10000
1000
E modulus, psi
Notes: Specific gravity of 2.65 is assumed
For soils, high strain estimate is typically 5% - 10% of low strain modulus
Rock dynamic to static modulus estimate is from Van Heerden (1987)
High strain static estimate trend is fit using the 5% soil criteria at lowest
seismic velocities (soils) and rock criteria at highest seismic velocities (rock)
Goodman Jack
& GSI rating
Plate-load tests
static modulus range used to estimate
subsidence magnitudes (see Figure 5)
(850)
100
1000
10000
S-wave velocity, f/s (Poisson's ratio 0.33 assumed)
High strain (static) modulus
Low strain (dynamic) modulus
Rock high strain estimate
5% low strain modulus
10% low strain modulus
P-wave scale
log scale
field static modulus
laboratory static modulus